

The Role of Interleukin 6 and Obesity in the Development of Hepatocellular Carcinoma

Inaugural-Dissertation

zur Erlangung des Doktorgrades
der Mathematisch-Naturwissenschaftlichen Fakultät
der Universität zu Köln



vorgelegt von
Sabine Gruber
aus Kerpen

Köln 2013

Thesis committee:

Prof. Dr. Jens C. Brüning

PD. Dr. F. Thomas Wunderlich

Prof. Dr. Peter Kloppenburg

Tag der mündlichen Prüfung: 29.11.2013

Contents

Abbreviations	xv
Abstract	xvi
Zusammenfassung	xvii
1 Introduction	1
1.1 Hepatocellular carcinoma	1
1.1.1 Linking inflammation to HCC	3
1.2 Linking obesity to HCC	4
1.2.1 Linking chronic low grade inflammation in obesity to HCC	6
1.3 Interleukin 6 signaling pathway	8
1.3.1 JAK/Stat-signaling	10
1.3.2 MAPK-signaling	11
1.4 Apoptosis	13
1.4.1 Extrinsic apoptotic pathway	14
1.4.2 Intrinsic apoptotic pathway	14
1.4.3 B-cell lymphoma (Bcl-2) family	16
1.4.4 Missregulation of apoptosis in cancer	17
1.5 Objectives	18
2 Materials and Methods	19
2.1 Materials	19
2.1.1 Chemicals	19
2.1.2 Buffer and solutions	22

2.1.3	Kits	24
2.1.4	Enzymes	25
2.1.5	Standards	25
2.2	Animal care	26
2.3	Metabolic measurements	26
2.3.1	Serum extraction	26
2.3.2	Measuring of blood glucose level	27
2.3.3	Glucose tolerance test	27
2.4	Treatments	27
2.4.1	Diethylnitrosamine (DEN)-injection	27
2.4.2	IL-6 signaling	27
2.4.3	NK T cell induction	27
2.4.4	Constitutiv active GSK-3 via Adeno-associated-virus (AAV)	28
2.4.5	PI-3K-inhibitor	28
2.4.6	Depletion of regulatory T cells	29
2.4.7	PP-1 inhibition by Ocadaic acid	29
2.5	Organ preparation	29
2.5.1	Organ extraction	29
2.5.2	Tumor quantification in the liver	29
2.5.3	Liver status	30
2.6	Bio molecular methods - nucleic acids	31
2.6.1	DNA-isolation from tail cuts	31
2.6.2	RNA-isolation with RNAeasy kit	31
2.6.3	Determination of nucleic acid concentration	31
2.6.4	Polymerase chain reaction (PCR) for genotyping of mice . .	32
2.6.5	Agarose gel electrophoresis	33
2.6.6	Reverse transcription (RT)	34
2.6.7	Quantitative real-time PCR (qRT-PCR)	35
2.6.8	Chromatin Immunoprecipitation	36

2.7	Bio molecular methods - proteins	37
2.7.1	Extraction of proteins from mouse organs	37
2.7.2	Mitochondrial isolation	38
2.7.3	Bax treatment of isolated mitochondria	38
2.7.4	SDS-polyacrylamid-gelelectrophorese (SDS-PAGE)	38
2.7.5	Western blot analysis	38
2.7.6	Quantitation of western blots	40
2.8	Bio molecular methods - serum	40
2.8.1	Serum analysis	40
2.8.2	Insulin, Leptin, IL-6 and TNF α enzyme linked immuno sor- bent assay (ELISA)	41
2.8.3	AKT, Caspase-3, GSK-3 β and PI3K activity assay	41
2.9	Immunohistochemical and immunofluorescence stainings	41
2.9.1	HE staining	41
2.9.2	Mcl-1 staining	41
2.9.3	Oil Red O staining	41
2.9.4	TUNEL staining	42
2.9.5	Ki67 staining	42
2.10	Cell culture	42
2.10.1	Dual Luciferase Reporter Assay	42
2.10.2	Primary murine hepatocyte and human hepatoma culture .	43
3	Results	44
3.1	Obesity increases basal hepatic Stat-3 activation and impairs acute IL-6 responsiveness	44
3.2	Generation of IL-6R α knock out mice	46
3.3	HFD causes obesity in control and IL-6R $\alpha^{\Delta/\Delta}$ mice in the DEN- induced HCC model	48
3.4	IL-6R α deficiency protects against DEN-induced liver carcinogene- sis but obesity abrogates this effect and promotes HCC development	53

3.5	Obesity and IL-6 increase HCC development through the inhibition of mitochondrial apoptosis	59
3.6	GSK-3 β inhibition stabilizes Mcl-1 under obese conditions in HCC development	66
3.7	Obesity and IL-6 controlled expression of PP-1 α and Mule synergize to stabilize Mcl-1	74
3.8	Compensatory effects of IL-6 type cytokines and receptors	83
3.8.1	HFD causes obesity in control, IL-6R $\alpha^{\Delta/\Delta}$ and gp130 $L-KO$ mice	83
3.8.2	Inactivation of gp130 in hepatocytes protected against DEN-induced HCC development even under obese conditions	84
3.8.3	No compensation for IL-6R α deficiency by IL-6 type cytokines in HCC development upon HFD feeding	88
3.9	The cell-type specific role of the IL-6R α in the development of HCC	91
3.9.1	Less effects on body weight through HFD feeding in IL-6R α^{L-KO} , IL-6R α^{M-KO} and IL-6R α^{T-KO} mice	92
3.9.2	IL-6R α^{T-KO} mice are protected against DEN-induced HCC even on HFD	94
4	Discussion	102
4.1	IL-6R α deficiency protects against DEN-induced liver carcinogenesis, but obesity abrogates this effect	103
4.2	Similar extent of obesity in control and IL-6R $\alpha^{\Delta/\Delta}$ mice in the DEN-induced HCC model	105
4.3	Obesity and IL-6 increase HCC development through the inhibition of mitochondrial apoptosis	107
4.4	GSK-3 β inhibition stabilizes Mcl-1 via IL-6 signaling and under obese conditions in HCC development	109
4.5	Obesity and IL-6 controlled expression of PP-1 α and Mule synergize to stabilize Mcl-1	111

4.6	Obesity promotes liver carcinogenesis via Mcl-1 stabilization independent of IL-6R α signaling	114
4.7	Inactivation of gp130 in hepatocytes protects against DEN-induced HCC development even under obese conditions	116
4.8	IL-6R α^{T-KO} mice are protected against DEN-induced HCC even on HFD	117
4.9	Conclusion	119
5	Bibliography	120
6	Acknowledgments	137
7	Erklärung	138
8	Curriculum vitae	139

List of Figures

1.1	Cancer distribution and HCC incidence rates worldwide in 2011 . . .	2
1.2	Mortality from Cancer According to Body-Mass Index for U.S. Men in the Cancer Prevention Study	4
1.3	Prevalence of obesity in adults from 2001 and 2010	5
1.4	TNF α signaling pathway	9
1.5	IL-6 signaling pathway	11
1.6	Apoptotic pathway	15
3.1	IL-6 responsiveness in control mice on NCD and HFD	45
3.2	Inactivation of IL-6 signaling in IL-6R $\alpha^{\Delta/\Delta}$	47
3.3	Metabolic parameters of control and IL-6R $\alpha^{\Delta/\Delta}$ mice	49
3.4	Inflammatory signaling in control and IL-6R $\alpha^{\Delta/\Delta}$ mice	50
3.5	Extent of lipid burden in control and IL-6R $\alpha^{\Delta/\Delta}$ mice	52
3.6	Tumor burden macroscopic in control and IL-6R $\alpha^{\Delta/\Delta}$ mice	54
3.7	Liver damage of control and IL-6R $\alpha^{\Delta/\Delta}$ mice	55
3.8	Tumor burden microscopic in control and IL-6R $\alpha^{\Delta/\Delta}$ mice	56
3.9	Liver status of control and IL-6R $\alpha^{\Delta/\Delta}$ mice	58
3.10	Caspase 3 activity in the liver of control and IL-6R $\alpha^{\Delta/\Delta}$ mice	60
3.11	Cytochrome C release from mitochondria of control and IL-6R $\alpha^{\Delta/\Delta}$ mice	61
3.12	Pro- and anti-apoptotic proteins in tumor livers of control and IL- 6R $\alpha^{\Delta/\Delta}$ mice	63
3.13	Mcl-1 level in tumor livers of control and IL-6R $\alpha^{\Delta/\Delta}$ mice	65
3.14	GSK-3 β activity in tumor livers of control and IL-6R $\alpha^{\Delta/\Delta}$ mice	67

3.15	Puma and Noxa in livers of control and IL-6R $\alpha^{\Delta/\Delta}$ mice	68
3.16	GSK-3 β activity in initial phase of tumor development of control and IL-6R $\alpha^{\Delta/\Delta}$ mice	70
3.17	PI3K inhibition in tumor bearing control and IL-6R $\alpha^{\Delta/\Delta}$ mice	72
3.18	PI3K pathway in tumor bearing control and IL-6R $\alpha^{\Delta/\Delta}$ mice	73
3.19	PP-1 α expression and Stat-3 activation in control and IL-6R $\alpha^{\Delta/\Delta}$ mice	75
3.20	PP-1 promoter analysis in control and IL-6R $\alpha^{\Delta/\Delta}$ mice	77
3.21	Mule expression in control and IL-6R $\alpha^{\Delta/\Delta}$ mice	78
3.22	ChIP experiments with Mule promoter	79
3.23	Mule promoter analysis in control and IL-6R $\alpha^{\Delta/\Delta}$ mice	81
3.24	Correlation between Mule and Mcl-1 level in human HCC	82
3.25	Body weight of control, IL-6R $\alpha^{\Delta/\Delta}$ and gp130 $^{L-KO}$ mice	84
3.26	Tumor burden macroscopic in control, IL-6R $\alpha^{\Delta/\Delta}$ and gp130 $^{L-KO}$ mice	85
3.27	Tumor burden microscopic in control, IL-6R $\alpha^{\Delta/\Delta}$ and gp130 $^{L-KO}$ mice	86
3.28	Liver status of control, IL-6R $\alpha^{\Delta/\Delta}$ and gp130 $^{L-KO}$ mice	87
3.29	IL-6 type cytokines and receptors in tumor livers of control and IL-6R $\alpha^{\Delta/\Delta}$ mice	90
3.30	Metabolic status of control, IL-6R $\alpha^{\Delta/\Delta}$, IL-6R α^{L-KO} , IL-6R α^{M-KO} and IL-6R α^{T-KO} mice	93
3.31	Tumor burden macroscopic in control, IL-6R $\alpha^{\Delta/\Delta}$, IL-6R α^{L-KO} , IL-6R α^{M-KO} and IL-6R α^{T-KO} mice	95
3.32	Liver damage of control, IL-6R $\alpha^{\Delta/\Delta}$, IL-6R α^{L-KO} , IL-6R α^{M-KO} and IL-6R α^{T-KO} mice	96
3.33	Tumor burden microscopic in control, IL-6R $\alpha^{\Delta/\Delta}$, IL-6R α^{L-KO} , IL- 6R α^{M-KO} and IL-6R α^{T-KO} mice	97
3.34	Liver status of control, IL-6R $\alpha^{\Delta/\Delta}$, IL-6R α^{L-KO} , IL-6R α^{M-KO} and IL-6R α^{T-KO} mice	99

3.35	Tumor burden macroscopic in control, IL-6R $\alpha^{\Delta/\Delta}$ and IL-6R α^{T-KO} mice	101
4.1	Model of apoptosis-regulation in HCC via IL-6 signaling and obesity	115

List of Tables

0.1	Abbreviations	x
2.1	Chemicals	19
2.2	Buffer and solutions	22
2.3	Kits	24
2.4	Enzymes	25
2.5	Standards	25
2.6	Primer	32
2.7	PCR mix	32
2.8	PCR programmes	33
2.9	RT programm	34
2.10	RT mix	34
2.11	Oligonucleotides for qRT-PCR (applied Biosystems, Darmstadt, Germany)	35
2.12	Realtime mix	36
2.13	Antibodies	39

Abbreviations

Table 0.1: Abbreviations

Abbreviations	
°C	degree celsius
3	three prime end of DNA sequence
5′	five prime end of DNA sequence
αGalCer	αGalactosylceramide
μg	microgram
AAV	adeno-associated virus
AIF	apoptosis inducing factor
AKT	protein kinase B
Alfp	albumin promoter/α-fetoprotein enhancer
ALT	alanin transaminase
AP-1	activated protein 1
Apaf-1	apoptotic protease activating factor 1
APS	Ammonium persulfate
ASK	apoptosis signal-regulating kinase
AST	aspartate transaminase
Bak	Bcl-2 homologues antagonist/killer
Bax	Bcl-2-associated X protein
Bcl-2	B-cell lymphoma 2
Bcl-XL	B-cell lymphoma extra large
Bid	BH3 interacting-domain death agonist
BL6	black 6
BMI	body mass index

Continued on next page

Table 0.1 – continued from previous page

Abbreviations	
BW	body weight
CD	cluster of differentiation
cDNA	complementary DNA
ChIP	chromatin immunoprecipitation
c-Jun	Jun proto-oncogene
CNTF	ciliary neurotrophic factor
CNTRF	ciliary neurotrophic factor receptor
CO ₂	carbon dioxide
Cre	site-specific recombinase from phage P1 (cause recombination)
CTCF-1	cardiotrophin-like cytokine factor 1
Cul-1	Cullin 1
DAPI	4,6-diamidino-2-phenylindole
DEN	Diethylnitrosamine
DNA	Desoxyribonucleic acid
DR	Death receptor
EBI-3	Epstein-Barr virus induced gene 3
ECL	Enhanced chemiluminescence
EDTA	Ethylendiamine tetraacetate
ELISA	Enzyme Linked Immunosorbent Assay
ERK	extracellular signal-related kinase
Facs	Fluorescence-activated cell sorting
FBW7	F-box WD repeat-containing protein 7
FLD	fatty liver disease
Fos	FBJ osteosarcoma oncogene
g	gram
GFP	green fluorescent protein
GusB	Glucuronidase beta
gp130	glycoprotein 130

Continued on next page

Table 0.1 – continued from previous page

Abbreviations	
gp130 ^{f1/f1}	floxed gp130 gene
gp130 ^{L-KO}	hepatocyte specific deletion of gp130
GSK-3 β	glycogen synthase kinase 3 β
GSK-3 β CA	constitutive active GSK-3 β
h	hour
H ₂ O	water
HBV	hepatitis B virus
HCC	hepatocellular carcinoma
HCl	hydrochloric acid
HCV	hepatitis C virus
HEPES	N-2-hydroxyethylpiperazine-N'-2-ethansulfonic acid
HFD	high fat diet
IGF	insulin like growth factor
IgG	immunoglobulin G
I κ B α	inhibitor of NF- κ B
IKK	inhibitor of NF- κ B kinase
IL-6	Interleukin 6
IL-6R α	Interleukin 6 receptor α
IL-6R $\alpha^{\Delta/\Delta}$	deletion of IL-6R α gene in the whole body
IL-6R $\alpha^{f1/f1}$	floxed IL-6R α gene
IL-6R α^{L-KO}	hepatocyte specific deletion of IL-6R α
IL-6R α^{M-KO}	myeloid specific deletion of IL-6R α
IL-6R α^{T-KO}	T cell specific deletion of IL-6R α
IMM	inner mitochondrial membrane
<i>i.p.</i>	intraperitoneal
<i>i.v.</i>	intravenously
JAK	janus activated kinase
JNK	c-Jun N terminale kinase

Continued on next page

Table 0.1 – continued from previous page

Abbreviations	
KC	Kupffer cell
kg	kilogram
LIFR	leukemia inhibitory factor receptor
loxP	recognition sequence for Cre
LPS	Lipopolysaccharide
MAPK	mitogen activated protein kinase
Mcl-1	myeloid leukemia cell 1
MEK	MAP kinase-ERK kinase
mg	milligram
MKK	McKusick-Kaufman syndrome kinase
ml	milliliter
MLK	mixed-lineage protein kinase
mM	millimolar
mo	months
mRNA	messenger RNA
Mule	Mcl-1 ubiquitin ligase E3
NaCl	sodium chloride
NaF	sodium fluoride
NCD	normal chow diet
NEMO	NF- κ B essential modulator of IKK
NF- κ B	nuclear factor 'kappa light chain enhancer' of activated B cells
ng	nanogram
NKT cells	natural killer-like T cells
nm	nanometer
N-terminal	amino-terminal
OA	okadaic acid
OD	optical density
OMM	outer mitochondrial membrane

Continued on next page

Table 0.1 – continued from previous page

Abbreviations	
OSMR	oncostatin M receptor
p	phosphorylated
P21	postnatal day 21
p38	mitogen-activated protein kinase
PAGE	polyacrylamid-gelelectrophorese
PBS	phosphate buffered saline
PCR	polymerase chain reaction
PDK-1	Phosphoinositide-dependent protein kinase 1
PI3K	phosphoinositid 3 kinase
PIP3	Phosphatidylinositol (3,4,5)-triphosphate
PKB	Protein kinase B
PolIII	polymerase 2
PP-1	protein phosphatase 1 α
rpm	rounds per minutes
pTEN	phosphatase and tensin homolog
Puma	p53 upregulated modulator of apoptosis
PVDF	polyinylidene fluoride
qPCR	quantitative real time PCR
RAF	rapidly accelerated fibrosarcoma kinase
Ras	rat sarcoma protein
RNA	ribonucleic acid
RNase	Ribonuclease
RT	room temperature
S9	serine 9 residue
SAPK	stress-activated protein kinase
SCF-FBW	SKP1-cullin-F-box WD repeat-containing complex
SDS	Sodiumdodecylsulfate
SEM	standard error of the mean

Continued on next page

Table 0.1 – continued from previous page

Abbreviations	
sgp139	soluble gp130
SH2	src-homology
sIL-6R α	soluble Interleukin 6 receptor α
Socs-3	suppressor of cytokine signaling 3
Stat-3	signal transducer and activator of transcription 3
TAK	TGF activated kinase
TBS	Tris buffered saline
TEMED	Tetramethylethylenediamine
TNF α	tumor necrosis factor α
T ^{regs}	regulatory T cells
Tris	2-amino-2-(hydroxymethyl)-1,3-propanediol
TUNEL	Terminal deoxynucleotidyl transferase dUTP nick end labeling
UV	ultraviolet
V	Volt
v/v	volume per volume
W	watt
WAT	white adipose tissue
WHO	World health organisation
w/v	weight per volume
wk	weeks
WT	wild type

Abstract

Obesity is a constantly increasing health burden affecting more than 30% of the population of westernized countries. In addition to classical associated disorders, obesity was also previously reported to increase the incidence of hepatocellular carcinoma (HCC) development, in part through activation of obesity-associated pro-inflammatory signaling and the release of inflammatory cytokines such as $\text{TNF}\alpha$ and IL-6, both known as tumor-promoting cytokines. Nevertheless, how these inflammatory cytokines trigger HCC development is currently not fully understood.

The current work reports that abrogation of IL-6R α signaling in lean mice protects against DEN-induced HCC development. This HCC protection occurs via destabilization of anti-apoptotic Bcl-2 family member Mcl-1, thus promoting hepatocyte apoptosis. In lean mice IL-6 regulates the stability of Mcl-1 via inhibition of PP-1 α expression which promotes GSK-3 β inactivation by serine 9 residue phosphorylation. In addition, IL-6 suppresses expression of the Mcl-1 E3 ligase Mule. Consequently, IL-6R α deficiency activates PP1- α and Mule expression resulting in increased Mcl-1 turnover and protection against HCC development. In contrast, in obese mice inhibition of PP1- α and Mule expression leading to Mcl-1 stabilization occurs independent from IL-6 signaling.

Furthermore, the current work could demonstrate that IL-6R α signaling in T cells is essential for the development of HCC indicated by the protective effect of IL-6R α deficiency on T cells.

Collectively, this study provides evidence that IL-6 and obesity inhibit hepatocyte apoptosis through Mcl-1 stabilization thus promoting liver carcinogenesis.

Zusammenfassung

Adipositas ist ein konstant wachsendes Gesundheitsproblem, welches schon heute mehr als 30% der westlichen Bevölkerung betrifft. Zusätzlich zu den klassisch-assoziierten Krankheiten, erhöht Adipositas auch die Gefahr der hepatozellulärer Karzinomentwicklung (HCC). Dies geschieht teilweise durch Aktivierung von Adipositas-assoziierten Signalwegen, welche zur Freisetzung von tumorfördernden, inflammatorischen Zytokinen wie $\text{TNF}\alpha$ und IL-6 führen. Unbekannt ist jedoch wie diese Zytokine die Entwicklung von HCC auslösen. Die vorliegende Arbeit zeigt, dass die Inaktivierung des $\text{IL6R}\alpha$ normalgewichtige Mäusen vor der DEN induzierte HCC Entwicklung schützt. Durch die Destabilisierung von Mcl-1, einem Mitglied der Anti-apoptotischen Bcl-2 Familie, wird die Apoptose in Hepatozyten gefördert. Dies schützt die Leber vor der Entwicklung von HCC. In normalgewichtigen Mäusen reguliert IL-6 die Stabilität von Mcl-1 durch Hemmung der $\text{PP-1}\alpha$ Expression, welches wiederum die Inaktivierung von $\text{GSK-3}\beta$ fördert. Zusätzlich unterdrückt IL-6 die Expression der Mcl-1 ubiquitin ligase E3 Mule. In $\text{IL-6R}\alpha$ defizienten Mäusen wird die Expression von $\text{PP-1}\alpha$ und Mule aktiviert, dies führt zu einem erhöhten Umsatz von Mcl-1 und zum Ausbleiben von HCC. Im Gegensatz dazu führt bei Adipositas die Hemmung der $\text{PP-1}\alpha$ und Mule Expression zu einer Stabilisierung von Mcl-1, unabhängig von der IL-6 Signalübertragung. Desweiteren kann mit der vorliegenden Arbeit gezeigt werden, dass die $\text{IL-6R}\alpha$ -signalübertragung in T Zellen essentiell für die Entwicklung von HCC ist. Hinweise dafür liefert der schützende Effekt der $\text{IL-6R}\alpha$ -defizienz auf T Zellen. Insgesamt liefert diese Studie Beweise dafür, dass IL-6 und Adipositas die Apoptose in Hepatozyten durch Mcl-1 Stabilisierung hemmen und so die Leberkarzinogenese fördern.

1 Introduction

1.1 Hepatocellular carcinoma

Cancer is a general term for a large group of diseases that can occur in almost every part of the body. Cancer development is characterized by uncontrolled cell growth that leads to tumor formation and invasion of these cells to neighboring tissues [Croce, 2008]. Cancer is a disease which is more frequent in older ages. Due to an increase in the old population, the World Health Organisation (WHO) assumes an increase in the cancer-related mortality rate from 7.9 million (2007) to 11.5 million (2030) cases per year. In most industrialized countries, cancer is the second most frequent cause of death after cardiovascular diseases [Alwan, 2011].

Hepatocellular carcinoma (HCC) is the third most common cancer worldwide (Fig. 1.1A) and represents, with 85-90% of all primary liver cancers, the most common one [El-Serag & Rudolph, 2007]. The average mortality is 95% within 5 years due to limited treatment strategies and the late exhibition of clinical symptoms [Sherman, 2005; Villanueva *et al.*, 2010]. Therefore, HCC represents the third largest cause of cancer deaths worldwide, especially for men in low- and middle-income countries, such as Africa and Eastern Asia (Fig. 1.1B). Male individuals have a 4-fold increase in HCC incidence compared to women. These results could be confirmed by Maria *et al.* [2002] in mouse models. Accordingly, females have a lower incidence for HCC due to an estrogen-dependent mechanism [Naugler *et al.*, 2007]. However, the increasing incidence of HCC in industrialized countries cannot be neglected [El-Serag *et al.*, 2003].

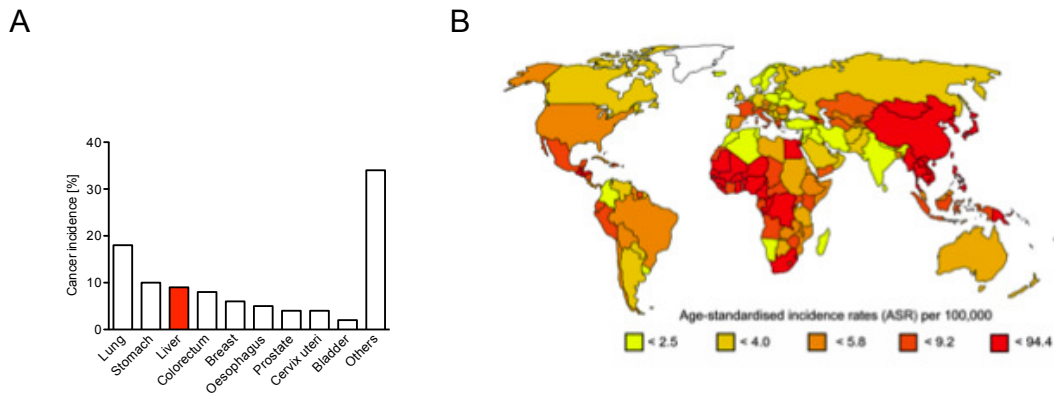


Figure 1.1: **Cancer distribution and HCC incidence rates worldwide in 2011**
 (A) Worldwide distribution of different cancer forms of both genders in percentage of total cancer numbers from 2011. (WHO globocan project) (B) Distribution of HCC incidence in 2011 (ASR per 100000). (WHO globocan project)

Cancer development and progression is influenced by genetic, epigenetic and environmental factors. HCC is linked to a variety of genetic predispositions, such as mutations in tumor suppressor genes, as well as to viral infections such as hepatitis B (HBC) or C (HCV), alcoholic liver disease, hemochromatosis and non-alcoholic steatohepatitis [Villanueva *et al.*, 2007; Fattovich *et al.*, 2004; Yoshioka *et al.*, 2004; Thorgeirsson & Grisham, 2002; Donato *et al.*, 2002; Yu *et al.*, 2001]. All of which cause liver damage and chronic inflammation and therefore promote HCC, which is characterized as a classic case of inflammation-linked cancer [Sanz-Cameno *et al.*, 2010; Mantovani *et al.*, 2008; Karin *et al.*, 2006; Karin & Greten, 2005; Balkwill & Mantovani, 2001].

1.1.1 Linking inflammation to HCC

Human studies could demonstrate that chronic inflammation in alcoholic hepatitis, HBV and HCV infections and steatohepatitis may lead to development of HCC [Abiru *et al.*, 2006; Sherman, 2005]. Even in mouse studies a strong correlation could be exhibit between the amount of liver damage during acute toxicity and inflammation and the extent of HCC development [Naugler *et al.*, 2007; Sakurai *et al.*, 2006; Maeda *et al.*, 2005]. Furthermore, Maeda and others could demonstrate that chemically or genetically induced HCC depends on inflammatory signaling [Sakurai *et al.*, 2006; Maeda *et al.*, 2005; Pikarsky *et al.*, 2004]. Liver injury and chronic inflammation that results in compensatory proliferation of differentiated hepatocytes, which are otherwise quiescent, is one of the major pathogenic mechanisms underlying HCC development [Sakurai *et al.*, 2006; Fausto, 1999; Maeda *et al.*, 2005]. The relevance of compensatory proliferation as a tumorigenic mechanism is supported by mouse genetic studies, using either the hepatic pro-carcinogen Diethylnitrosamine (DEN) as an inducer of HCC [Hui *et al.*, 2008; Sakurai *et al.*, 2006; Maeda *et al.*, 2005] or the conditional or complete inactivation of nuclear factor 'kappa light chain enhancer' of activated B cells (NF- κ B) signaling, needed for maintenance of hepatocyte survival [Luedde *et al.*, 2007]. The resulting necrosis of hepatocytes in these studies enhances mutagenesis in host cells, accumulation of double strand breaks and results in HCC [Karin, 2008; Sakurai *et al.*, 2006; Maeda *et al.*, 2005]. Furthermore, during chronic inflammation the infiltrating immune cells create a tumor microenvironment releasing elevated levels of pro-inflammatory cytokines such as tumor necrosis factor alpha (TNF α) and Interleukin 6 (IL-6) [Newell *et al.*, 2008; Xu *et al.*, 2003]. Liver injury and compensatory proliferation are strongly depending on IL-6 and the absence of this cytokine results in almost complete inhibition of DEN-induced HCC [Naugler *et al.*, 2007]. Furthermore, IL-6 deficient mice demonstrate reduced liver injury, apoptosis, necrosis and proliferation in hepatocytes after DEN-injection, characterizing inflammation as the major contributing factor in HCC development.

1.2 Linking obesity to HCC

Previous epidemiological studies identified obesity as a major risk factor for several cancer entities and demonstrated a 1.52 - 1.62-fold increase in relative risk of cancer related death [Calle *et al.*, 2003; Calle & Kaaks, 2004; Bianchini *et al.*, 2002]. The amount of increase in risk depends on the type of cancer, whereas HCC exhibited the strongest obesity-associated increase in tumor incidence with a 4.52-fold increase, particularly in men with a body mass index over 35 (Fig. 1.2) [Calle *et al.*, 2003]. Thus, the obesity-associated increase in HCC development gains substantial clinical relevance in the light of the current epidemical increase in obesity in westernized societies [Ford & Mokdad, 2008].

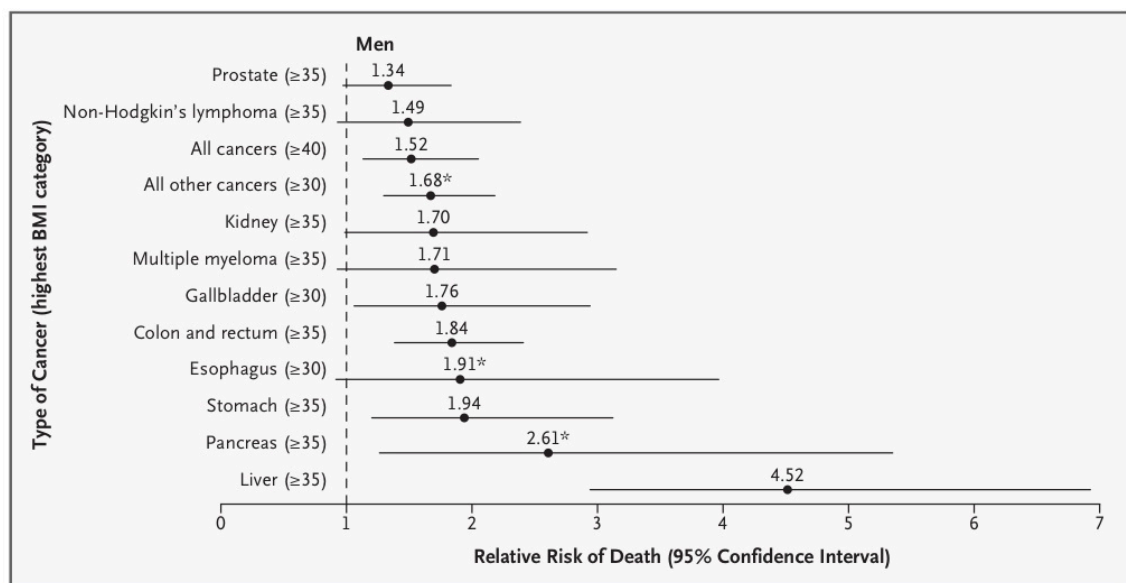


Figure 1.2: **Mortality from Cancer According to Body-Mass Index for U.S. Men in the Cancer Prevention Study**

For each relative risk, comparison between men in highest BMI category (indicated in parentheses) and men in reference category (BMI, 18.5 to 24.9). Asterisks indicate relative risks for men who never smoked. Results were significant ($p \leq 0.05$) for all cancer sites. [Calle *et al.*, 2003]

Obesity is a constantly increasing health burden affecting more than 30% of the population of westernized countries. Obesity is defined as a condition of abnormal or excessive body fat accumulation that is a consequence of a sustained positive energy balance. That means consuming more calories than spending,

resulting in excessive storage of lipids in the adipose tissue. A more sedentary lifestyle in western societies with reduced physical work and the increased availability of food due to the industrialization contributes further to a positive energy balance.

In 2008, approximately 1.5 billion adults were overweight, of which over 200 million men and approximately 300 million women were obese. Following recordings of each country in the WHO European Region from 2008, over 50% of both men and women have a body mass index (BMI = weight in kilograms / size in meters²) higher than 25 and thus considered to be overweight. Nearly 23% of these were obese indicated by a BMI above 30 (Fig. 1.3 [Berghofer, 2008]).

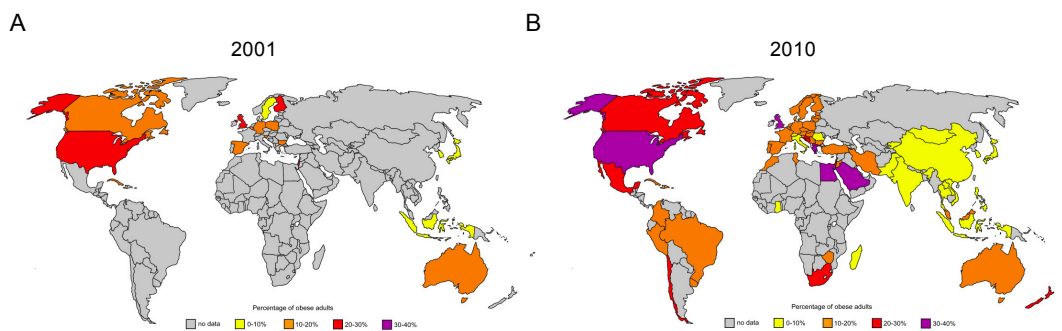


Figure 1.3: **Prevalence of obesity in adults from 2001 and 2010**

The worldwide prevalence of obese adults (BMI >30) compared from 2001 and 2010. Datas were obtained from the WHO.

The association between fat accumulation and HCC was known for a long time [El-Serag & Rudolph, 2007; Caldwell *et al.*, 2004]. Fatty liver disease (FLD) turned out to be one of the major risk factors for HCC which rapidly increased over the last years in western countries. Obesity and FLD lead to steatosis and cirrhosis and thereby increase the incidence of HCC [Yoshioka *et al.*, 2004; Calle *et al.*, 2003].

While the current study was being completed, Park *et al.* [2010] could demonstrate that genetically and dietary-induced obesity enhances development of chemically induced HCC. Moreover, earlier studies described that consumption of high fat diet (HFD) resulted in increased formation of pre-neoplastic lesions in response to DEN administration in rats [Wang *et al.*, 2009]. However, these rats

were not evaluated for HCC and the mechanism underlying increased formation of the lesions was not determined.

Another recent study used mice with hepatocyte-specific deficiency of the regulatory subunit NF- κ B essential modulator (NEMO) of the inhibitor of kappa B kinase (IKK) complex or the IKKs itself (Nemo/IKK $\gamma^{\Delta hep}$), which spontaneously develop liver damage, hepatosteatosis and HCC on a normal chow diet (NCD) [Luedde *et al.*, 2007]. These mice revealed enhanced development of hepatosteatosis and liver damage after HFD-feeding, which ultimately results in accelerated tumor development in the liver [Wunderlich *et al.*, 2008]. However, the pre-existing hepatosteatosis and spontaneous liver damage in Nemo/IKK $\gamma^{\Delta hep}$ mice upon NCD feeding prevented the conclusive demonstration that obesity per se rather than chronic liver damage, caused by the absence of NF- κ B, is responsible for tumor promotion. Furthermore, the mechanism by which obesity accelerates HCC development in these mice was not determined.

1.2.1 Linking chronic low grade inflammation in obesity to HCC

The excessive weight gain during obesity is associated with a chronic low grade inflammatory state. The concept of chronic low grade inflammation in response to obesity was first demonstrated by elevated expression of TNF α in the white adipose tissue (WAT) [Hotamisligil *et al.*, 1993]. Follow-up studies confirmed the observation in humans, where WAT also expresses increased TNF α upon obesity, which was decreased after weight loss [Gonzalez *et al.*, 1999; Dandona *et al.*, 1998; Hotamisligil *et al.*, 1995; Kern *et al.*, 1995]. Additional work demonstrated that the chronic low grade inflammation in obesity is not only locally in WAT, but also systemically, indicated by elevated plasma concentrations of circulating TNF α and IL-6 [Nishimura *et al.*, 2009; Xu *et al.*, 2003; Bastard *et al.*, 2000; Mohamed-Ali *et al.*, 1997; Hotamisligil *et al.*, 1993]. During the development of obesity, immune cells, such as macrophages and T cells, infiltrate tissues, such as WAT or liver, and lead to increased secretion of TNF α and IL-6 [Nishimura *et al.*, 2009; Xu *et al.*,

2003]. The tumor promoting effect of HFD depends to a large extent on this elevated levels of $\text{TNF}\alpha$ and IL-6, both of which are tumor-promoting cytokines [Park *et al.*, 2010; Lin & Karin, 2007].

Liver injury and compensatory proliferation are strongly depending on IL-6 and the absence of this cytokine results in almost complete inhibition of DEN-induced HCC [Naugler *et al.*, 2007]. Additionally, it could be demonstrated that obesity increases IL-6 level compared to lean mice and thereby accelerates tumor development [Park *et al.*, 2010]. IL-6 may not be the only mediator responsible for obesity-induced cancer promotion, however, it is well established that its production is elevated in obese mice due to the low-grade inflammatory response caused by lipid accumulation [Arkan *et al.*, 2005; Shoelson *et al.*, 2007; Solinas *et al.*, 2007; Hotamisligil, 2006].

1.3 Interleukin 6 signaling pathway

IL-6 is a pleiotropic cytokine largely responsible for the hepatic response to infections or systemic inflammation, often termed the "acute phase response". IL-6 regulates activation of phagocytosis and acute phase proteins such as the c-reactive protein or serum amyloid A in the inflammation process [Barton, 1996]. Moreover, IL-6 plays a key role in the transition from innate to adaptive immunity by initiating differentiation of T- and B-lymphocytes [Brooks *et al.*, 1985].

The IL-6 gene consists of 5 exons whose expression results in an inactive pre-peptide of 212 amino acids which is then cleaved into the active form of 184 amino acids. IL-6 has several splice forms and is posttranslationally modified by glycosylation and phosphorylation [Parekh *et al.*, 1992]. The membrane bound IL-6 receptor (IL-6R) is expressed on hepatocytes, macrophages, T lymphocytes and endothelial cells [Barton, 1996]. The heterotrimeric receptor consists of two signal transduction β -chains glycoprotein 130 (gp130) and one IL-6R α -chains. Gp130 is widely used by a cohort of cytokines receptors, especially by the IL-6 type cytokine receptor family including Interleukin 11 receptor (IL-11R), oncostatin M receptor (OSMR), ciliary neurotrophic factor receptor (CNTFR), Interleukin 27 receptor (IL-27R), Epstein-Barr virus induced gene 3 (EBI-3) and leukemia inhibitory factor receptor (LIFR) [Zhang *et al.*, 1994]. In contrast the IL-6R α chain is specific for IL-6 signaling in hepatocytes, macrophages, endothelial cells and T-lymphocytes [Hibi *et al.*, 1996].

Besides the classical membrane bound IL-6 receptor signaling an alternative pathway exists using a soluble form of the IL-6 receptor (sIL-6R α). The sIL-6R α is either created by shedding of the extracellular part of the membrane bound IL-6 receptor which is triggered by the c-reactive protein or is produced by alternative splicing of the messenger RNA (mRNA) [Jones *et al.*, 1999]. A complex of IL-6 and the sIL-6R α can bind to the gp130 signaling chain at virtually all cell types, thereby rendering also cells responsible to IL-6 which do not express the IL-6R α chain [Graeve *et al.*, 1996]. This kind of IL-6 signaling was described as "transsig-

nalizing" which can be inhibited by soluble gp130 (sgp130) [Chalaris *et al.*, 2007].

IL-6 expression is regulated by $\text{TNF}\alpha$ signaling which activates a dual kinase system (Fig. 1.4). On the one hand, $\text{TNF}\alpha$ leads to survival which is mediated by the IKK kinases phosphorylating the inhibitor of $\text{NF-}\kappa\text{B}$ ($\text{I}\kappa\text{B}\alpha$), thus, liberating $\text{NF-}\kappa\text{B}$ transcription factors to induce IL-6 transcription and proliferation [Karin, 2008]. On the other hand, $\text{TNF}\alpha$ induced apoptosis as a consequence of c-Jun N terminal kinase (JNK) activation phosphorylating the classical activated protein 1 (AP-1) [Karin & Gallagher, 2005; Ventura *et al.*, 2003].

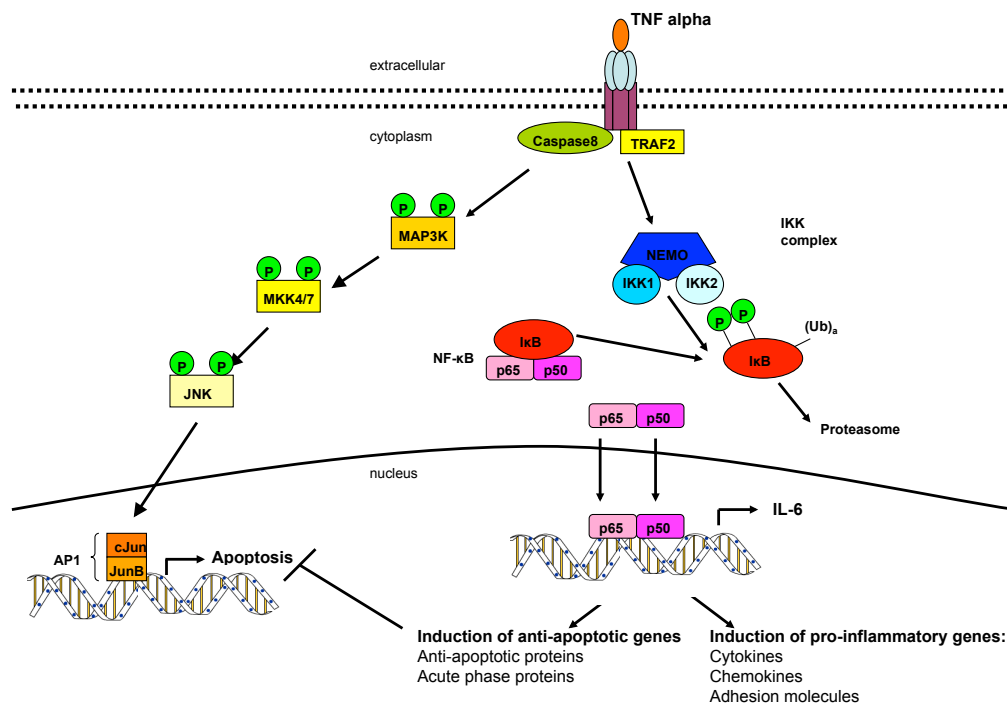


Figure 1.4: $\text{TNF}\alpha$ signaling pathway

$\text{TNF}\alpha$ binds to its receptor and mediates signaling by the IKK complex (IKK1, IKK2, NEMO). The IKK complex phosphorylates $\text{I}\kappa\text{B}$ leading to its ubiquitination and degradation by the proteasome. The transcription factor $\text{NF-}\kappa\text{B}$ translocates to the nucleus and activates transcription of target genes such as IL-6. Alternatively, the $\text{TNF}\alpha$ receptor phosphorylates MAP3K mediated by Caspase 8 leading to phosphorylation of MKK which results in JNK activation. c-Jun, phosphorylated by JNK forms AP-1 with the JunB proteins and regulates target genes.

1.3.1 JAK/Stat-signaling

Upon IL-6 binding to the IL-6R α , the gp130 complex recruits Janus-activated-kinases (JAK) [O'Shea *et al.*, 2002]. JAKs provide tyrosine kinase activity at the activated IL-6R α . These JAKs bind to the intracellular receptor domains and phosphorylate tyrosines of the IL-6R α after JAK dimers phosphorylate each other [O'Shea *et al.*, 2002]. These phosphorylated tyrosines of the receptor are binding sites for proteins containing src- homology 2 (SH2) domains [O'Shea *et al.*, 2002]. Signal transducer and activator of transcription 3 (Stat-3) binds to the receptor by its SH2 domain and thereby tyrosin 705 of Stat-3 is phosphorylated by the JAKs [O'Shea *et al.*, 2002]. This induces a conformational change and creates new SH2 binding sites at the Stat-3 surface [Akira, 1997]. Therefore, Stat-3 dissociates from the IL-6R α , forms homodimers, translocates into the nucleus and enhances or inhibits transcription of target genes (Fig. 1.5) [Ramadori & Christ, 1999; Akira, 1997].

One of the target genes of Stat-3 is the suppressor of cytokine signaling (Socs) 3 [Endo *et al.*, 1997]. Socs-3 in turn negatively regulates the IL-6 mediated signaling transduction pathway in a negative feedback loop (Fig. 1.5). On the one hand, Socs-3 binds to phosphorylated tyrosine at the IL-6R α and therefore occupies binding sites for Stat-3. On the other hand, Socs-3 binds directly to JAKs thereby reducing JAK kinase activity [Kawazoe *et al.*, 2001; Naka *et al.*, 1999, 1997; Bjørbaek *et al.*, 1998; Endo *et al.*, 1997].

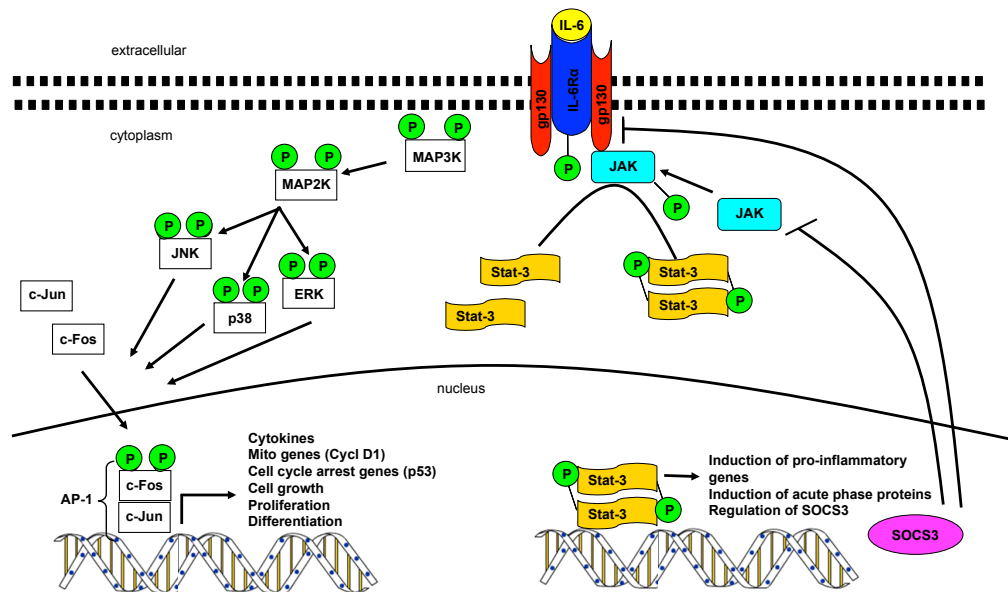


Figure 1.5: **IL-6 signaling pathway**

IL-6 binds to its receptor, composed of gp130 and IL6R α . Gp130 recruits JAKs which phosphorylate the receptor after transphosphorylation. The phosphorylated receptor recruits Stat-3 which is phosphorylated by JAKs and forms homodimers. These dimers translocate to the nucleus and induce transcription of target genes.

1.3.2 MAPK-signaling

Additionally to the JAK/Stat pathway, IL-6 activates the mitogen-activated protein kinase (MAPK) pathway (Fig. 1.5). The MAPK pathway regulates embryonic development, cell differentiation, cell proliferation and apoptosis and is activated by mitogens, cytokines or cellular stress [Davis *et al.*, 2002; Davis, 2000]. Three groups of MAPK are described consisting of JNK, the extracellular signal-related kinases (ERK) and the p38 protein kinases (Fig. 1.5) [Ramadori & Christ, 1999].

JNK is mainly activated by pro-inflammatory cytokines such as TNF α and IL-6 or by cellular stress [Weston & Davis, 2002]. The signal transduction from the receptor to the MAP3K is not yet fully elucidated. However, it was demonstrated

that mixed-lineage protein kinase (MLK) 1, apoptosis signal-regulating kinase (ASK) 1, MAP kinase-ERK kinase (MEK) 1/4, TGF activated kinase (TAK) 1 and JNK 1-3 are participating in this signaling pathway [Davis, 2000; Baud *et al.*, 1999]. Finally, JNK phosphorylates c-Jun which forms a homodimer or heterodimer with other Jun- or FBJ osteosarcoma oncogene- (Fos) proteins to produce AP-1 [Weston & Davis, 2002; Karin & Chang, 2001]. AP-1 activation regulates cytokine production, enhances transcription of mitotic genes such as Cyclin D1 and reduces expression of cell cycle arrest genes such as p53 [Angel & Karin, 1991].

The ERK signaling pathway involves MEK 1 and 2, rapidly accelerated fibrosarcoma kinase (RAF) and ERK 1 and 2 and regulates cell growth, proliferation and differentiation [Zhang *et al.*, 2004]. Over-expression and activation of ERK can be detected in many types of cancer [Jin *et al.*, 2013; Bartholomeusz *et al.*, 2012; Caja *et al.*, 2009; Zhang *et al.*, 2004].

The p38 pathway is activated by stress, UV light and osmotic stress. This pathway involves signaling of MLK and ASK-1 as well as TAK, McKusick-Kaufman syndrome kinase (MKK) 3/6, p38 and MAPK α/β and results in similar outcomes as the ERK pathway [Shi & Gaestel, 2002; Tibbles & Woodgett, 1999].

1.4 Apoptosis

Evading or inhibiting apoptosis is one of the hallmarks in the development of cancer [Hanahan & Weinberg, 2000]. The hypothesis that apoptosis serves as a barrier to cancer was first raised in 1972, when Kerr, Wyllie, and Currie described massive apoptosis in the cells populating rapidly growing, hormone-dependent tumors following hormone withdrawal [Kerr *et al.*, 1972].

Apoptosis is the process of programmed cell death and can be induced by several stimuli including cellular stress, UV-light, DNA damage and virus infections [Green, 2005]. Apoptosis leads to characteristic morphological cell changes, including cell shrinkage, nuclear fragmentation, chromatin condensation and chromosomal DNA fragmentation, which subsequently results in cell death [Hanahan & Weinberg, 2011]. In contrast to necrosis, which is a form of traumatic cell death, apoptosis is necessary during an organism's life cycle, for example for the separation of fingers and toes in a developing human embryo [Haruta *et al.*, 2011]. Furthermore, apoptosis is necessary to eliminate cells with DNA damage and keeps proliferating tissue in balance [Hanahan & Weinberg, 2011]. Missregulation of apoptosis results in wide range of pathophysiological consequences, including carcinogenesis and Alzheimer's disease [Rohn, 2010]. The apoptotic process is tightly regulated and divided into two pathways which can overlap. On the one hand the extrinsic pathway mediated by membrane-bound death receptors, such as the TNF-receptor, on the other hand the intrinsic pathway mediated intracellular via the mitochondria [Hanahan & Weinberg, 2011].

1.4.1 Extrinsic apoptotic pathway

The extrinsic apoptotic pathway is mediated via death receptors (DR) from the TNF-receptor family, including Fas (CD95/Apo1), TNFR, DR3, DR4, DR5, DR6, NGFR and EDAR [Bhardwaj & Aggarwal, 2003]. After binding of the ligand at the extracellular, cysteine-rich part of the DR, adapter proteins are recruited to the intracellular part of the receptor which cleaves and thereby activates Caspase 8 (Fig. 1.6A) [Hengartner, 2000]. This leads to recruitment of Caspase 3. Caspase 3 is cleaved by Caspase 9 and thereby activated which results in degradation of cellular components (Fig. 1.6A) [Malhi *et al.*, 2010].

1.4.2 Intrinsic apoptotic pathway

The key element of the intrinsic apoptotic pathway are the mitochondria which are the central sensory organelle that can respond to DNA damage. The double membrane of the mitochondria consists of the inner and the outer membrane. The inner, impermeable mitochondrial membrane (IMM) consists of many invaginations called cristae and harbor different enzyme complexes essential for the respiratory chain. The outer, semi-permeable mitochondrial membrane (OMM) comprises different membrane-bound protein complexes which allow the exchange of small molecules and proteins between mitochondria and cytosol. The intermembrane space (IMS) contains pro-apoptotic factors such as cytochrome C, apoptosis inducing factor (AIF) or endonuclease G which cannot pass through the constitutive protein channel and stay in the IMS. (Fig. 1.6B) The mitochondria respond to DNA damage by mitochondrial outer membrane permeabilization [Green, 2005; Chipuk *et al.*, 2006]. By forming pores, cytochrome C can be released into the cytoplasm and interact with apoptotic protease activating factor-1 (Apaf-1) (Fig. 1.6C) [Green, 2005; Chipuk *et al.*, 2006]. Recruitment of pro-Caspase 9 to the complex then leads to formation of the apoptosome, cleavage of Caspase 9 and activation of Caspase 3 (Fig. 1.6C) [Green, 2005; Chipuk *et al.*, 2006].

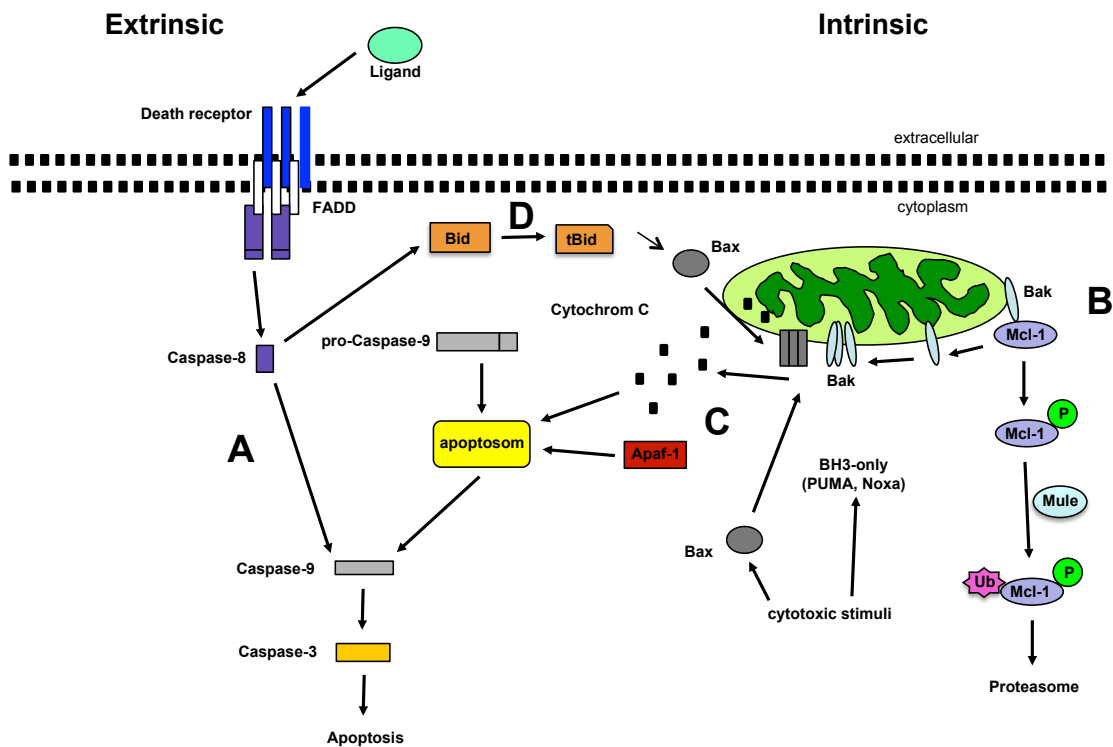


Figure 1.6: **Apoptotic pathway**

(A) After stimulation by extrinsic signals adapter proteins are recruited to the receptor, Caspase 8 is recruited and activated which results in cleavage and thereby activation of Caspase 3. (B) In the physiological state Mcl-1 exists in a complex with Bak associated with the OMM. (C) After cytotoxic stimuli Mcl-1 is separated from Bak by active BH3-only proteins, phosphorylated, ubiquitinated by Mule and degraded by the proteasome. Bak and Bax can oligomerise and integrate in the OMM to form pores which leads to the release of cytochrome C. Cytochrome C interacts with Apaf-1 and recruits Caspase 9 to form the apoptosome which leads to cleavage and activation of Caspase 3. (C) The intrinsic pathway can be activated via extracellular signals by Bid. Caspase 8, activated via DR signaling, can cleave Bid and the resulting truncated Bid (tBid) interacts with Bax and leads to the integration in the OMM.

1.4.3 B-cell lymphoma (Bcl-2) family

The balance between anti- and pro-apoptotic members of the Bcl-2 protein family regulates mitochondrial outer membrane permeabilization and the efflux of cytochrome C in response to cellular damage [Brunelle & Letai, 2009]. The Bcl-2 protein family consists of pro-apoptotic proteins such Bcl-2 homologues antagonist/killer (Bak) and Bcl-2-associated X protein (Bax) and anti-apoptotic proteins such as Bcl-2, Bcl-XL and Myeloid leukemia cell 1 (Mcl-1). Another sub-group consists of the pro-apoptotic BH3-only proteins such as p53 upregulated modulator of apoptosis (Puma) and phorbol-12-myristate-13-acetate-induced protein 1 (PMAIP1), also known as Noxa, which have only one of the four Bcl-2 homology domains [Thomas *et al.*, 2010]. These proteins promote apoptosis by binding at anti-apoptotic proteins [Brinkmann *et al.*, 2013; Eskes *et al.*, 2000].

Bax and Bak are constitutively expressed. Bak is associated with the OMM whereas Bax is located in the cytosol (Fig. 1.6C). After initiation of apoptosis, Bim binds at Bax which leads to a conformational change and to translocation to the OMM (Fig. 1.6C) [Ren *et al.*, 2010]. Bax oligomerise with Bak, integrates into the OMM and creates pores which leads to the release of cytochrome C (Fig. 1.6C) [Malhi *et al.*, 2010].

To avoid a constitutive activation of apoptosis, anti-apoptotic proteins are bound to Bax and Bak to suppress membrane permeabilization. Bak is bound by Mcl-1 at the OMM which can be detached via replacement by Noxa (Fig. 1.6C) [Ren *et al.*, 2010]. After phosphorylation Mcl-1 is ubiquitinated by the Mcl-1 ubiquitin ligase E3 (Mule) and degraded by the proteasome [Zhong *et al.*, 2005].

The extrinsic and intrinsic apoptotic pathway are connected via BH3 interacting-domain death agonist (Bid). Caspase 8, activated via death receptor signaling, can cleave Bid and the resulting truncated Bid (tBid) interacts with Bax and leads to integration in the OMM (Fig. 1.6D) [Eskes *et al.*, 2000].

1.4.4 Missregulation of apoptosis in cancer

The discovery of the upregulation of the Bcl-2 oncogene in follicular lymphoma [Korsmeyer, 1992] and its recognition as having anti-apoptotic activity opened up the investigation of apoptosis in cancer at the molecular level [Vaux *et al.*, 1988]. Further insights into the myc-Bcl-2 interaction emerged later from studying the effects of a myc oncogene on fibroblasts cultured under low serum conditions. Widespread apoptosis was induced in myc-expressing cells cultured in serum-free media and the consequent apoptosis could be abrogated by exogenous survival factors, by forced overexpression of Bcl-2 or the related Bcl-XL protein or by disruption of the FAS death signaling circuit [Hueber *et al.*, 1997]. Collectively, the data indicate that the apoptotic program of the cell can be triggered by an overexpressed oncogene. Indeed, elimination of cells bearing activated oncogenes by apoptosis may represent the primary means by which such mutant cells are continually eliminated from the tissues.

1.5 Objectives

Hepatocellular carcinoma (HCC) and obesity are intimately connected diseases and their incidences are steadily increasing worldwide. Thus, the obesity-associated increase in HCC development gains substantial clinical relevance.

Previous work clearly evidenced the promoting role of IL-6 in liver tumorigenesis [Naugler *et al.*, 2007]. Nevertheless, how IL-6 signaling facilitates HCC growth in the tumor itself or in the tumor microenvironment or whether both are affected by IL-6 still remains elusive.

To precisely define the effects of IL-6 signaling pathway in tumors and in cells contributing to the tumor microenvironment through a loss of function approaches in mice, the IL-6R α was genetically deleted in the entire body, hepatocytes, myeloid cell and T cells of mice, respectively. A DEN induced liver carcinogenesis approach was applied to these mice to confirm the previously published protection of IL-6 signaling deficient animals to DEN induced HCC development and to elucidate the underlying mechanism. Moreover, a group DEN injected mice were also exposed to HFD feeding since HFD increased tumor number and size in different HCC tumor model [Park *et al.*, 2010; Wunderlich *et al.*, 2008].

Taken together, these experiments should determine the molecular mechanisms and the cell type (s) responsible for mediating the recently published protection to HCC development in IL-6 knock out mice. Thus, this work will clarify whether the tumor originating from hepatocytes or specific cell types contributing to the microenvironment such as macrophages and T lymphocytes mediate IL-6's ability to promote tumor growth in the HCC mouse model.

2 Materials and Methods

2.1 Materials

2.1.1 Chemicals

Table 2.1: **Chemicals**

Chemical	Supplier
β -mercaptoethanol	Applichem, Darmstadt, Germany
ϵ -aminocaproic acid	Sigma-Aldrich, Seelze, Germany
0.9% saline (sterile)	Delta Select, Pfullingen, Germany
2,2,2-Tribromoethanol (Avertin)	Sigma-Aldrich, Seelze, Germany
2-Methyl-2-Butanol	Sigma-Aldrich, Seelze, Germany
Acetic acid	Merck, Darmstadt, Germany
Acetone	KMF Laborchemie, Lohmar, Germany
Acrylamide	Roth, Karlsruhe, Germany
Agarose	Peqlab, Erlangen, Germany
Agarose (Ultra Pure)	Invitrogen, Karlsruhe, Germany
Ammonium Acetate	Merck, Darmstadt, Germany
Ammoniumpersulfat (APS)	Sigma-Aldrich, Seelze, Germany
Aprotinin	Sigma-Aldrich, Seelze, Germany
Bacillol	Bode Chemie, Hamburg, Germany
Benzamidine	Sigma-Aldrich, Seelze, Germany
Bovine serum albumin (BSA)	Sigma-Aldrich, Seelze, Germany
Bromphenol blue	Merck, Darmstadt, Germany
Calcium chloride	Merck, Darmstadt, Germany
Chloroform	Merck, Darmstadt, Germany

Continued on next page

Table 2.1 – continued from previous page

Chemical	Supplier
Desoxy-ribonucleotid-triphosphates (dNTPs)	Amersham, Freiburg, Germany
Developer G153	AGFA, Mortsel, Belgium
Dimethylsulfoxide (DMSO)	Merck, Darmstadt, Germany
di-Natriumhydrogenphosphat	Merck, Darmstadt, Germany
Di-thiothreitol	Applichem, Darmstadt, Germany
Enhanced chemiluminescence (ECL) Kit	Perbio Science, Bonn, Germany
Ethanol, absolute	Applichem, Darmstadt, Germany
Ethidium bromide	Sigma-Aldrich, Seelze, Germany
Ethylendiamine tetraacetate (EDTA)	Applichem, Darmstadt, Germany
Fixer G354	AGFA, Mortsel, Belgium
Forene (isoflurane)	Abbot GmbH, Wiesbaden, Germany
Glucose 20%	DeltaSelect, Pfullingen, Germany
Glycerol	Serva, Heidelberg, Germany
Glycine	Applichem, Darmstadt, Germany
HEPES	Applichem, Darmstadt, Germany
Hydrochloric acid (37%)	KMF Laborchemie, Lohmar, Germany
Hydrogen peroxide	Sigma-Aldrich, Seelze, Germany
Insulin	Novo Nordisk, Bagsvaerd, Denmark
Isopropanol (2-propanol)	Roth, Karlsruhe, Germany
Magnesium chloride	Merck, Darmstadt, Germany
Methanol	Roth, Karlsruhe, Germany
Nitrogen (liquid)	Linde, Pullach, Germany
N-Nitrosodiethylamine	Sigma-Aldrich, Seelze, Germany
Paraformaldehyde (PFA)	Sigma-Aldrich, Seelze, Germany
Phenylmethylsulfonylfluoride (PMSF)	Sigma-Aldrich, Seelze, Germany
Phosphate buffered saline (PBS)	Gibco BRL, Eggenstein, Germany
Potassium chloride	Merck, Darmstadt, Germany

Continued on next page

Table 2.1 – continued from previous page

Chemical	Supplier
Potassium dihydrogenphosphat	Merck, Darmstadt, Germany
Potassium hydroxide	Merck, Darmstadt, Germany
Sodium acetate	Applichem, Darmstadt, Germany
Sodium chloride	Applichem, Darmstadt, Germany
Sodium citrate	Merck, Darmstadt, Germany
Sodium dodecyl sulfate	Applichem, Darmstadt, Germany
Sodium fluoride	Merck, Darmstadt, Germany
Sodium heparin (Liquemin)	Roche, Grenzach-Wyhlen, Switzerland
Sodium hydrogen phosphate	Merck, Darmstadt, Germany
Sodium hydroxide	Applichem, Darmstadt, Germany
Sodium orthovanadate	Sigma-Aldrich, Seelze, Germany
Tetramethylethylenediamine (TEMED)	Sigma-Aldrich, Seelze, Germany
Tissue Freezing Medium	Jung, Heidelberg, Germany
Tramadolhydrochlorid (Tramal)	Grünenthal, Aachen, Germany
Trishydroxymethylaminomethane (Tris)	Applichem, Darmstadt, Germany
Triton X-100	Applichem, Darmstadt, Germany
Trizol	Applichem, Darmstadt, Germany
Tween 20	Applichem, Darmstadt, Germany
Vectashield Mounting Medium with DAPI	Vector, Burlingame, USA
Western Blocking Reagent	Roche, Mannheim, Germany

2.1.2 Buffer and solutions

Table 2.2: Buffer and solutions

Buffer/Solution	Composition
Anode buffer 1	0,3 M Tris
	20% (v/v) Methanol
Anode buffer 2	25 mM tris
	20% (v/v) Methanol
Antibody Solution	5% (v/v) Roche Western Blocking
	Reagent in TBS-T
Avertin-injectable solution	20.3 mg/ml Avertin Stocksolution
	mixed in 0.9 % NaCl
	steril filter and store at 4°C in the dark
Avertin-stocksolution	1.6 mg/ml Avertin
	in 2-Methyl-2-Butanol
	incubate for 12 h at RT
Cathode buffer	40 mM 6-Aminocapron acid
	0.01 % (v/v) SDS
	20% (v/v) Methanol
Organ Lyses Buffer	50 mM HEPES
	1 % Triton X-100
	50 mM NaCl
	0.1 M NaF
	10 mM EDTA
	10 mM Sodium orthovanadat
	0.1 % (w/v) SDS
	2 mM Benzamidin
	10 µl/ml Aprotinin
	adjust pH 7.4
2 mM PMSF	

Continued on next page

Table 2.2 – continued from previous page

Buffer/Solution	Composition
PBS (1x)	137 mM NaCl
	2.7 mM KCl
	8.1 mM Na ₂ HPO ₄
	1.5 mM KH ₂ PO ₄
	adjust pH 7.4
SDS-PAGE electrophoresis buffer (10x)	0.25 M Tris
	2 M Glycin
	35 mM SDS
SDS-protein-loading-buffer (4x)	250 mM Tris-HCl, pH 6.8
	200 mM DTT
	8% (v/v) SDS
	0.04% (w/v) Bromphenolblue
	40% (v/v) Glycerol
Stripping solution	0.7% β -Mercaptoethanol
	2% (v/v) SDS
	12.5% 0.5 M Tris, pH 6.8
TAE (50x)	2 M Tris
	50 mM EDTA
	adjust pH 8 with acetate acid
Tail-Lyses-Buffer	100 mM Tris-HCl, pH 8.5
	200 mM NaCl
	5 mM EDTA
	0.2% (w/v) SDS
TBS (10x)	1.47 M NaCl
	0.2 M Tris
	adjust pH 7.4
TBS-Tween (1x)	1 x TBS
	0.1% Tween20

Continued on next page

Table 2.2 – continued from previous page

Buffer/Solution	Composition
TE-Buffer	10 mM Tris-HCl, pH 7.4
	10 mM EDTA, pH 7.8
Western Blocking solution	10% (v/v) Roche Western Blocking
	Reagent in TBS-T

2.1.3 Kits

Table 2.3: Kits

Kit	Company
Real-time detection PCR	
TaqMan universal PDR master mix	Applied Biosystems, Darmstadt, Germany
Reverse transcription PCR	
Reverse transcription core kit	Qiagen, Hilden, Germany
SuperScript III first-strand kit	Invitrogen, Karlsruhe, Germany
RNA isolation	
RNAeasy extraction kit	Quiagen, Hilden, Germany
peqGOLD TriFast	Peqlab, Erlangen, Germany
Developing of western blots	
Enhanced chemiluminescence kit	Amersham Pharmacia Biotech, Freiburg, Germany

2.1.4 Enzymes

Table 2.4: **Enzymes**

Enzymes	Supplier
DNase	Promega, Mannheim, Germany
Proteinase K	Roche Diagnostics, Basel, Swiss
DreamTaq	ThermoScientific, Schwerte, Germany
RNase A	ThermoScientific, Schwerte, Germany

2.1.5 Standards

Table 2.5: **Standards**

Standard	Company
GeneRuler™ DNA ladder mix	ThermoScientific, Schwerte, Germany
PageRuler™ protein ladder	ThermoScientific, Schwerte, Germany

2.2 Animal care

Keeping of mice, used for the experiments, occurred in agreement with the animal protection guidelines of the district president of Cologne. The authorization for animal procedures was approved by the district government of Cologne and in accordance with NIH guidelines. Authorization for accomplishment of the experiments: 50.203.2 – K 13, 35/03 Genetic analysis of molecular mechanisms in the regulation of gluconeogenesis and glucose disposal. The mice were housed in a constant 12 hour day-night-cycle, the room temperature was constantly 22°C and they had ad libitum access to food and drinking water. After weaning (P21), mice were separated by sex and were kept in groups of 2 to 5 animals per cage. During weaning the mice were marked by eartags. For genotyping by PCR the tail top was cut. During the experiments the mice were exposed to high fat diet (HFD; C1057; Altromin) containing 32.7 % carbohydrates, 20 % protein, and 35.5 % fat (55.2 % of calories from fat) or normal chow diet (NCD; Teklad Global Rodent 2918; Harlan) containing 53.5 % carbohydrates, 18.5 % protein, and 5.5 % fat (12 % of calories from fat).

2.3 Metabolic measurements

2.3.1 Serum extraction

Blood samples were taken from the mice by two different methods. Blood was either collected from the tail vene or from the submandibular veins by piercing the cheek with a lancet. For coagulation the blood was stored on ice for 30 minutes and afterwards centrifuged for 60 minutes at 13.000 rpm at 4 °C. The blood serum was collected and frozen at -20 °C until further application.

2.3.2 Measuring of blood glucose level

For measuring blood glucose level Glucomen® blood glucose meter was used. Therefore the tail vene was cut and a drop of blood was transferred to Glucomen®-test strip.

2.3.3 Glucose tolerance test

A glucose tolerance test was used to test metabolic reaction of mice to hyperglycemic stimuli. Therefore mice were fasted for 6 hours and afterwards injected with 2 mg/g body weight glucose *i.p.*. Blood glucose levels were measured before, 15, 30, 60 and 120 minutes after injection.

2.4 Treatments

2.4.1 Diethylnitrosamine (DEN)-injection

Liver tumors were induced by DEN to investigate the role of IL-6 in hepatocarcinogenesis. Mice were injected intra peritoneal (*i.p.*) with 25 mg/kg DEN (Sigma) 15 days after birth for long term studies. Tumor development was investigated for 8 months. For short term studies 8 weeks old mice were injected *i.p.* with 100 mg/kg DEN and sacrificed 4, 12, 24 hours or 48 hours after injection.

2.4.2 IL-6 signaling

50 ng recombinant IL-6 was injected either via the Vena carva or via tail vene in 8 weeks old mice to induce IL-6 signaling and mice were sacrificed at different time points.

2.4.3 NK T cell induction

Eight weeks old mice were injected *i.p.* with 4 μ g Galactosylceramide to specifically activate NK T cells and sacrificed at different time points.

2.4.4 Constitutiv active GSK-3 via Adeno-associated-virus (AAV)

8 weeks old mice were injected with 5×10^1 viral particles 5 days before DEN treatment to test the effect of constitutive active GSK-3 β (GSK-3 β CA). Adeno-associated viral vector particle production was carried out by calcium phosphate transient co-transfection of the vector plasmid p87GSK-3CA or pscAAV/EGFP, pXR8 AAV serotype 8 helper plasmid (kindly provided by James Wilson, University of Pennsylvania, Philadelphia, USA) and pXX6-80 adenovirus helper plasmid (kindly provided by Jude Samulski, University of North Carolina at Chapel Hill, USA) into human embryonic kidney 293 (HEK293) cells. p87GSK-3 β CA contained the TTR-promoter driven GSK-3CA cassette that was amplified from mouse liver cDNA using primers 5NcomycGSKCA: ccATGGGCGGCGAGCA-GAAACTCATCTCTGAAGAGGATCTGTCGGGGCGACCGAGAACCACCgCC TTTGCGGAGAGCTGCAAGCC and 3NotGsk3: GCGGCCGCTCAGGTGGAGT TGAAGCTG and subsequently cloned into p87 using restriction endonucleases NcoI and NotI thereby replacing the luciferase transgene by GSK-3CA. p87 is designed for production of AAV8-inverted terminal repeat (ITR)-flanked self-complementary AAV vector genomes. HEK293 cells were harvested post transfection and subjected to benzonase treatment after lysis. AAV particles were purified using a discontinuous iodixanol gradient (15-60%). Recombinant viral particle titer was determined by qPCR and found to be 2×10^9 per μ l for AAV8 TTR GSK-3 β CA and $3,3 \times 10^8$ for AAV8 GFP. The control vector encoding for GFP was produced accordingly.

2.4.5 PI-3K-inhibitor

8 month old mice injected with 25 mg/kg DEN were treated with 1 mg of PI3K inhibitor GDC-0941 by oral gavage daily for 10 days to inhibit PI3K and were subsequently sacrificed. GDC-0941 was dissolved as previously described (Sos et al., 2009).

2.4.6 Depletion of regulatory T cells

Thirteen days old mice were injected with 1 mg α CD25 antibody to deplete regulatory T cells before injection with 100 mg/kg DEN injection on day 15 initiates tumor development.

2.4.7 PP-1 inhibition by Ocadaic acid

Eight weeks old mice were injected *i.p.* with 0.75 μ g/kg BW ocadaic acid to specifically inhibit PP-1 activity 1 hour before DEN injection. Mice were sacrificed at different time points.

2.5 Organ preparation

2.5.1 Organ extraction

After 8 weeks (short-term experiments) and 8 month (long-term experiments), respectively, mice were sacrificed with CO₂. Blood was taken from the heart, liver, muscle, white adipose tissue and brain were extracted and shock frozen in liquid nitrogen. A small part of the liver was embedded in tissue freezing medium for subsequent tissue slices. The big lobe of the liver of mice from the long-term experiments was deposite in formalin for further analysis. White adipose tissue was weighed. The organs were stored at -80 °C until further application.

2.5.2 Tumor quantification in the liver

For the macroscopical quantification tumor numbers in livers of eight months old mice were determined. Livers were extracted and tumors were counted which were visible by eye. The big lobe of the liver from eight months old mice (long-term experiment) was deposited in formalin and sent to Beate Straub, a pathologist in the Institute of Pathology in the University Hospital in Heidelberg, for microscopical analyses.

2.5.3 Liver status

Quantitation of inflammation measured in the big liver lobe of DEN-injected 8 month old mice was performed by the following score:

1 = mild inflammation (mild portal inflammation, 3-5 single cell necrosis, no grouped necrosis)

2 = moderate inflammation (moderate portal inflammation, 6-9 single cell necrosis, 1 grouped necrosis)

3 = severe inflammation (severe portal inflammation, more than 10 single cell necrosis, more than 1 grouped necrosis)

Quantitation of steatosis measured in the big liver lobe of DEN-injected 8 month old mice was performed by the following score:

1 = 0 - 10%

2 = 11 - 50 %

3 = above 50 %

Quantitation of fibrosis measured in the big liver lobe of DEN-injected 8-month mice was performed by the following score:

1 = increased portal connective tissue

2 = early formation of septa

2.6 Bio molecular methods - nucleic acids

2.6.1 DNA-isolation from tail cuts

To isolate genomic DNA from tailcuts, tails were incubated with 600 μ l tail lysis buffer containing Proteinase K (1:100) at 55°C over night. On the next day lysed tails were centrifuged for 10 minutes at 10.000 rpm to collect coat residues. The supernatant was mixed with 600 μ l isopropanol for precipitation of DNA. The mix was centrifuged at 13.000 rpm for 15 minutes, the supernatant was discarded and pellet was washed with 200 μ l 70 % ethanol. After centrifugation at 13.000 rpm for 10 minutes, the supernatant was again discarded and DNA pellet dried for 15 minutes. The DNA was resuspended in 50 μ l Tris-EDTA buffer containing RNase A (1:1000).

2.6.2 RNA-isolation with RNAeasy kit

To obtain pure RNA for real-time analysis RNAeasy Mini Kit (Qiagen) was used. The procedure was performed according to the RNAeasy Mini Kit protocol for purification of total RNA from animal tissue.

2.6.3 Determination of nucleic acid concentration

For quantitation of DNA or RNA in solution a spectral photometer was used. The photometer measured optical density at a wavelength of 260 nm. The absorption of purine and pyrimidine aromatic bases is maximal at this wavelength. The following formula was used for determination of DNA:

$$C [\text{ng}/\mu\text{l}] = \text{OD}_{260} \times D \times E$$

C = concentration of DNA solution OD₂₆₀ = absorption at 260 nm D = dilution factor E = extinction coefficient

Around 50 μ g/ml double-stranded DNA or 40 μ g/ml RNA or single-stranded DNA corresponds to an OD₂₆₀ of 1. Optical density of a wavelength at 280 nm was measured to detect protein contaminations. A ratio between 1.8 – 2.0 (OD₂₆₀

/OD280) shows minimal protein contaminations. Measurements were done in the NanoDrop® instrument.

2.6.4 Polymerase chain reaction (PCR) for genotyping of mice

Table 2.6: **Primer**

Primer notation	Sequence
5'Cre	ACG AGT GAT GAG GTT CGC A
3'Cre	ATG TTT AGC TGG CCC AAA TGT
5'IL6Ex3	CCA GAG GAG CCC AAG CTC TC
3'IL6a	TAG GGC CCA GTT CCT TTA T
5GK12	CCGCGGGCGATCGCCTAGG
5'gp130	GGT GGC TGA TTC ACC TGC A
3'gp130	TAC GCT GGG CAG CGT CCT
gp130 delta	AAC ACA CTC ATG CTG AAA CC

Table 2.7: **PCR mix**

Reagent	Amount
H ₂ O	20.1 μ l
Buffer	2.5 μ l
dNTPs	0.2 μ l
Primer	0.25 μ l per primer
DreamTaq	0.2 μ l
DNA	1.5 μ l

Table 2.8: PCR programmes

PCR	Programm
Cre	95°C 30 sec
	95°C 30 sec
	54°C 30 sec
	72°C 1 min
	72°C 5 min
	4°C endless
IL-6R α	94°C 3 min
	94°C 45 sec
	54°C 45 sec
	72°C 1.30 min
	72°C 10 min
	4°C endless
gp130	94°C 4 min
	94°C 30 sec
	54°C 30 sec
	72°C 45 min
	72°C 10 min
	4°C endless

2.6.5 Agarose gel electrophoresis

Gel electrophoresis was used to separate DNA with different size.

2.6.6 Reverse transcription (RT)

A RT-PCR was performed to produce cDNA for real-time analysis. Using the High Capacity cDNA Reverse Transcription Kit from Applied Biosystems, RT-PCR was performed according to manufacturer's instructions.

Table 2.9: RT programm

Temperature	Time
25°C	10 min
37°C	2 h
85°C	5 min
4°C	endless

Table 2.10: RT mix

Reagent	Amount
RNase free H ₂ O	4.2 µl
10x Buffer	2 µl
dNTPs	0.8 µl
random Oligos	2 µl
reverse transkriptase	0.25 µl
RNA	1-2 µg in 10 µl

2.6.7 Quantitative real-time PCR (qRT-PCR)

Quantitative qRT-PCR was performed to measure expression levels, using Taq-Man probes from Applied biosystem. The qRT-PCR was performed as followed.

Table 2.11: Oligonucleotides for qRT-PCR (applied Biosystems, Darmstadt, Germany)

Probe	Order number
Bak	Mm00432042m1
Bax	Mm00432045m1
Bbc3	Mm00519268m1
Bcl-2	Mm00477631m1
Bclxl	Mm00437783m1
Clcf-1	Mm0136492m1
Cntf	Mm00446373m1
Cntfr	Mm00516693m1
Ctf-1	Mm00432772m1
Cul1	Mm00516318m1
Ebi-3	Mm00469294m1
Fbxw7	Mm00504452m1
gp130	Mm00438665m1
Gusb	Mm00446953m1
Huwe1	Mm00615533m1
IL-6	Mm00446190m1
IL-11	Mm00434162m1
IL-33	Mm00505403m1
IL-6ra	Mm00439649m1
IL-11ra	Mm00494938m1
IL-20ra	Mm00555504m1
Lif	Mm00434762m1
Lifr	Mm00442942m1
Mcl-1	Mm01257352g1

Continued on next page

Table 2.11 – continued from previous page

Probe	Order number
Osm	Mm01193966m1
Osmr	Mm01307326m1
Pmaip1	Mm00451763m1
Pp1ca	Mm00453291g1
Puma	Mm00437783m1

Table 2.12: Realtime mix

Reagent	Amount
DEPC- H ₂ O	3.4 μ l
MasterMiix (TaqMan)	6 μ l
probe	0.6 μ l
cDNA	2 μ l

2.6.8 Chromatin Immunoprecipitation

HepG2 cells were grown on 15cm dishes to 80-90% confluency in EF Medium. Cells were stimulated with 200 ng/ml human IL-6 (#200-006, PeproTech) for 45 minutes and subsequently crosslinked with 1% PFA for 10 minutes at room temperature. The reaction was quenched with addition of 1.7 ml 1.25 M Glycine for 5 minutes and cells were washed twice with PBS. Cells were scraped off the plates in 2 ml PBS, supplemented with protease inhibitor (Roche cOmplete protease inhibitor cocktail), and collected in 15 ml falcon tubes (700 xg, 5 minutes, 4°C). The cell pellet was resuspended in 1 ml cell lysis buffer (5 mM HEPES, 140 mM NaCl, 1 mM EDTA, 10% Glycerol, 0.25% Triton X-100, 1 mM PMSF, Roche cOmplete protease inhibitor cocktail) and rotated for 15 minutes at 4°C. Cells were collected (700 xg, 5 minutes, 4°C), resuspended in 1 ml MNase Buffer (0.32 M Sucrose, 50 mM Tris-HCL pH7.5, 4 mM MgCl₂, 1 mM CaCl₂, 0.1 mM PSMF, Roche cOmplete protease inhibitor cocktail, 300u MNase [Thermo Scientific]) and

incubated at 4°C for 60 minutes. Cells were collected (700 xg, 5 minutes, 4°C), re-suspended in 1 ml nuclear lysis buffer (50 mM Tris-HCL pH8.0, 10 mM EDTA, 1% SDS, 1 mM PMSE, Roche cOmplete protease inhibitor cocktail) and again rotated for 15 minutes at 4°C. The cell suspension was sonicated with 20 pulses a 30 seconds (Branson Sonifier 250, output control 4, duty cycle 50%, 90 seconds cooldown between pulses). 100 µl cell suspension, containing 1x10⁶ cells, were used per immunoprecipitation. Subsequent sample handling was done with the EZ-ChIP kit (#17-371, Millipore) according to the manufacturer's instructions. Immunoprecipitation was performed with an antibody against RNA-Polymerase II, mouse IgG (both included with the kit) and an antibody against p-Stat3 Y705 (#9145, Cell-Signaling). Precipitation of the promoter regions was analyzed by PCR, utilizing the primers 5hMULEChIP (GAGGGAAGGAGTCTGGATAAT) and 3hMULEChIP (CCGATC-TAGGTGTCTAGAGC) or 5hMULEUSChIP (GCATTGTATGATTGTACTACAGTT-TAT) and 3hMULEUSChIP (CCAGCGGTTACTCTTCTAAGAA) for MULE, resulting in 296 bp and 180 bp fragments respectively; 5hPP1CACHIP (AGTGCGCTG GGAATTCAGCC) and 3hPP1CACHIP (GAGGCGCCCAGCCCTGT) for PP1CA, resulting in a 307 bp fragment.

2.7 Bio molecular methods - proteins

2.7.1 Extraction of proteins from mouse organs

To extract proteins from mouse organs the organs were covered with 1 ml organ lysis buffer and homogenized with an Ultraturrax. Afterwards the homogenate was centrifuged for one hour at 13.000 rpm at 4 °C. After centrifugation the clear medial of the three phases was collected in a new tube and the protein content was measured by the Warburg-method. The absorption of the protein solution was measured at 280 nm.

2.7.2 Mitochondrial isolation

Isolation of mitochondria from mouse liver was done as previously described (Frezza et al., 2007). Mitochondria were washed twice in MSB (400mM manitol, 10 mM KH₂PO₄, 50 mM Tris-HCl, 0.5% BSA, pH 7.2) and protein concentrations were determined (BCA Protein Assay, Pierce).

2.7.3 Bax treatment of isolated mitochondria

100 μ g mitochondria, supported with 1 mM ATP, 5 μ M rotenone and 4 mM MgCl₂, were treated with increasing amounts of recombinant Bax protein (0.25 μ g-1 μ g; SignalChem) for 30' at 30°C. After centrifugation (20.000g), the supernatant was further analyzed by western-blot for release of cytochrome c.

2.7.4 SDS-polyacrylamid-gelelectrophorese (SDS-PAGE)

For electrophoretic separation by means of their molecular size protein samples were diluted with organ lyses buffer and 4x SDS-loading dye to a concentration of 10 μ g/ μ l. The samples were heated to 98 °C for 5 minutes to denaturate proteins for SDS binding. In the experiments 10 % and 15 % resolving gels where used.

2.7.5 Western blot analysis

For determination of protein levels, proteins, which were separated by SDS-PAGE, were transferred onto a Polyvinylidendifluorid (PVDF)-membrane. A Semi-Dry-Blot and a Wet-Blot were used bevor blocking for one hour in 1 % Western Blocking reagent in TBS-T. First antibody were diluted in 0,5 % Western Blocking reagent (antibody dilution in 2.13) and incubated at 4° C over night. The second antibody were diluted in 0.5 % Western Blocking reagent (antibody dilution in 2.13) and incubated for one hour at room temperature. For detection 10 ml ECL was used for one minute. For reuse membrane was stripped 30 minutes in a 56°C water bath with stripping solution.

Table 2.13: **Antibodies**

Antibodies	Type	Dilution	Supplier
α -panAKT	rabbit, monoclonal	1:1000	Cell Signaling, Danvers, USA
α -Bax	rabbit, monoclonal	1:500	Santacruz, Heidelberg, Germany
α -Bcl-2	rabbit, monoclonal	1:500	Santacruz, Heidelberg, Germany
α -BclXL	rabbit, monoclonal	1:500	Santacruz, Heidelberg, Germany
α -Calnexin	rabbit, monoclonal	1:1000	Millipore, Germany
α -cleaved Caspase 3	rabbit, monoclonal	1:500	Cell Signaling, Danvers, USA
α -Complex II	rabbit, monoclonal	1:1000	Santacruz, Heidelberg, Germany
α -GSK-3 β	rabbit, monoclonal	1:1000	Cell Signaling, Danvers, USA
α -Mcl-1	rabbit, monoclonal	1:2000	Rockland Inc., Gilbertsville, PA 19525
α -pAKT	rabbit, monoclonal	1:1000	Cell Signaling, Danvers, USA
α -pERK 1/2	rabbit, monoclonal	1:1000	Cell Signaling, Danvers, USA
α -pGSK-3 β	rabbit, monoclonal	1:1000	Cell Signaling, Danvers, USA
α -pJNK	rabbit, monoclonal	1:1000	Cell Signaling, Danvers, USA

Continued on next page

Table 2.13 – continued from previous page

Antibodies	Type	Dilution	Supplier
α -Puma	rabbit, monoclonal	1:1000	Cell Signaling, Danvers, USA
α -pStat-3	rabbit, monoclonal	1:1000	Cell Signaling, Danvers, USA
α -rabbit, conjugated with peroxi- dase	rabbit, monoclonal	1:1000	Sigma, Deisenhofen, Germany

2.7.6 Quantitation of western blots

Quantitation of Western blots was done by Quantity One by BioRad.

2.8 Bio molecular methods - serum

2.8.1 Serum analysis

For evaluation of liver injury, levels of glutamate-pyruvate-transaminase and aspartate-aminotransferase in the serum were measured. Level of triglycerides and cholesterol were also measured. Serum was diluted 1:10 in 0.9 % NaCl and measured in the central lab of the university hospital in cologne.

2.8.2 Insulin, Leptin, IL-6 and TNF α enzyme linked immuno sorbent assay (ELISA)

Serum insulin (mouse Insulin ELISA, Crystal Chem inc.), serum leptin (mouse leptin ELISA, Crystal Chem inc.), serum TNF α (Quantikine Immunoassay ELISA TNF α , R&D Systems), serum sgp130 (Glucoprotein 130 ELISA kit, antikörper-online), serum IL-6 sR (Quantikine Immunoassay ELISA IL-6, R&D Systems) and serum IL-6 (Quantikine Immunoassay ELISA IL-6, R&D Systems) were determined by ELISA according to manufacturer's instructions.

2.8.3 AKT, Caspase-3, GSK-3 β and PI3K activity assay

AKT activity (AKT kinase assay, Cell Signaling), Caspase-3 activity, (PathScan Cleaved Caspase 3 ELISA kit, Cell Signaling), GSK-3 β activity (GSK-3 β activity assay, sigma-aldrich) and PI3K activity (PI-3 kinase activity assay, echolon) in liver lysates were determined according to manufacturer's instructions.

2.9 Immunohistochemical and immunofluorescence stainings

2.9.1 HE staining

For histological analysis of tumors formalin-fixed liver specimen were embedded in paraffin, 2 μ m sections were cut and stained with hematoxylin/eosin, distase-PAS silver stain.

2.9.2 Mcl-1 staining

For histological analysis of tumors formalin-fixed liver specimen were embedded in paraffin, 2 μ m sections were cut and stained Mcl-1 (abcam #32087) or HUWE1 (lifespan biosciences LS-B1359/20559).

2.9.3 Oil Red O staining

Steatosis was detected by Oil-Red-O Staining.

2.9.4 TUNEL staining

Tissue sections were used for DeadEnd Fluorometric TUNEL system (Promega) according to manufacturer's instructions to detect apoptotic cells. TUNEL-positive cells were quantified using image tool software (Imaris 7.0).

2.9.5 Ki67 staining

To detect proliferating cells, tissue sections were stained with Ki67 antibody (#ab15580, Abcam) and donkey α -rabbit red (#711-025-152, Jackson). Ki67-positive cells were quantified using image tool software (Imaris 7.0).

2.10 Cell culture

2.10.1 Dual Luciferase Reporter Assay

For the pTE-MULE-Luc reporter construct generation, 1000 bp promoter region of the mouse MULE locus were inserted downstream of the luciferase open reading frame in the pTE-Luc plasmid instead of the CAG promoter (Jordan et al., 2011, Nat Cell Biol). The MULE promoter was amplified by PCR with the primers 5MluMule (ACGCGTTATAGACTTTAGGCAGTCTG) and 3NcoMule (CCATGGTTTTTCAGTTTTCTGATTAAAG). Insertion into pTE-Luc was performed with NcoI-MluI double restriction. HepG2 were plated on 6-well plates and transfected with 1000 ng DNA (100 ng pRL-Null and 900 ng pTE-MULE-Luc) using the Lipofectamine 2000 transfection reagent (Invitrogen) according to the manufacturer's instructions. 24 hours after transfection, cells were pre-incubated with 20 μ M STAT3 inhibitor for 1 hr (#573099, Calbiochem, DMSO vehicle, manufacturer's instruction were followed) and subsequently stimulated with 250 ng/ml human IL-6 (#200-006, PeproTech) over night respectively. Dual luciferase reporter assays were performed 48 hours after transfection using a luciferase Assay System (Promega) according to the manufacturer's instructions.

2.10.2 Primary murine hepatocyte and human hepatoma culture

Anesthetized mice were perfused 5 min with EBSS solution (Gibco, 4155-048) containing 0.5 mM EGTA via vena cava. Subsequently, mice were perfused with 50 ml EBSS (Gibco, 24010-043) containing 10 mM Hepes, 15 mg Collagenase Type II (Worthington) and 2 mg Trypsin inhibitor (Sigma). After perfusion, the liver was transferred in 10 ml ice cold EBSS (Gibco, 24010-043) containing 10 mM Hepes. The gall bladder was removed and hepatocytes were released from the cell association. The cell suspension was pressed through a sieve with 20 μ m mesh and centrifuged for 5 min. at 500 g at 4°C. The supernatant was removed and the pellet was washed twice in William's E medium (PPA) containing 6 ml sodium pyruvate, 6 ml non essential amino acids, 30 ml FCS, 6 ml Penicillin/Streptomycin, 6 ml Glucose, 11,5 ml Hepes and 6 ml Glutamate. Subsequently, the pellet was dissolved in 10 ml medium. The viability should be >90 %, as determined by trypan blue dye exclusion. 3×10^6 hepatocytes isolated from control and IL-6R α -deficient animals were incubated with medium containing DEN at different concentrations for 48 h. Subsequently, mitochondria and cytosolic fractions were separated and used for Western blot analysis. Hep3B cells were cultivated in hepatocyte medium and stimulated with 50 ng human IL-6 (#200-006, PeproTech) for the indicated time. Neutralization of hIL-6R using anti-IL-6R α (R&D mab227) and control rat IgG (BD 554682) was performed prior to IL-6 treatment.

3 Results

3.1 Obesity increases basal hepatic Stat-3 activation and impairs acute IL-6 responsiveness

To determine the molecular mechanisms mediating the recently published protection to HCC development in IL-6 deficient mice, the IL-6R α was genetically deleted in the entire body and a DEN induced liver carcinogenesis approach was applied. Furthermore, DEN injected mice were exposed to HFD feeding to determine the effect of obesity to HCC development.

IL-6 initiates downstream signaling by binding to the IL-6 receptor (IL-6R), whose activation results in multiple downstream signaling events in the liver such as activation of the JAK/Stat-3 and MAPK/ERK pathways [Heinrich *et al.*, 1998].

To determine the time course of IL-6 activated downstream signaling 8 weeks old control mice were injected with 50 ng IL-6 / g BW intravenously (*i.v.*) and phosphorylation of several downstream targets were analysed by western blot after 30, 60, 120 and 240 minutes. Phosphorylation of Stat-3 appeared already 30 min post IL-6 injection and progressively declined thereafter whereas activation of ERK-1/2 was detected after 30 min and progressively increasing up to 120 min (Fig. 3.1A). However, IL-6 injection did not activate hepatic JNK phosphorylation in control mice (Fig. 3.1A). Next, dose response to IL-6 in lean control mice was measured by western blotting. IL-6-induced Stat-3 activation in liver was detected upon injection of 3 ng IL-6/g body weight (BW) intraperitoneally (*i.p.*), but increased dose-dependently when 30 and 300 ng IL-6/g BW were applied (Fig. 3.1B). To investigate the effect of obesity to IL-6 signaling lean and obese

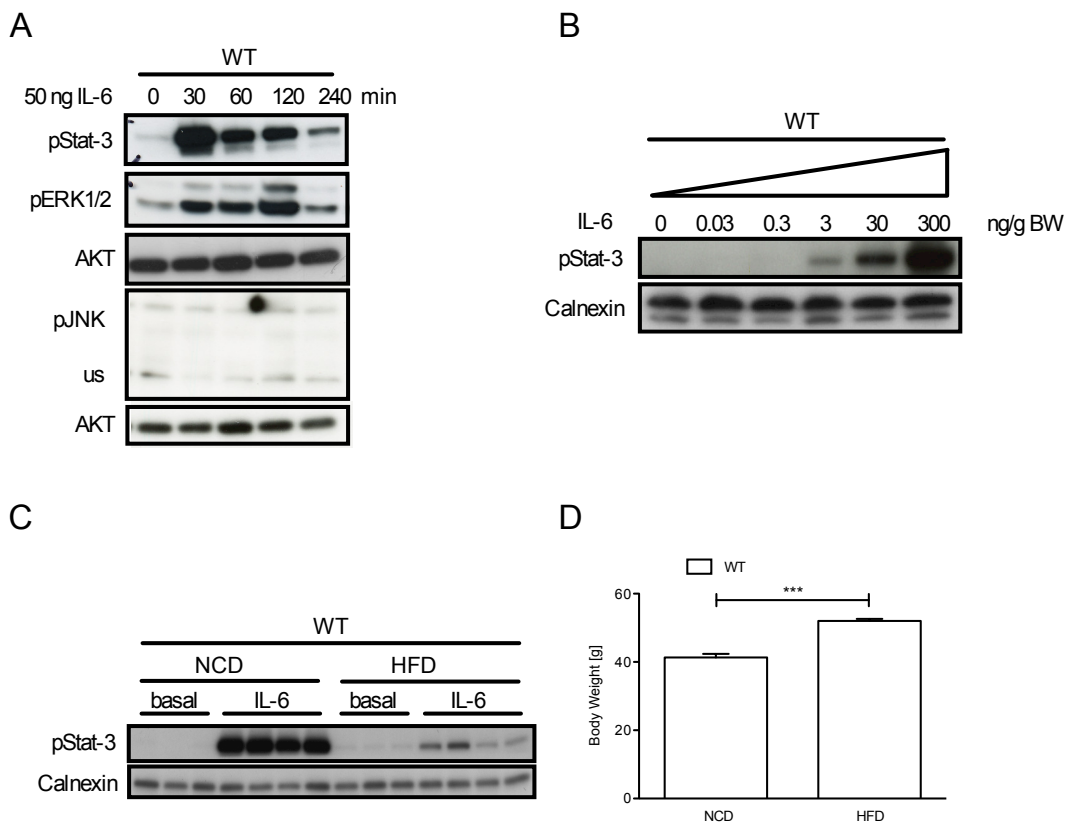


Figure 3.1: **IL-6 responsiveness in control mice on NCD and HFD**

(A) Western blot analysis using pStat-3, pERK1/2, pJNK, and AKT antibodies on liver tissue from 8 wk C57BL/6 mice after *i.v.* injection of 50 ng IL-6 / g BW. (B) Western blot analysis using pStat-3 and Calnexin antibodies on liver tissue from control mice 1 hr post *i.p.* injection of indicated amounts of IL-6 / g BW. (C) Western blot analysis using pStat-3 and Calnexin antibodies on liver tissue of control mice exposed to NCD or HFD for 23 wk before and 1 hr after *i.p.* injection of 50 ng IL-6 / g BW. (D) Body weight of from C at 24 wk (n=7). Displayed values are means \pm S.E.M.; *, $p \leq 0.05$; **, $p \leq 0.01$; ***, $p \leq 0.001$ versus control. Data in B/C/D produced in collaboration with Jan Mauer.

mice were injected with 50 ng IL-6/g BW *i.p.* (Fig. 3.1C/D). While injection of 50 ng IL-6/g BW induced a strong hepatic activation of Stat-3 in lean mice, this response was massively decreased in obese control mice (Fig. 3.1C/D). Furthermore, livers from obese mice displayed increased Stat-3 activation in the basal state compared to lean mice (Fig. 3.1C/D).

Collectively, these experiments demonstrate that obesity increases basal Stat-3 activation and impairs the responsiveness to acute IL-6 stimulation.

3.2 Generation of IL-6R α knock out mice

To address the role of IL-6R α signaling in the development of hepatocellular carcinoma (HCC), a conditional IL-6R α mouse strain, in which exon 2 and 3 of the IL-6R α gene are flanked by loxP sites (IL-6R $\alpha^{fl/fl}$) was used [Wunderlich *et al.*, 2010]. These mice were crossed to mice expressing the Cre recombinase under the control of the human cytomegalovirus minimal promoter [Schwenk *et al.*, 1995] and further intercrossed with siblings leading to mice lacking the IL-6R α in the whole body (IL-6R $\alpha^{\Delta/\Delta}$). IL-6R $\alpha^{fl/fl}$ mice served as controls throughout experiments.

Determination of efficiency and specificity was previously shown in "The role of Interleukin 6 in the development of hepatocellular carcinoma" [Gruber, 2009]. As this work is mainly focussed on the liver, determination of efficiency in the liver was tested again (Fig. 3.2A). qPCR of liver cDNA of control and IL-6R $\alpha^{\Delta/\Delta}$ mice revealed the absence of IL-6R α expression in IL-6R $\alpha^{\Delta/\Delta}$ mice (Fig. 3.2A). Accordingly, IL-6 was unable to induce hepatic Stat-3 phosphorylation in IL-6R $\alpha^{\Delta/\Delta}$ mice, whereas CNTF potently induced Stat-3 activation in these mice (Fig. 3.2B). Furthermore, Lipopolysaccharide (LPS) was observed to potently induce Stat-3 and JNK phosphorylation in control mice but failed to activate Stat-3 in IL-6R $\alpha^{\Delta/\Delta}$ mice (Fig. 3.2B). Thus, the experiments revealed successful inactivation of IL-6 signaling in IL-6R $\alpha^{\Delta/\Delta}$ mice while the responsiveness to alternative IL-6R α -independent gp130 cytokines such as CNTF remained unaltered.

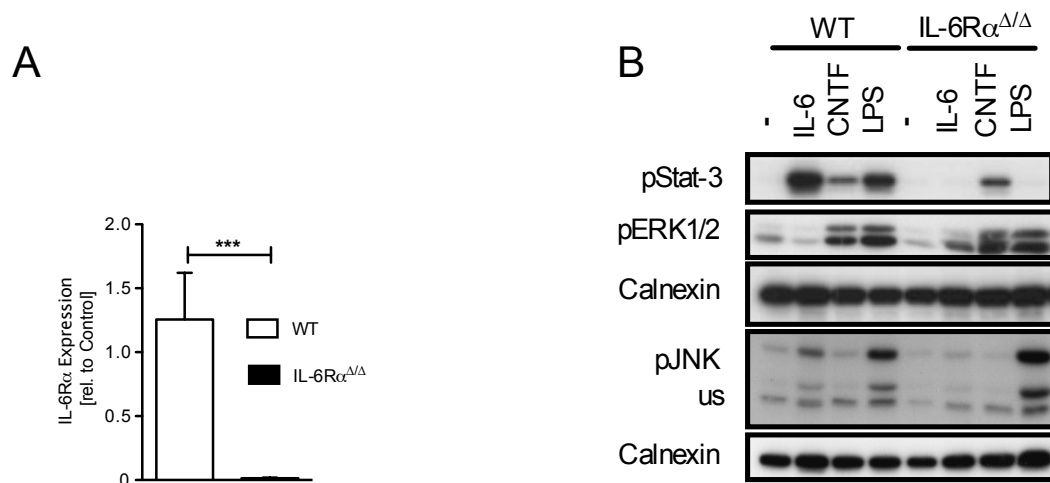


Figure 3.2: **Inactivation of IL-6 signaling in IL-6R $\alpha^{\Delta/\Delta}$**

(A) qPCR of IL-6R α in livers of control and IL-6R $\alpha^{\Delta/\Delta}$ mice (n=6). (B) Western blot analysis using pStat-3, pERK1/2, pJNK and Calnexin antibodies on liver tissue from 8 wk old control and IL-6R $\alpha^{\Delta/\Delta}$ mice after *i.p.* injection of 100 ng IL-6, CNTF and LPS. Displayed values are means \pm S.E.M.; *, $p \leq 0.05$; **, $p \leq 0.01$; ***, $p \leq 0.001$ versus control. Data in B produced in collaboration with Justus Ackermann

3.3 HFD causes obesity in control and IL-6R $\alpha^{\Delta/\Delta}$ mice in the DEN-induced HCC model

HCC represents a classical inflammation-induced cancer entity whose development is significantly enhanced under obese conditions. To investigate whether IL-6R α deficiency affects HCC development under lean and obese conditions, male IL-6R $\alpha^{f1/f1}$ and IL-6R $\alpha^{\Delta/\Delta}$ mice were injected with 25 mg/kg BW DEN *i.p.* at 15 days of age and separated after weaning in cohorts fed either a NCD or HFD for 8 month. To examine whether IL-6R α deficiency has an impact on metabolic or inflammatory state different parameters were measured.

As expected, upon HFD feeding body weight was significantly increased both in IL-6R $\alpha^{\Delta/\Delta}$ and control mice compared to mice fed a NCD, whereas no differences could be detected between genotypes both upon NCD and HFD feeding (Fig. 3.3A).

Previously, it could be shown that HFD feeding impairs glucose metabolism [Xu *et al.*, 2003]. Hence, an *i.p.* Glucose tolerance test was performed, demonstrating an unaltered glucose clearance between IL-6R $\alpha^{\Delta/\Delta}$ and control mice under NCD conditions (Fig. 3.3B). Upon HFD feeding both IL-6R $\alpha^{\Delta/\Delta}$ and control mice revealed an impaired glucose tolerance, which was further impaired in IL-6R $\alpha^{\Delta/\Delta}$ under HFD conditions (Fig. 3.3B).

Recent studies could demonstrate that serum Insulin and Leptin levels increase upon HFD feeding [Benoit *et al.*, 2004]. Therefore concentrations of circulating Insulin and Leptin were measured by ELISA. Insulin levels were significantly increased upon HFD feeding both in IL-6R $\alpha^{\Delta/\Delta}$ and control mice, but no differences could be detected between the genotypes neither on NCD nor on HFD conditions (Fig. 3.3C). Upon NCD no difference in Leptin levels could be detected between the genotypes, whereas HFD feeding led to a significant increase of serum Leptin levels both in IL-6R $\alpha^{\Delta/\Delta}$ and control mice (Fig. 3.3D). While the Leptin level in control mice was doubled under HFD conditions compared to NCD conditions,

IL-6R $\alpha^{\Delta/\Delta}$ mice revealed a 4-fold increase in serum Leptin level upon HFD compared to NCD feeding (Fig. 3.3D), suggesting a greater impairment in Leptin signaling.

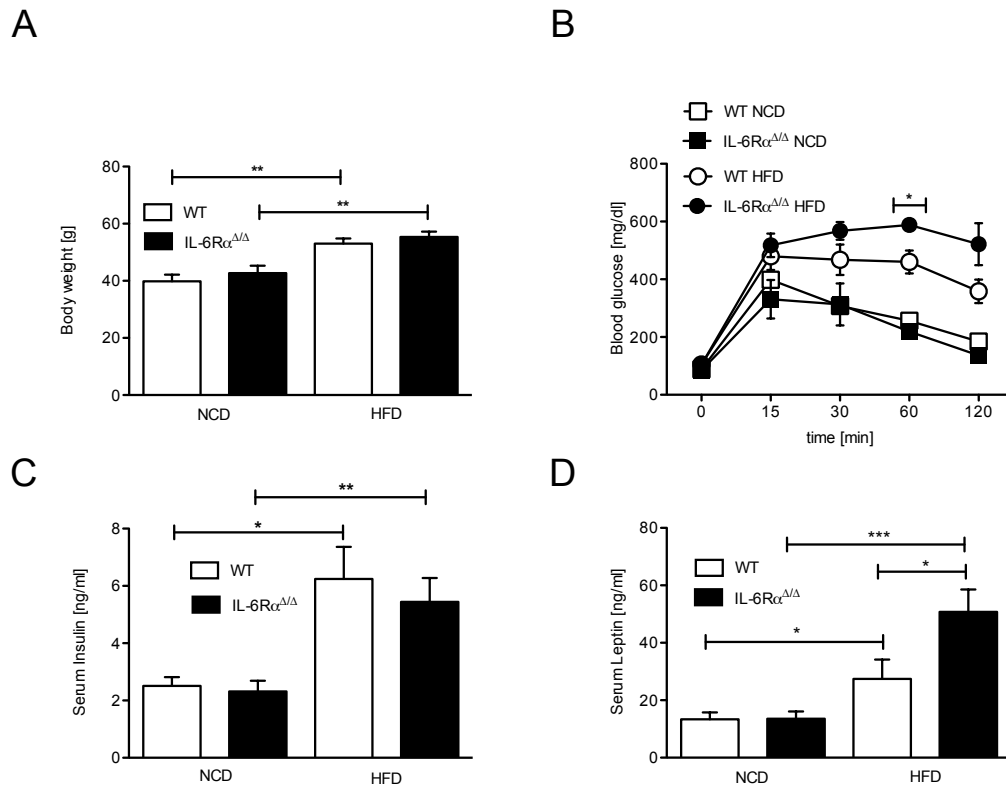


Figure 3.3: **Metabolic parameters of control and IL-6R $\alpha^{\Delta/\Delta}$ mice**

(A) Weight determination of 8 month (mo) control and IL-6R $\alpha^{\Delta/\Delta}$ mice (n=15) injected with 25 mg/kg DEN at 15 days of age and exposed to NCD or HFD after weaning. (B) Glucose tolerance test of 8 mo control and IL-6R $\alpha^{\Delta/\Delta}$ mice (n=6). Examination of (C) serum Insulin concentrations and (D) serum Leptin concentrations by ELISA from DEN-injected 8 mo control and IL-6R $\alpha^{\Delta/\Delta}$ mice (n=8). Displayed values are means \pm S.E.M.; *, $p \leq 0.05$; **, $p \leq 0.01$; ***, $p \leq 0.001$ versus control.

To determine the inflammatory status of IL-6R $\alpha^{\Delta/\Delta}$ and control mice after 8 month of tumor development, inflammatory cytokine such as TNF α and IL-6 were measured by ELISA in the sera of these mice. As expected, TNF α and IL-6 measurements revealed a significant increase in sera of control and IL-6R $\alpha^{\Delta/\Delta}$ mice under obese conditions (Fig. 3.4A/B). These data demonstrate that IL-6R α deficiency did not affect HFD-induced obesity or obesity-induced insulin resis-

tance and inflammation.

However, alternative modulation of IL-6 type cytokine signaling by trans- signaling of soluble receptors such as sIL-6R α and sgp130 might also contribute to obesity-induced inflammation. Therefore, sIL-6R α and sgp130 levels in the serum were measured. While in IL-6R α -deficient mice the sIL-6R α was consistently at the lowest detection level but unchanged between control mice on both diets (Fig. 3.4C), sgp130 was reduced in obese IL-6R $\alpha^{\Delta/\Delta}$ mice compared to lean but comparable to control animals upon HFD feeding (Fig. 3.4D).

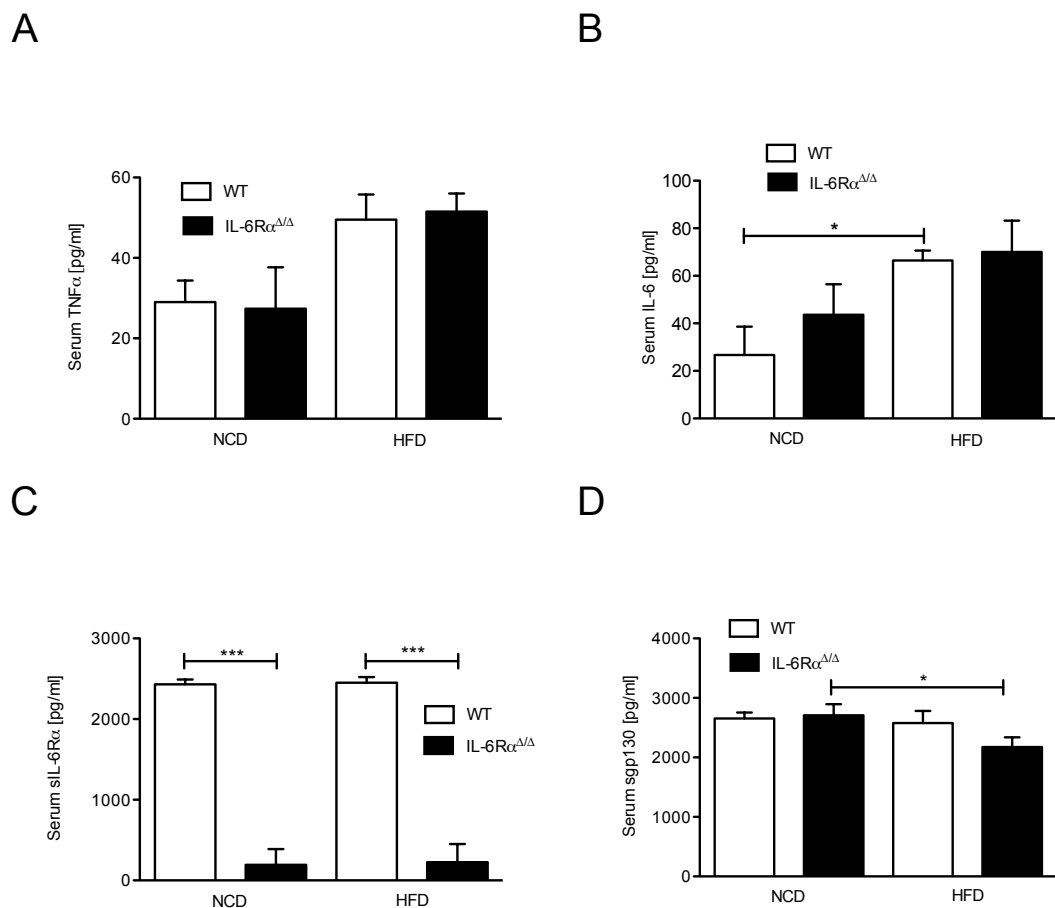


Figure 3.4: **Inflammatory signaling in control and IL-6R $\alpha^{\Delta/\Delta}$ mice**

(A) Examination of serum TNF α concentrations, (B) serum IL-6 concentrations, (C) serum sIL-6R concentrations and (D) serum sgp130 concentrations by ELISA from DEN-injected 8 mo control and IL-6R $\alpha^{\Delta/\Delta}$ mice (n=8). Displayed values are means \pm S.E.M.; *, $p \leq 0.05$; **, $p \leq 0.01$; ***, $p \leq 0.001$ versus control.

To determine the extent of circulating lipids in the blood, cholesterol and triglyceride level in the serum were measured by ELISA. Cholesterol measurement revealed similar levels in control and IL-6R $\alpha^{\Delta/\Delta}$ mice fed either a NCD or HFD before DEN treatment (Fig. 3.5A). After DEN treatment Cholesterol levels significantly increased upon NCD feeding but remained similar between genotypes (Fig. 3.5A). Upon HFD feeding no alteration could be detected in both genotypes compared to untreated mice (Fig. 3.5A). Triglyceride level were completely unaltered between treated and non-treated mice, diets and genotypes (Fig. 3.5B). To determine lipid accumulation in the liver Oil red O staining of liver sections of the four different groups of mice were performed. These stainings revealed increased hepatic fat storage in mice exposed to HFD feeding in both control and IL-6R $\alpha^{\Delta/\Delta}$ animals, although lipid accumulation was comparable between the genotypes (Fig. 3.5C).

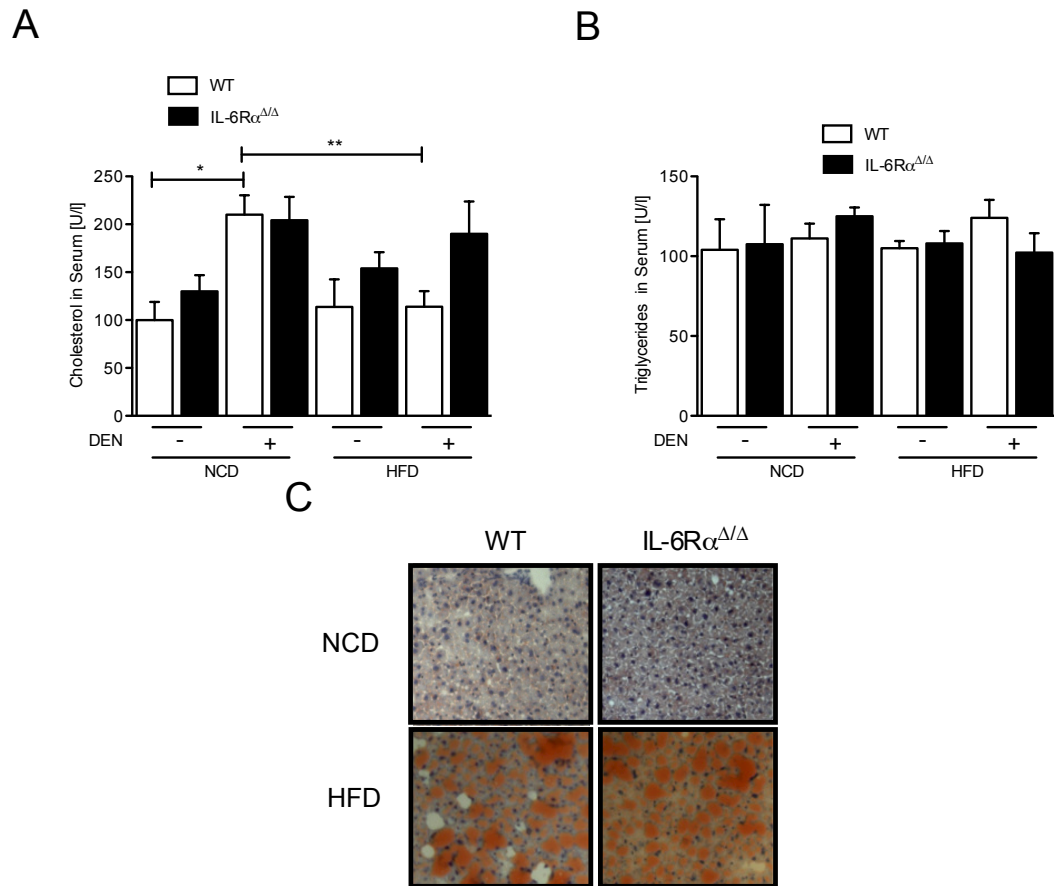


Figure 3.5: Extent of lipid burden in control and IL-6R $\alpha^{\Delta/\Delta}$ mice. (A) Examination of serum Cholesterol level and (B) serum Triglyceride level of untreated (-) or DEN-injected (+) 8 mo control and IL-6R $\alpha^{\Delta/\Delta}$ mice (n=10). (C) Oil Red O stainings of liver sections obtained from DEN-injected 8 mo control and IL-6R $\alpha^{\Delta/\Delta}$ mice. Displayed values are means \pm S.E.M.; *, $p \leq 0.05$; **, $p \leq 0.01$; ***, $p \leq 0.001$ versus control.

Taken together, these experiments demonstrate that HFD exposure causes similar levels of obesity in both control and IL-6R $\alpha^{\Delta/\Delta}$ mice upon DEN induction.

3.4 IL-6R α deficiency protects against DEN-induced liver carcinogenesis but obesity abrogates this effect and promotes HCC development

In the next step tumor development in 8 mo-old DEN-treated control and IL-6R $\alpha^{\Delta/\Delta}$ mice, that had been exposed to either NCD or HFD feeding, was investigated by visual inspection. Male control NCD-fed mice developed approximately 30 macroscopically visible liver tumors (Fig. 3.6A/B). 66% of the tumors were smaller than 2 mm (Fig. 3.4C) whereas 33% reached a size of more than 2 mm (Fig. 3.6D). Similar to IL-6-deficient mice [Naugler *et al.*, 2007], IL-6R α deficiency potently protected mice from developing DEN-induced HCC upon NCD feeding (Fig. 3.6A/B). In line with previous studies, obesity increased tumor burden to approximately 50 tumors in control mice (Fig. 3.6A/B) [Park *et al.*, 2010]. However, when IL-6R $\alpha^{\Delta/\Delta}$ mice were fed a HFD, the protective effect of IL-6R α deficiency on HCC development was abrogated as DEN treatment induced significantly higher tumor numbers in these mice comparable to control mice upon HFD feeding (Fig. 3.6A/B).

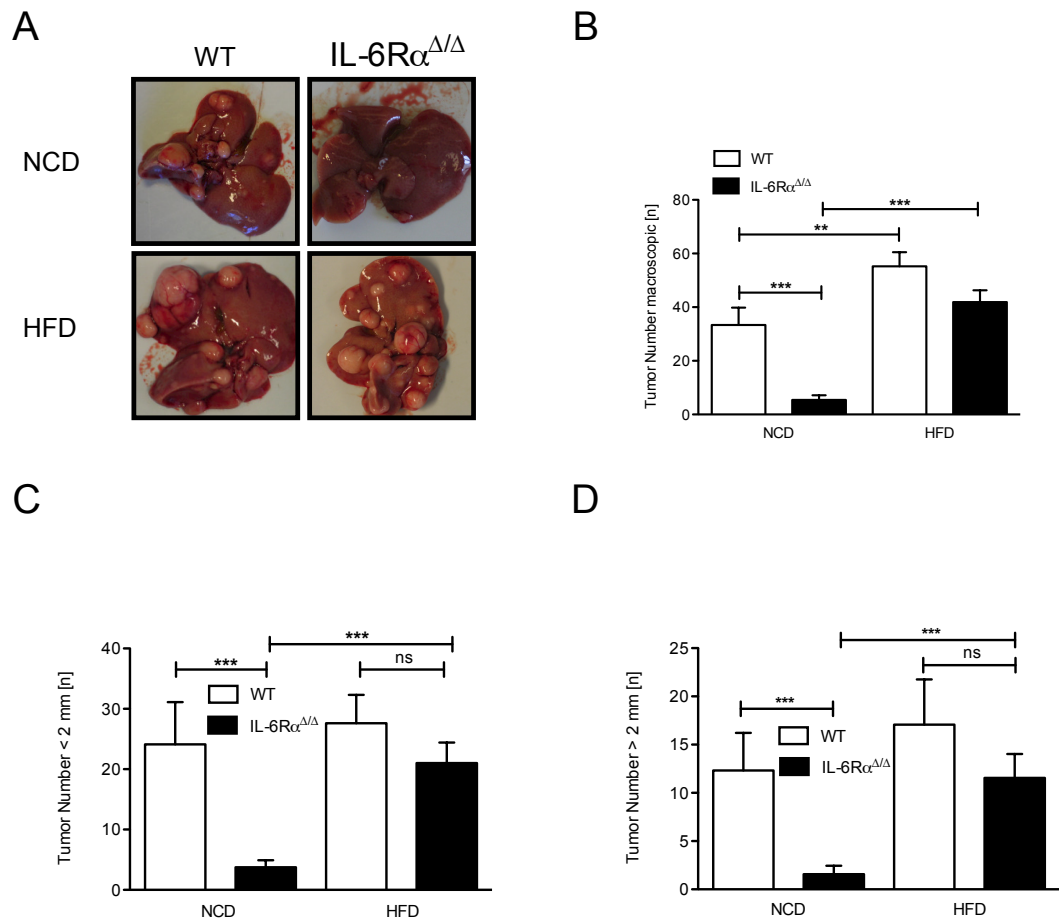


Figure 3.6: **Tumor burden macroscopic in control and IL-6R $\alpha^{\Delta/\Delta}$ mice**

(A) Livers of 8 mo control and IL-6R $\alpha^{\Delta/\Delta}$ mice injected with 25 mg/kg BW DEN at 15 days of age. (B) Quantitation of macroscopic tumor multiplicity determined by visual inspection in DEN-injected 8 mo control and IL-6R $\alpha^{\Delta/\Delta}$ mice (n=15). (C) Enumeration of tumor number for < 2 mm and (D) > 2 mm as determined by visual inspection of DEN-injected 8 mo control and IL-6R $\alpha^{\Delta/\Delta}$ mice (n=15). Displayed values are means \pm S.E.M.; *, $p \leq 0.05$; **, $p \leq 0.01$; ***, $p \leq 0.001$ versus control.

Recent studies observed that HFD feeding induce hepatic steatosis that can eventually lead to the development of liver damage and steatohepatitis that in turn might result in HCC development [Fujii *et al.*, 2013; Nault & Zucman-Rossi, 2010]. As an indirect indicator of liver damage, the activity of the liver aspartate transaminase (AST) and alanin transaminase (ALT) were measured in the serum of IL-6R $\alpha^{\Delta/\Delta}$ and control mice fed either a NCD and or HFD before and after DEN treatment. AST and ALT levels were not significantly different in the serum

of control and IL-6R $\alpha^{\Delta/\Delta}$ mice fed either a NCD or HFD before DEN treatment (Fig. 3.7A/B). After DEN treatment serum AST levels significantly increased to the same extent both in control and IL-6R $\alpha^{\Delta/\Delta}$ mice fed on either a NCD or HFD, whereas no significant difference could be detected between NCD and HFD fed mice (Fig.3.7A/B). Serum ALT levels of control and IL-6R $\alpha^{\Delta/\Delta}$ mice revealed no increase after DEN treatment neither on NCD nor on HFD feeding (Fig. 3.7A/B).

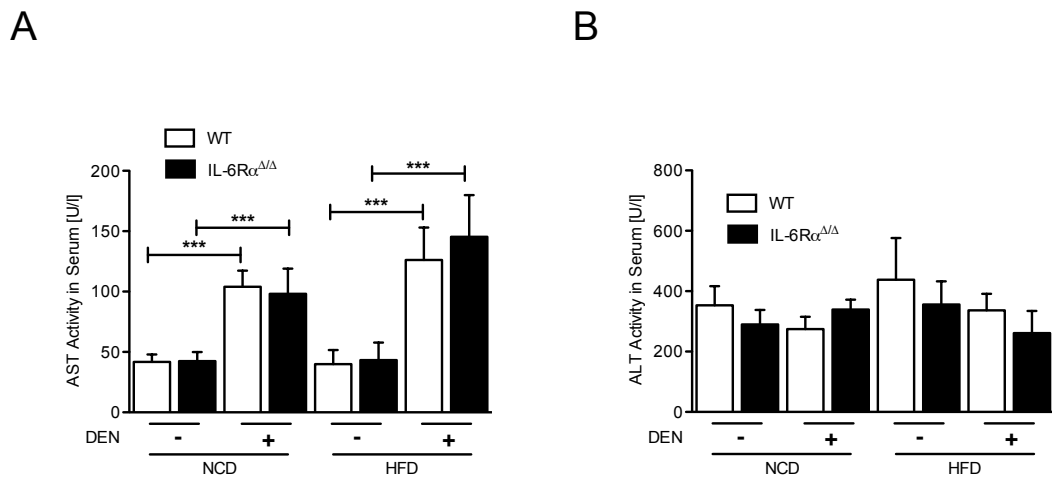


Figure 3.7: **Liver damage of control and IL-6R $\alpha^{\Delta/\Delta}$ mice**

(A) Determination of serum AST and (B) ALT activity of untreated (-) or DEN-injected (+) 8 mo control and IL-6R $\alpha^{\Delta/\Delta}$ mice (n=6). Displayed values are means \pm S.E.M.; *, $p \leq 0.05$; **, $p \leq 0.01$; ***, $p \leq 0.001$ versus control.

Histological investigation of HE-stained liver sections confirmed that NCD-fed IL-6R $\alpha^{\Delta/\Delta}$ mice had significantly decreased number of HCC foci when compared to NCD-fed control mice (Fig. 3.8A/B). Although, this difference was not as large as observed upon macroscopic inspection (Fig.3.8A/B). Strikingly, HFD feeding restored the carcinogenic capability of DEN in IL-6R $\alpha^{\Delta/\Delta}$ animals as the number of HCC foci increased to the same extent in control mice and IL-6R $\alpha^{\Delta/\Delta}$ mice upon HFD feeding (Fig. 3.8A/B). Furthermore, tumor size was significantly decreased in IL-6R $\alpha^{\Delta/\Delta}$ mice upon NCD feeding compared to control, whereas this effect was blunted upon HFD feeding demonstrated by similar increase in tumor size in both IL-6R $\alpha^{\Delta/\Delta}$ and control mice upon HFD feeding (Fig. 3.8C).

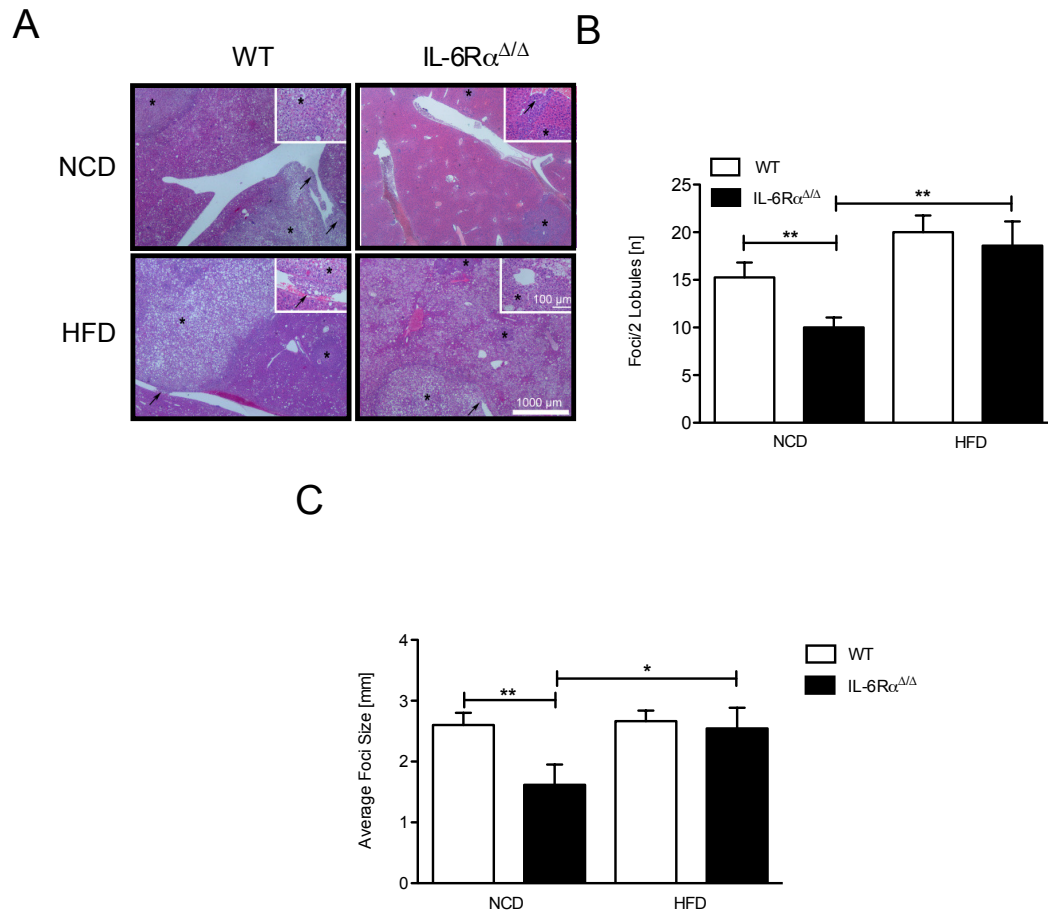


Figure 3.8: **Tumor burden microscopic in control and IL-6R $\alpha^{\Delta/\Delta}$ mice**
 (A) HE-stained sections of livers from DEN-injected 8 mo control and IL-6R $\alpha^{\Delta/\Delta}$ mice. Asterisks indicate tumor foci; arrows indicate tumorous blood vessel infiltrates. (B) Quantitation of tumor number per 2 lobules counted on liver sections from 8 mo control and IL-6R $\alpha^{\Delta/\Delta}$ mice (n=15). (C) Quantitation of tumor size measured in the big liver lobe of DEN-injected 8 mo control and IL-6R $\alpha^{\Delta/\Delta}$ mice (n=15). Displayed values are means \pm S.E.M.; *, $p \leq 0.05$; **, $p \leq 0.01$; ***, $p \leq 0.001$ versus control. Data produced in collaboration with Beate Straub.

Moreover, the extent of inflammation as assessed by quantitation of infiltrating immune cells was significantly reduced in livers of IL-6R $\alpha^{\Delta/\Delta}$ mice compared to control mice exposed to a NCD feeding (Fig. 3.9A). In contrast, HFD feeding significantly increased liver inflammation in both control and IL-6R $\alpha^{\Delta/\Delta}$ animals (Fig. 3.9A). Previous studies demonstrated that HFD feeding induce hepatocyte steatosis that can result in HCC development [Fujii *et al.*, 2013; Nault & Zucman-

Rossi, 2010]. Livers of IL-6R $\alpha^{\Delta/\Delta}$ mice fed a NCD revealed a significantly reduced extent of steatosis compared to control mice (Fig. 3.9B). Upon HFD feeding the extent of steatosis significantly increased both in control and IL-6R $\alpha^{\Delta/\Delta}$ mice (Fig. 3.9B). Additionally necrotic hepatocytes per two lobules were counted which revealed no significant alterations between the genotypes but a significant increase of necrotic cells in both control and IL-6R $\alpha^{\Delta/\Delta}$ mice upon HFD feeding (Fig. 3.9C). Fibrosis is often connected with the development of liver cancer, therefore the extent of fibrosis was determined by score [Luedde & Schwabe, 2011]. Similar to the analysis of necrotic cells no significant alteration could be detected between the genotypes but an significant higher extent of fibrosis upon HFD feeding in both control and IL-6R $\alpha^{\Delta/\Delta}$ mice (Fig. 3.9D).

Taken together, these data demonstrate that obesity promotes HCC development and progression and renders tumor development independent of IL-6R α signaling, thus abrogating the protective function of IL-6R α deficiency under NCD conditions.

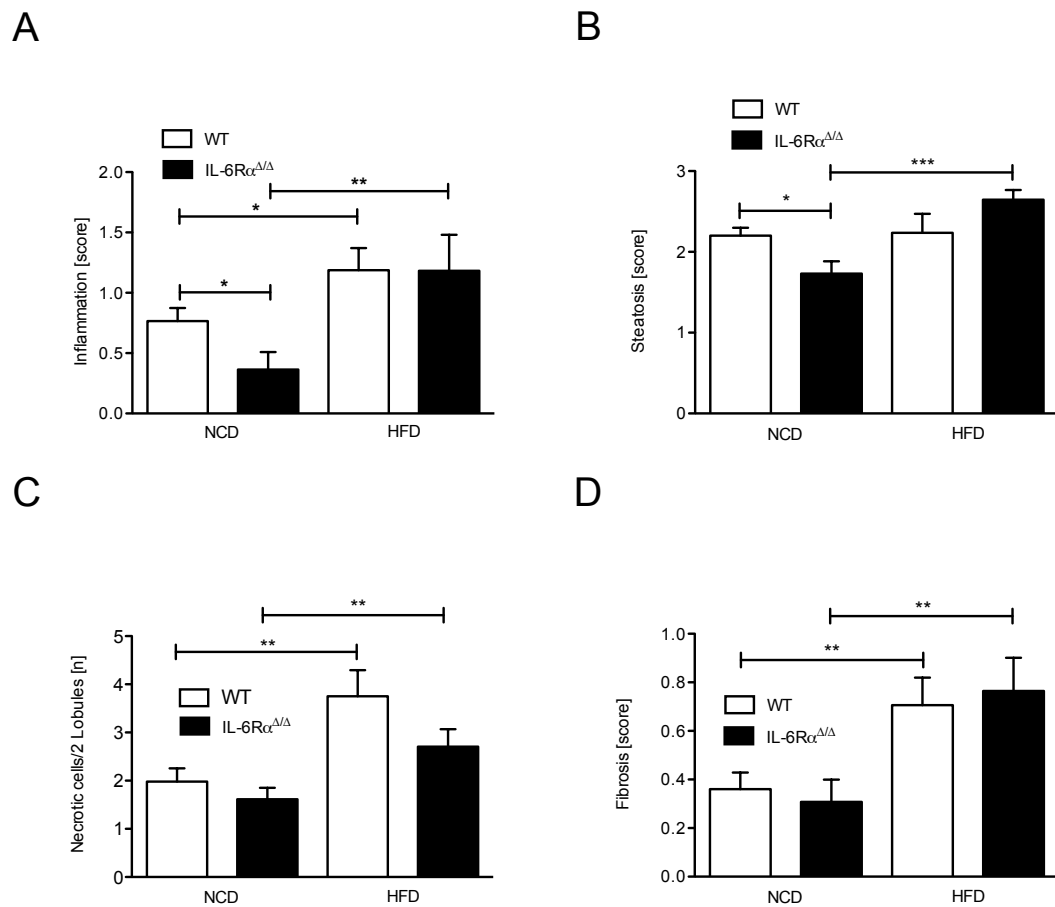


Figure 3.9: Liver status of control and IL-6R $\alpha^{\Delta/\Delta}$ mice

(A) Quantitation of inflammation measured in the big liver lobe of DEN-injected 8 mo control and IL-6R $\alpha^{\Delta/\Delta}$. 1 = mild inflammation (mild portal inflammation, 3-5 single cell necrosis, no grouped necrosis); 2 = moderate inflammation (moderate portal inflammation, 6-9 single cell necrosis, 1 grouped necrosis); 3 = severe inflammation (severe portal inflammation, more than 10 single cell necrosis, more than 1 grouped necrosis) (n=15). (B) Quantitation of steatosis measured in the big liver lobe of DEN-injected 8 mo control and IL-6R $\alpha^{\Delta/\Delta}$. 1 = 0 - 10%; 2 = 11 - 50 %; 3 = above 50 % (C) Quantitation of necrotic cells measured in the big liver lobe of DEN-injected 8 mo control and IL-6R $\alpha^{\Delta/\Delta}$. (D) Quantitation of fibrosis measured in the big liver lobe of DEN-injected 8 mo control and IL-6R $\alpha^{\Delta/\Delta}$. 1 = increased portal connective tissue; 2 = early formation of septa (n = 15) Displayed values are means \pm S.E.M.; *, p \leq 0.05; **, p \leq 0.01; ***, p \leq 0.001 versus control. Data produced in collaboration with Beate Straub.

3.5 Obesity and IL-6 increase HCC development through the inhibition of mitochondrial apoptosis

IL-6 is a potent survival signal in hepatocytes and deletion of its receptor may thus affect hepatocyte death signaling and survival. Therefore, apoptosis in the livers of the different cohorts of mice was examined by determining the presence of active Caspase 3 by activity assay and western blot analysis.

Increased Caspase 3 activation was detected in liver lysates derived from NCD fed IL-6R $\alpha^{\Delta/\Delta}$ mice upon DEN treatment compared to control mice upon NCD feeding (Fig. 3.10A). Upon HFD feeding Caspase 3 activation was significantly decreased in IL-6R α deficient mice compared to NCD-fed IL-6R $\alpha^{\Delta/\Delta}$ mice (Fig. 3.10A). In comparison to control mice upon HFD feeding, IL-6R $\alpha^{\Delta/\Delta}$ mice exhibited the same level of Caspase 3 activation upon HFD feeding (Fig. 3.10A). In line with this observation, Caspase 3 cleavage and thereby activation increased upon a single DEN injection in livers of IL-6R $\alpha^{\Delta/\Delta}$ mice compared to control mice (Fig. 3.10B). These data were further substantiated by the finding that AST and ALT activity was elevated in sera of IL-6R $\alpha^{\Delta/\Delta}$ mice upon acute DEN injection which is another strong indicator of liver damage (Fig. 3.10C/D).

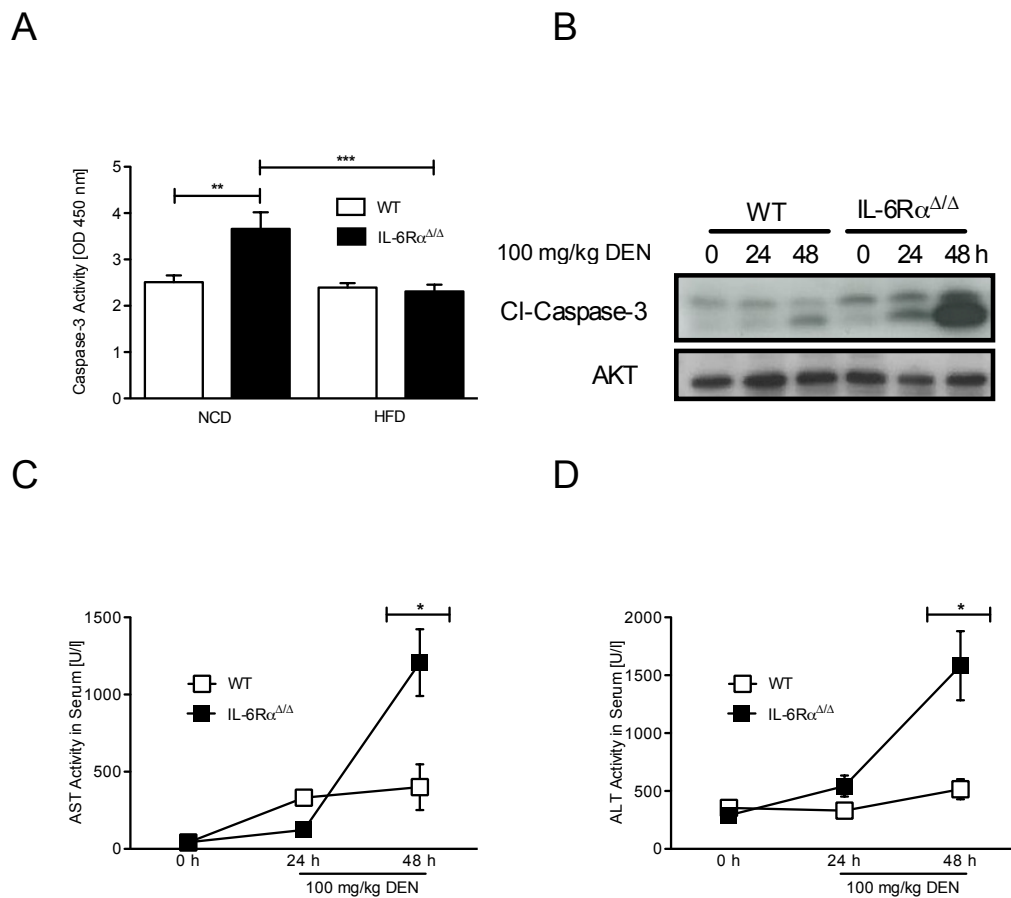


Figure 3.10: **Caspase 3 activity in the liver of control and IL-6R $\alpha^{\Delta/\Delta}$ mice**

(A) Determination of Caspase 3 activity using an ELISA based assay on liver lysates from DEN-injected 8 mo control and IL-6R $\alpha^{\Delta/\Delta}$ mice (n=5). (B) Western blot analysis using cleaved Caspase 3 and AKT antibodies on liver tissue from 8 wk control and IL-6R $\alpha^{\Delta/\Delta}$ mice fed on a NCD sacrificed at the indicated time points after a 100 mg/kg DEN injection. (C) Determination of serum AST and (D) ALT activity to assess liver damage in 8 wk control and IL-6R $\alpha^{\Delta/\Delta}$ mice fed on a NCD sacrificed at the indicated time points after a 100 mg/kg BW DEN injection (n=6). Displayed values are means \pm S.E.M.; *, $p \leq 0.05$; **, $p \leq 0.01$; ***, $p \leq 0.001$ versus control.

Mitochondria represent a central sensory organelle that can respond to DNA damage by mitochondrial outer membrane permeabilization. This process is tightly regulated by Bcl-2 protein family members such as Bcl-2, Bcl-XL, Mcl-1, Bak or Bax [Brunelle & Letai, 2009]. To experimentally address whether increased DEN-induced apoptosis in IL-6R $\alpha^{\Delta/\Delta}$ mice is a consequence of enhanced mitochondrial apoptotic response, freshly isolated mitochondria from livers of naive

control and IL-6R $\alpha^{\Delta/\Delta}$ mice were incubated with increasing amounts of recombinant Bax protein and the release of mitochondrial Cytochrome C was measured by western blot analysis. These data demonstrated that mitochondria derived from the livers of IL-6R $\alpha^{\Delta/\Delta}$ mice were more susceptible to recombinant Bax as indicated by the increased release of Cytochrome C in the cytosol compared to control mice (Fig. 3.11A). Consistently, IL-6R α -deficient hepatocytes demonstrated concentration dependent cytosolic Cytochrome C levels in response to DEN (Fig. 3.11B) as well as increased Cytochrome C at the mitochondria itself (Fig. 3.11C).

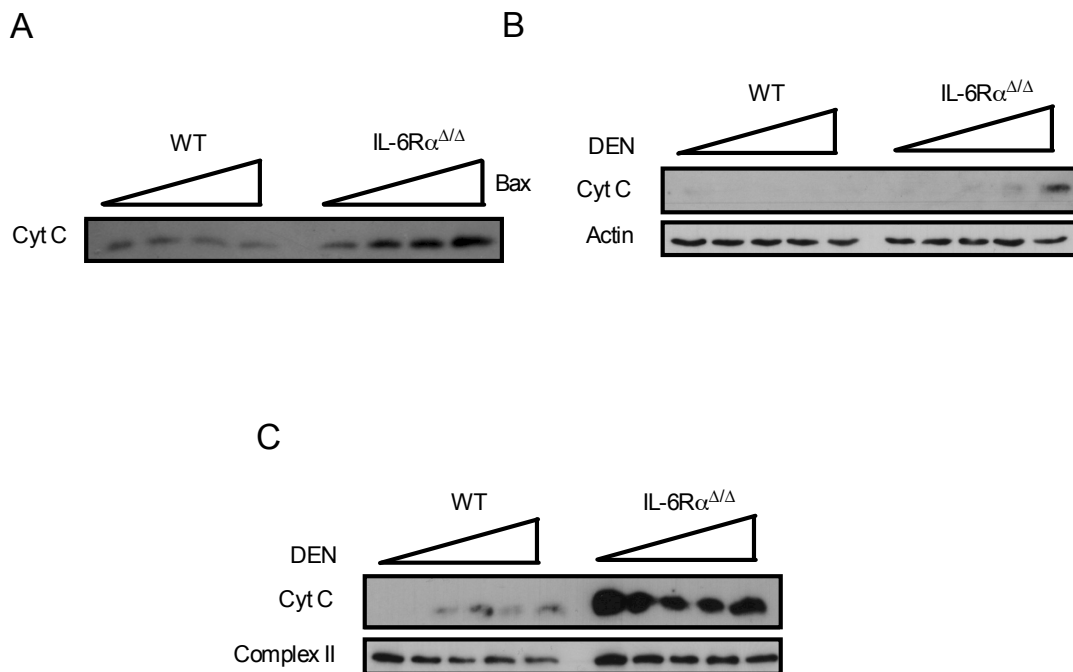


Figure 3.11: Cytochrome C release from mitochondria of control and IL-6R $\alpha^{\Delta/\Delta}$ mice
(A) Cytochrome C release of isolated mitochondria after treatment with increasing concentrations of recombinant Bax. Mitochondria were isolated from naive 8 wk control and IL-6R $\alpha^{\Delta/\Delta}$ mice fed a NCD. **(B)** Western blot analysis using Cytochrome C and Actin antibodies of cytosolic extracts and **(C)** western blot analysis using Cytochrome C and Complex II antibodies of mitochondrial extracts from primary hepatocytes isolated from 8 wk control and IL-6R $\alpha^{\Delta/\Delta}$ mice that were treated with 0, 0.25, 0.5, 1 and 5 mM DEN for 48h in culture. Displayed values are means \pm S.E.M.; *, $p \leq 0.05$; **, $p \leq 0.01$; ***, $p \leq 0.001$ versus control. Data produced in collaboration with Jens Seeger.

The balance between anti- and pro-apoptotic members of the Bcl-2 protein family regulates mitochondrial outer membrane permeabilization and the efflux of Cytochrome C in response to cellular damage [Brunelle & Letai, 2009]. The presence of the anti-apoptotic Bcl-2 protein family members Mcl-1, Bcl-2 and Bcl-XL at mitochondria has been shown to prevent Cytochrome C release, whereas pro-apoptotic protein such as Bax and Bak stimulate Cytochrome C release [Brunelle & Letai, 2009]. To investigate levels of these proteins at the mitochondria of tumor bearing mice, western blot analysis of mitochondrial extracts, derived from tumor livers of the different cohorts of mice, was performed. This analysis revealed a reduced mitochondrial level of Mcl-1 in NCD fed IL-6R $\alpha^{\Delta/\Delta}$ mice (Fig. 3.12A). Interestingly, upon HFD-feeding mitochondrial Mcl-1 protein levels were restored to comparable levels in both control and IL-6R α -deficient animals (Fig. 3.12A). Furthermore, levels of pro-apoptotic protein Bax were decreased in NCD fed IL-6R $\alpha^{\Delta/\Delta}$ mice, an effect which was blunted upon HFD feeding (Fig. 3.12A). Notably, protein levels of Bcl-2, Bcl-XL and Bak were not altered between diets and genotypes (Fig. 3.12A). Strikingly, qPCR analyses of liver cDNA of the four different groups of mice revealed that the transcriptional levels of the corresponding genes were largely unaltered (Fig. 3.12B) suggesting that the reduced Mcl-1 content of mitochondria of IL-6R $\alpha^{\Delta/\Delta}$ mice might be caused by a posttranslational regulatory mechanism.

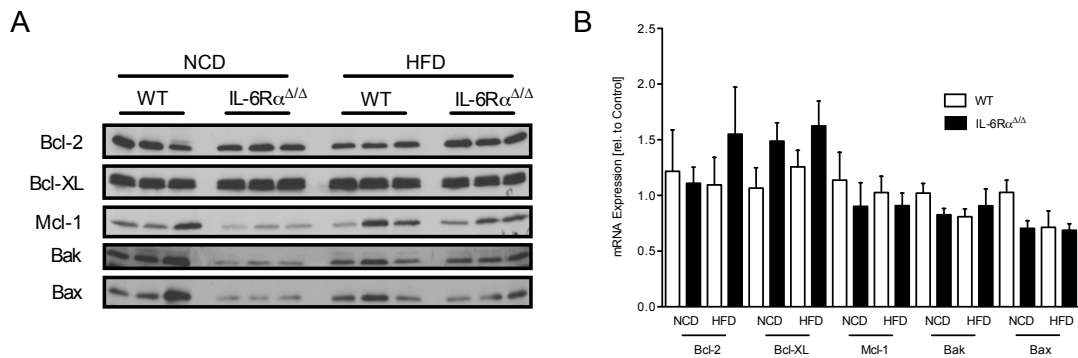


Figure 3.12: **Pro- and anti-apoptotic proteins in tumor livers of control and IL-6R $\alpha^{\Delta/\Delta}$ mice**

(A) Western blot analysis using Bcl-2, Bcl-XL, Mcl-1, Bak, Bax and Complex II antibodies on isolated mitochondria from DEN-injected 8 mo control and IL-6R $\alpha^{\Delta/\Delta}$ mice. (B) qPCR of Bcl-2, Bcl-XL, Mcl-1, Bak and Bax on livers from DEN-injected 8 mo control and IL-6R $\alpha^{\Delta/\Delta}$ mice. (n=6). Displayed values are means \pm S.E.M.; *, $p \leq 0.05$; **, $p \leq 0.01$; ***, $p \leq 0.001$ versus control. Data in A produced in collaboration with Jens Seeger.

Consistent with these data, immunohistochemistry of mouse liver sections demonstrated that HFD feeding significantly increased Mcl-1 protein abundance in the tumors independent from IL-6R α signaling (Fig. 3.13A/B). The tumor-associated Mcl-1 expression was further analyzed in dissected HCCs from livers of the different groups of mice by western blot analysis, demonstrating that Mcl-1 protein was decreased in HCCs of lean IL-6R α deficient mice compared to control tumors, while HFD feeding increased Mcl-1 protein in HCCs of control as well as IL-6R $\alpha^{\Delta/\Delta}$ mice (Fig. 3.13C).

Hepatocyte apoptosis has been shown to result in compensatory proliferation of adjacent hepatocytes to cause HCC development [Bisgaard *et al.*, 1998]. IL-6 is thought to contribute to hepatocyte proliferation and DEN administration to male mice results in IL-6 production that depends on IKK β in myeloid cells, most likely the resident macrophages called Kupffer cells (KCs) Naugler *et al.* [2007]; Cressman *et al.* [1996]. In addition to preventing IL-6 production, ablation of IKK β in myeloid cells prevents compensatory proliferation, one of the main tumor promoting mechanisms [Maeda *et al.*, 2005].

Thus, proliferation of hepatocytes in response to DEN-induced apoptosis in lean control and IL-6R $\alpha^{\Delta/\Delta}$ mice (Fig. 3.13D) was compared. While hepatocyte proliferation was significantly reduced in IL-6R α -deficient animals without DEN injection, DEN-induced compensatory proliferation of hepatocytes was comparable between control and IL-6R $\alpha^{\Delta/\Delta}$ mice as examined through quantitation of Ki67-positive hepatocytes in livers of these mice (Fig. 3.13D).

Taken together, these experiments demonstrate that under NCD conditions, loss of IL-6 signaling sensitizes hepatocytes to damage-induced apoptosis without impairments in compensatory proliferation. However, under HFD conditions, hepatocyte apoptosis is inhibited – even in the absence of IL-6R α signaling.

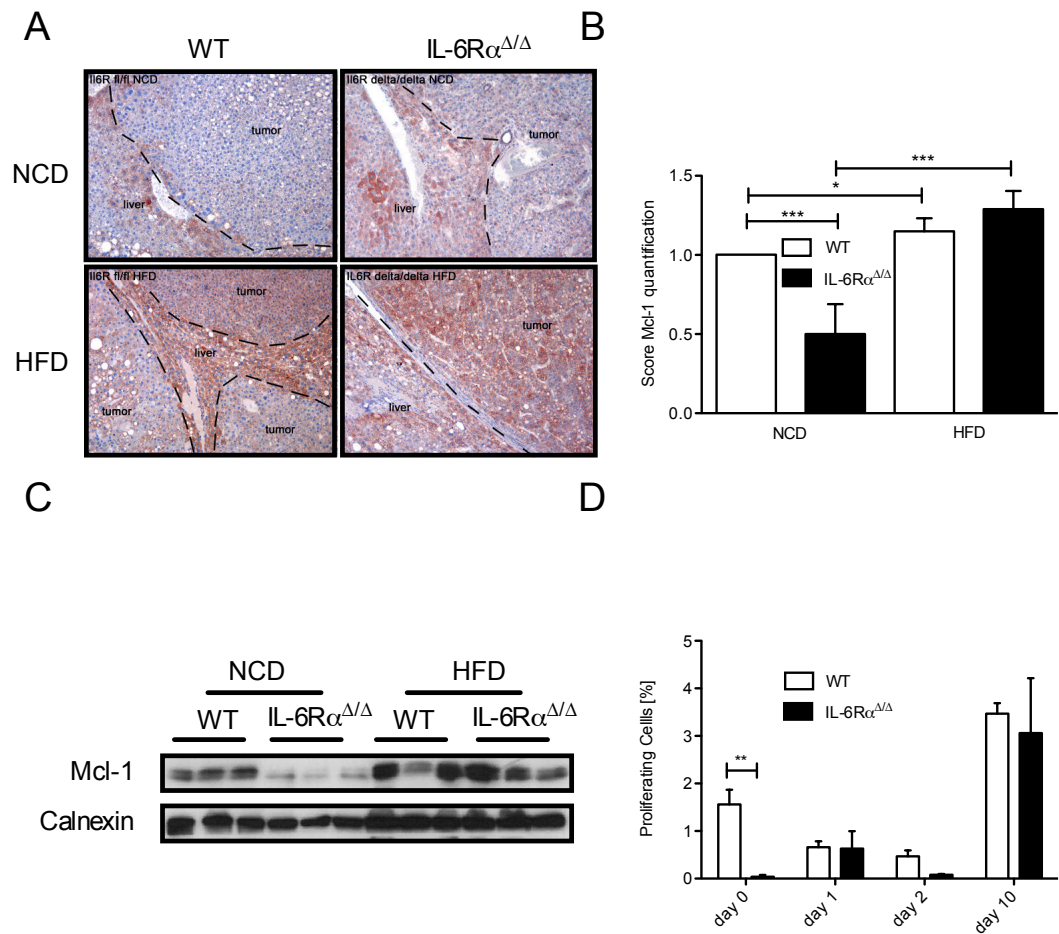


Figure 3.13: **Mcl-1 level in tumor livers of control and IL-6R $\alpha^{\Delta/\Delta}$ mice**

(A) Representative Mcl-1-stained sections of livers from DEN-injected 8 mo control and IL-6R $\alpha^{\Delta/\Delta}$ mice. Dashed lines discriminate tumor and normal liver tissue. (B) Quantitation of Mcl-1 in tumors of the big liver lobe from DEN-injected 8 mo control and IL-6R $\alpha^{\Delta/\Delta}$ mice. 0 = no Mcl-1, 1 = low Mcl-1, 2 = high Mcl-1 (C) Western blot analysis using Mcl-1 and Calnexin antibodies on isolated tumors from DEN-injected 8 mo control and IL-6R $\alpha^{\Delta/\Delta}$ mice. (D) Quantitation of proliferating, Ki67 positive hepatocytes in liver sections from 8 wk control and IL-6R $\alpha^{\Delta/\Delta}$ mice sacrificed at indicated time points upon injection of 100 mg/kg BW DEN (n=3). Displayed values are means \pm S.E.M.; *, $p \leq 0.05$; **, $p \leq 0.01$; ***, $p \leq 0.001$ versus control. Data in A/B produced in collaboration with Beate Straub.

3.6 GSK-3 β inhibition stabilizes Mcl-1 under obese conditions in HCC development

The Mcl-1 protein comprises a N-terminal PEST domain that is responsible for its short half-life. Among the numerous protein kinases that have been implicated in the regulation of Mcl-1, glycogen synthase kinase 3 β (GSK-3 β) is known to play a pivotal role in controlling Mcl-1 protein stability [Maurer *et al.*, 2006]. GSK-3 β is a serine/threonine protein kinase that, unlike most other protein kinases, is constantly active but becomes inactivated upon phosphorylation at serine residue 9 (S9) [Cross *et al.*, 1995]. Interestingly, inactivation of GSK-3 β via phosphorylation at S9 increases stabilization and accumulation of Mcl-1 protein and thereby prevents apoptosis [Ding *et al.*, 2007].

To address the role of GSK-3 β action in Mcl-1 protein stability during HCC development, GSK-3 β phosphorylation in the livers of DEN-treated control and IL-6R $\alpha^{\Delta/\Delta}$ mice upon either a NCD or HFD feeding was analysed. Remarkably, GSK-3 β was less phosphorylated at S9 and thus more active in livers of IL-6R $\alpha^{\Delta/\Delta}$ mice upon NCD feeding (Fig. 3.14A/B), whereas total GSK-3 β levels were unaltered (Fig. 3.14A/C). Interestingly, GSK-3 β S9 phosphorylation was reconstituted and Mcl-1 levels were increased in livers of IL-6R $\alpha^{\Delta/\Delta}$ mice when exposed to HFD feeding (Fig. 3.14A). Consistent with these observations, direct assessment of GSK-3 β kinase activity revealed significantly enhanced GSK-3 β activity in livers of IL-6R $\alpha^{\Delta/\Delta}$ mice fed a NCD but not a HFD (Fig. 3.14D).

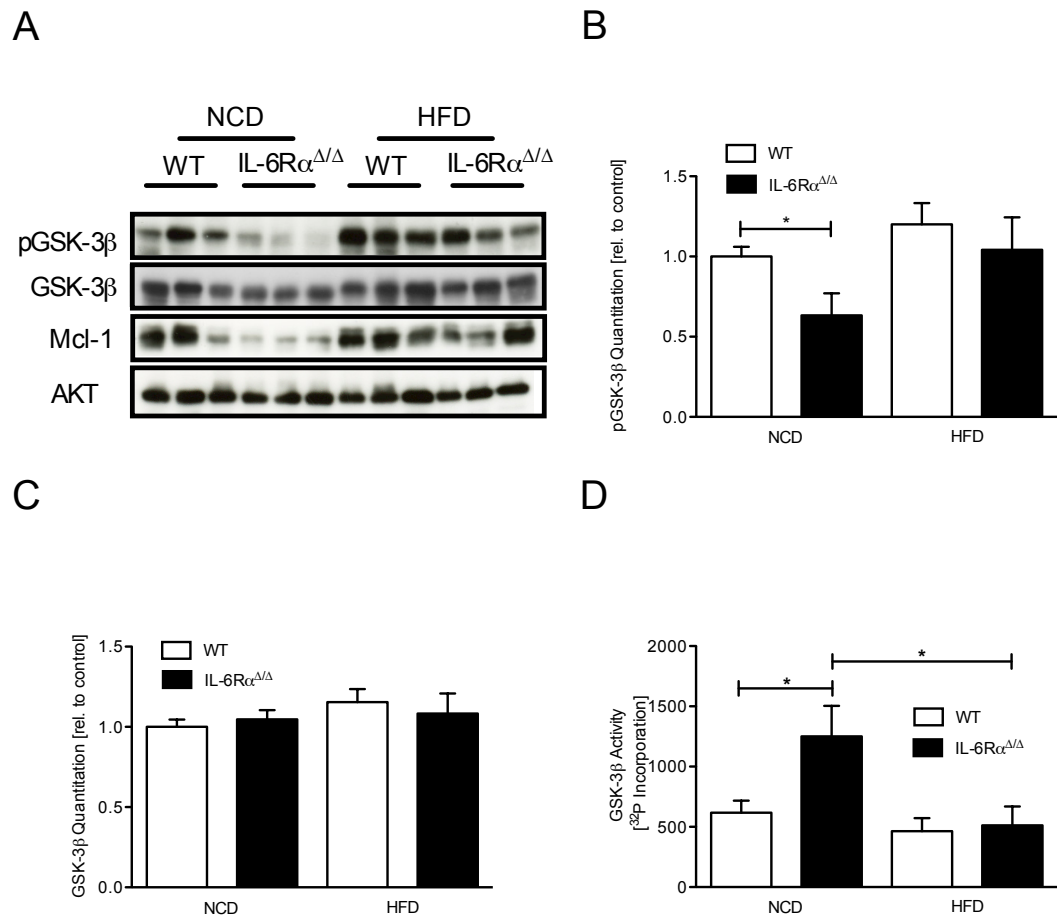


Figure 3.14: GSK-3 β activity in tumor livers of control and IL-6R $\alpha^{\Delta/\Delta}$ mice
(A) Western blot analysis using pGSK-3 β , GSK-3 β , Mcl-1, and AKT antibodies on liver tissue from DEN-injected 8 mo control and IL-6R $\alpha^{\Delta/\Delta}$ mice. **(B)** Quantitation of pGSK-3 β level and **(C)** GSK-3 β level from A relative to AKT levels. **(D)** Determination of GSK-3 β activity in liver lysates from DEN-injected 8 mo control and IL-6R $\alpha^{\Delta/\Delta}$ mice (n=5). Displayed values are means \pm S.E.M.; *, $p \leq 0.05$; **, $p \leq 0.01$; ***, $p \leq 0.001$ versus control.

Active GSK-3 β has been previously demonstrated to regulate apoptosis through expression of the BH3 only member PUMA that antagonizes Mcl-1 to sensitize for apoptosis [Charvet *et al.*, 2011]. Consistently, PUMA expression was 2-fold increased in tumor livers of IL-6R $\alpha^{\Delta/\Delta}$ mice but restored under obese conditions (Fig. 3.15A). However, in the initial phase of tumor development PUMA expression was unchanged between genotypes (Fig. 3.15B). Of note, expression of NOXA was unchanged between genotypes and diets (Fig. 3.15C).

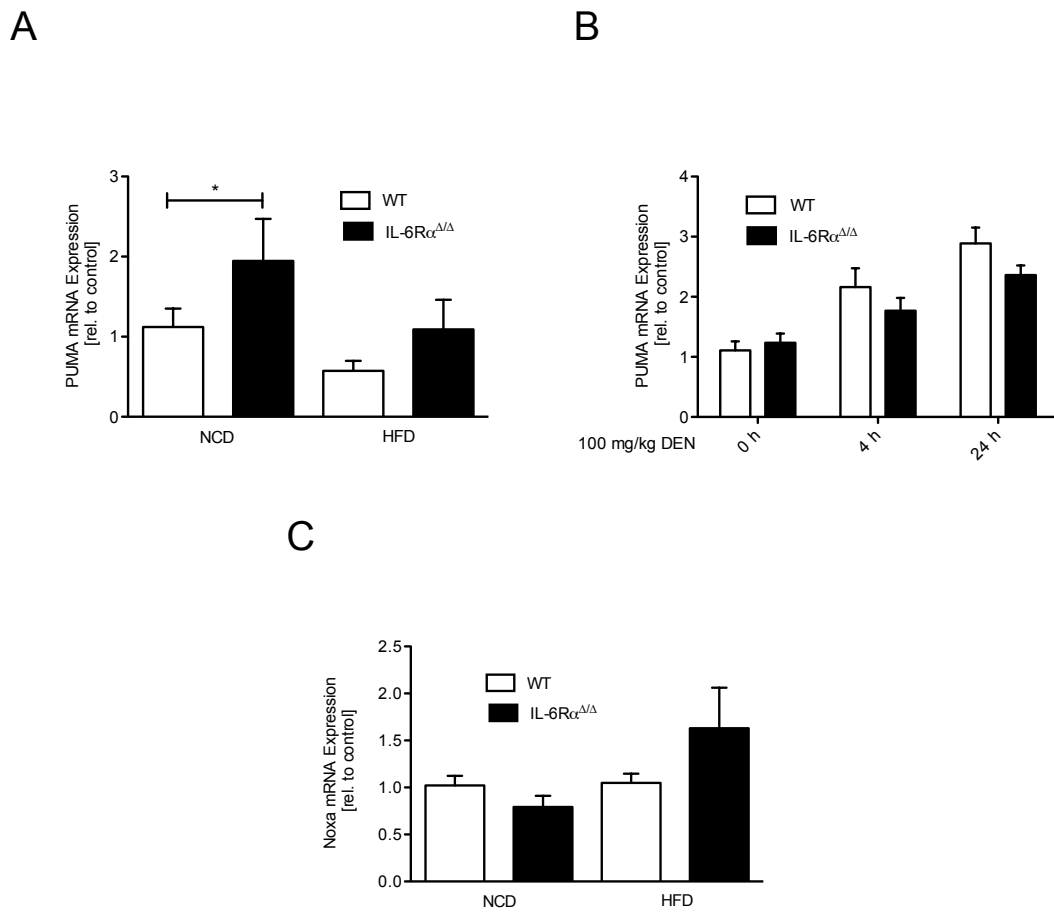


Figure 3.15: **Puma and Noxa in tumor livers of control and IL-6R $\alpha^{\Delta/\Delta}$ mice**

(A) qPCR of Puma in liver of DEN-injected 8 mo male control and IL-6R $\alpha^{\Delta/\Delta}$ mice (n=6). (B) qPCR of PUMA in livers of 8 wk control and IL-6R $\alpha^{\Delta/\Delta}$ mice after injection of 100 mg/kg DEN. (C) qPCR of Noxa in liver of DEN-injected 8 mo male control and IL-6R $\alpha^{\Delta/\Delta}$ mice (n=6). Displayed values are means \pm S.E.M.; *, $p \leq 0.05$; **, $p \leq 0.01$; ***, $p \leq 0.001$ versus control.

Next it was examined whether inactivation of GSK-3 β is a downstream event of IL-6 signaling that in turn stabilizes Mcl-1. Indeed, injection of IL-6 in control mice resulted in marked phosphorylation of GSK-3 β at S9 already 30 min post-injection, which was paralleled by increased Mcl-1 protein levels (Fig. 3.16A). To assess Mcl-1 stability and GSK-3 β activity in the initial phase of tumor development, control and IL-6R $\alpha^{\Delta/\Delta}$ animals were injected with 100 mg/kg DEN and Mcl-1 expression and GSK-3 β phosphorylation were determined.

While in control mice DEN injection stabilized Mcl-1 over time as a consequence of GSK-3 β inactivation, this response was largely blunted in IL-6R $\alpha^{\Delta/\Delta}$ mice (Fig. 3.16B). Mcl-1 stabilization as well as GSK-3 β phosphorylation in controls corresponded with circulating IL-6 that peaked 8 h upon injection (Fig. 3.16C), whereas Mcl-1 stability was maintained up to 24 h (Fig. 3.16B). However, PUMA protein levels peaked in both genotypes 24h after DEN injection (Fig. 3.16B) indicating that a GSK-3 β independent mechanisms control PUMA expression. Thus, abrogation of IL-6 signaling resulted in decreased Mcl-1 protein expression during the early phases of DEN-induced liver tumorigenesis (Fig. 3.16B).

To directly address the role of GSK-3 β regarding Mcl-1 stabilization in vivo, control mice were injected with adeno-associated viral vectors (AAV) expressing either GFP or a myc-tagged constitutive active GSK-3 β variant (GSK-3 β CA) harboring a serine to alanine substitution at position 9 of GSK-3 β (S9A). Western blot analysis using Mcl-1 antibody demonstrated that expression of GSK-3 β CA in livers of control mice reduced Mcl-1 protein level after DEN injection (Fig. 3.16D), similar to the observation in IL-6R $\alpha^{\Delta/\Delta}$ (Fig. 3.16B). In line with the previous experiment, PUMA levels failed to correlate with GSK-3 β activity under acute DEN conditions, although increased PUMA protein could be observed in non-injected GSK-3 β CA expressing livers (Fig. 3.16D).

These experiments therefore reveal that GSK-3 β inactivation by phosphorylation at S9 is required during the initial phases of tumorigenesis to stabilize Mcl-1 protein levels.

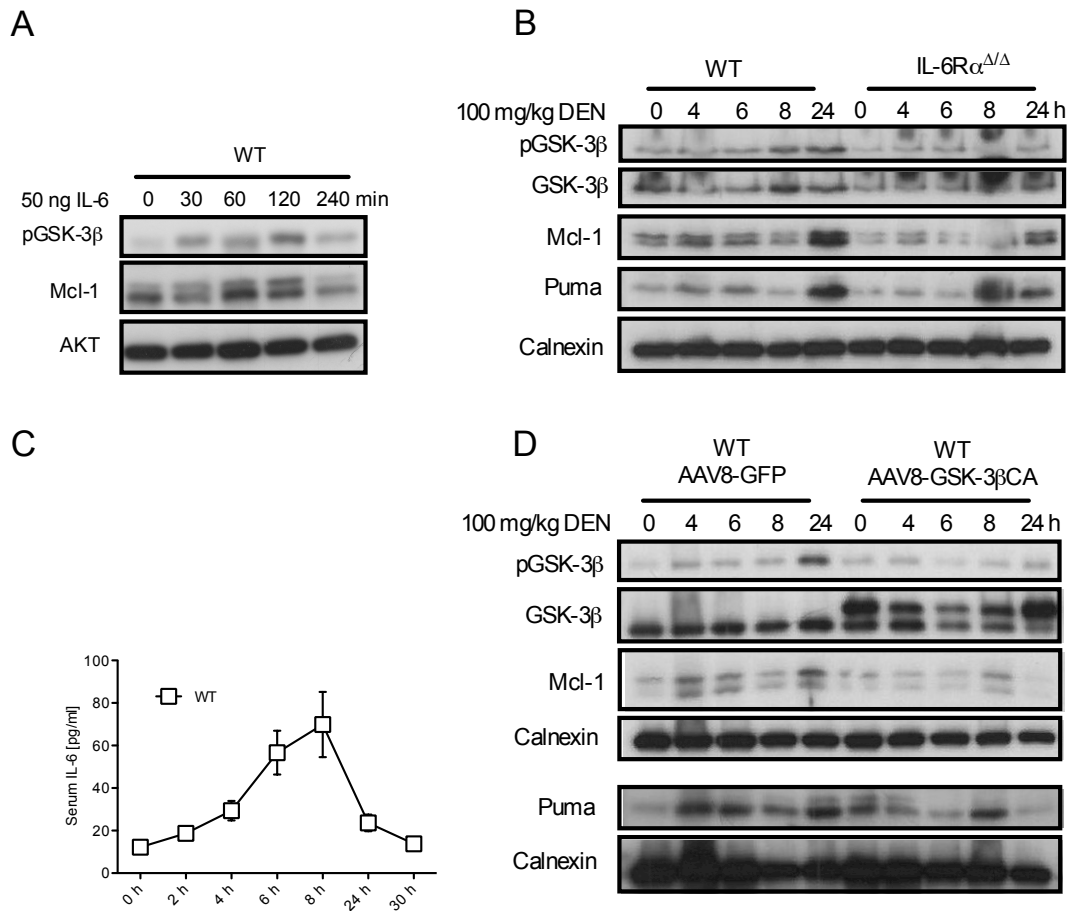


Figure 3.16: GSK-3 β activity in initial phase of tumor development of control and IL-6R $\alpha^{\Delta/\Delta}$ mice

(A) Western blot analysis using pGSK-3 β , Mcl-1, and AKT antibodies on liver tissue from 8 wk control mice fed on NCD after *i.v.* injection of 50 ng IL-6. (B) Western blot analysis using pGSK-3 β , GSK-3 β , Mcl-1, Puma and Calnexin antibodies on liver tissue from 8 wk male control and IL-6R $\alpha^{\Delta/\Delta}$ mice fed on NCD sacrificed at indicated time points after injection of 100 mg/kg DEN. (C) Examination of serum IL-6 concentrations by ELISA taken from DEN-injected 8 wk control mice at the indicated time points (n=10). (D) Western blot analysis using pGSK-3 β , GSK-3 β , Mcl-1, Puma and Calnexin antibodies on liver tissue from 8 wk control mice pre-infected with AAV8 viruses expressing GFP or GSK-3 β CA at indicated time points after injection of 100 mg/kg BW DEN. Displayed values are means \pm S.E.M.; *, $p \leq 0.05$; **, $p \leq 0.01$; ***, $p \leq 0.001$ versus control. Data in D produced in collaboration with Claudia Wunderlich.

GSK-3 β S9 phosphorylation mainly occurs through the action of Phosphatidylinositol 3-kinase (PI3K) signaling [Cross *et al.*, 1995]. The PI3K/AKT pathway, which transmits anti-apoptotic survival signals, is likely involved in mitigating apoptosis in a substantial fraction of human tumors [Jiang & Liu, 2008; Cully *et al.*, 2006]. To determine the role of PI3K signaling in DEN-induced HCC development of HFD fed mice, HCC-bearing HFD fed control mice were treated with the specific PI3K inhibitor GDC-0941.

Accordingly, administration of GDC-0941 to tumor-bearing HFD fed mice resulted in reactivation of GSK-3 β (Fig. 3.17A). Consequently, Mcl-1 protein levels were reduced in the livers of these mice when compared to HFD fed control mice, though livers of NCD fed IL-6R $\alpha^{\Delta/\Delta}$ mice still exhibited less Mcl-1 protein (Fig. 3.17A). Furthermore, the reduction of Mcl-1 protein by inhibition of PI3K in tumor-bearing HFD fed control mice resulted in an increase of TUNEL-positive cells – a marker for apoptosis (Fig. 3.17B/C). Moreover, Ki67 staining of tumor liver sections demonstrated that PI3K inhibition reduced hepatocyte proliferation (Fig. 3.17D/E). Importantly, the quantitative evaluation of apoptosis and hepatocyte proliferation in livers of PI3K inhibitor-treated HFD fed control mice revealed a significant increase in apoptosis and reduction in proliferation comparable to that observed for NCD-fed IL-6R $\alpha^{\Delta/\Delta}$ mice, which are protected against HCC development.

However regardless of the result obtained from the pharmacological inhibition of PI3K, the formation of PIP3 was similar in the cohorts of mice independent on diet and genotype (Fig. 3.18A). Even downstream AKT activity was unaltered in those groups of mice as examined on one hand by phosphorylation of AKT at serine 473 (Fig. 3.18B/C) as well as by the ability of immunoprecipitated AKT to phosphorylate a GSK-3 β S9 including peptide on the other (Fig. 3.18D).

Thus, PI3K/AKT signaling is active but not altered in the absence of IL-6R α signaling in HCC development independent on dietary condition.

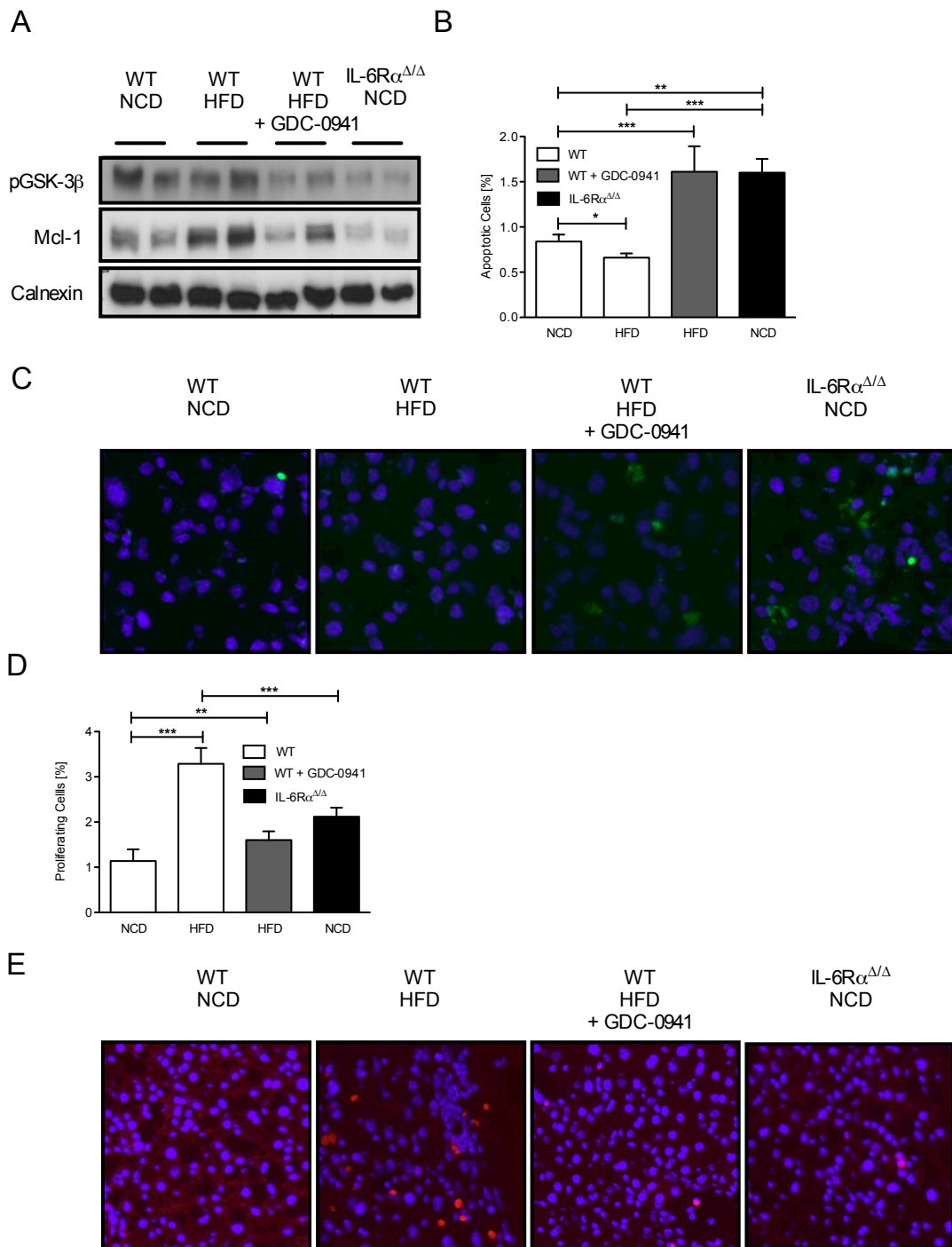


Figure 3.17: **PI3K inhibition in tumor bearing control and IL-6R $\alpha^{\Delta/\Delta}$ mice**

(A) Western blot analysis using pGSK-3 β , Mcl-1 and Calnexin antibodies on liver tissue from DEN-injected 8 mo control and IL-6R $\alpha^{\Delta/\Delta}$ mice treated with GDC-0941 or with vehicle. (B) Quantitation of C (n=4). (C) TUNEL stainings of tumor liver sections from DEN-injected 8 mo IL-6R $\alpha^{\Delta/\Delta}$ and control mice treated with or without GDC-0941. (D) Quantitation E (n=4). (E) Ki67 staining of tumor liver sections from DEN-injected 8-mo IL-6R $\alpha^{\Delta/\Delta}$ and control mice treated with or without GDC-0941. Displayed values are means \pm S.E.M.; *, $p \leq 0.05$; **, $p \leq 0.01$; ***, $p \leq 0.001$ versus control.

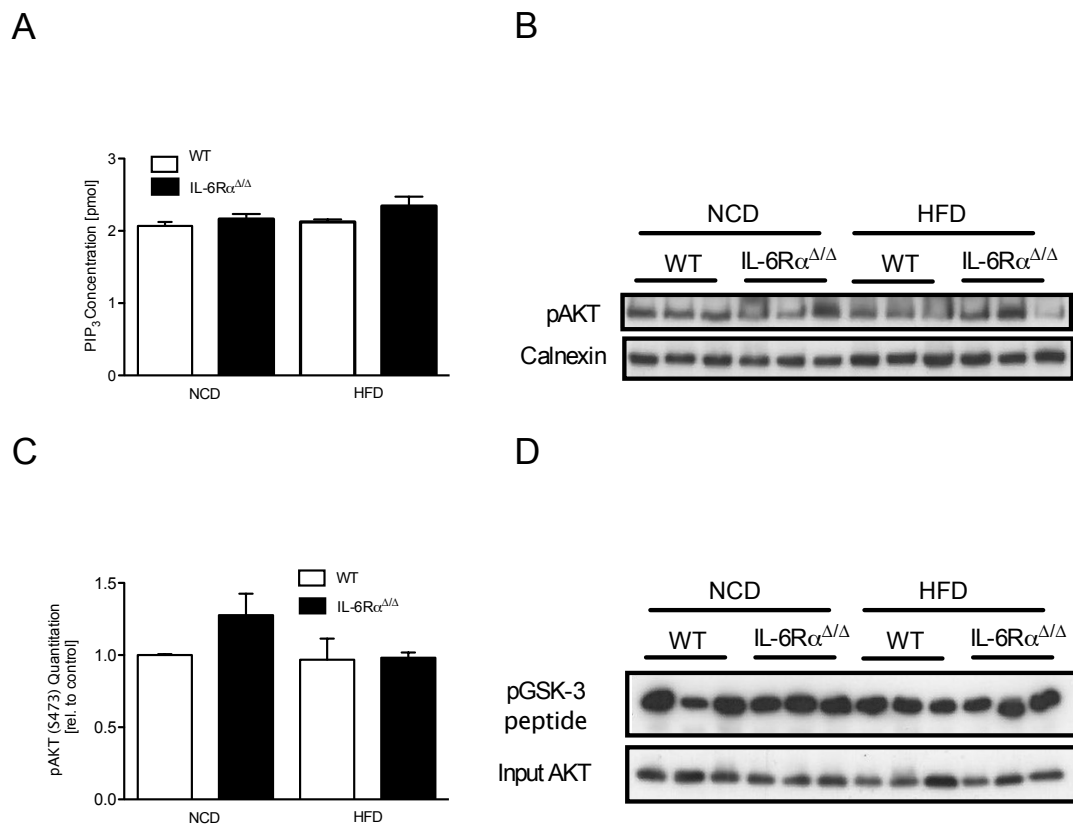


Figure 3.18: **PI3K pathway in tumor bearing control and IL-6R $\alpha^{\Delta/\Delta}$ mice**

(A) Determination of PIP₃ concentration in liver lysates from DEN-injected 8 mo control and IL-6R $\alpha^{\Delta/\Delta}$ mice examined by PI3K activity assay (n=6). (B) Western blot analysis of liver lysates from DEN-injected 8 mo control and IL-6R $\alpha^{\Delta/\Delta}$ mice using pAKT and Calnexin antibodies. (C) Quantitation of pAKT level from B relative to Calnexin (n=6). (D) AKT kinase activity assay of liver lysates from DEN-injected 8 mo control and IL-6R $\alpha^{\Delta/\Delta}$ mice. Immunoprecipitated AKT was incubated in a reaction with GSK-3 β peptide. Western blots of reaction and input using pGSK-3 β and AKT antibodies. Displayed values are means \pm S.E.M.; *, $p \leq 0.05$; **, $p \leq 0.01$; ***, $p \leq 0.001$ versus control.

3.7 Obesity and IL-6 controlled expression of PP-1 α and Mule synergize to stabilize Mcl-1

Hence alteration of PI3K/AKT activity in lean IL-6R α -deficient animals failed to explain increased GSK-3 β action, the expression levels of protein phosphatase 1 α (PP-1 α) that catalyzes the reverse reaction, namely GSK-3 β dephosphorylation at S9 were examined. Strikingly, expression levels of PP-1 α were more than 2-fold increased in IL-6R α -deficient mice in the DEN-induced HCC protocol when compared to controls (Fig. 3.19A). Transcriptional control of IL-6 regulated gene expression is mainly mediated through the transcription factor Stat-3, whose activation was reduced in lean IL-6R $\alpha^{\Delta/\Delta}$ mice in acute as well as chronic DEN experiments (Fig. 3.19B/C). Evidently, not only the restored hepatic Stat-3 activation in obese IL-6R $\alpha^{\Delta/\Delta}$ mice occurred independent of IL-6 but also the remaining DEN-induced Stat-3 activation in lean IL-6R $\alpha^{\Delta/\Delta}$ mice, thus indicating another obesity- and/or DEN-induced factor that activates Stat-3 in the absence of IL-6R α (Fig. 3.19B/C).

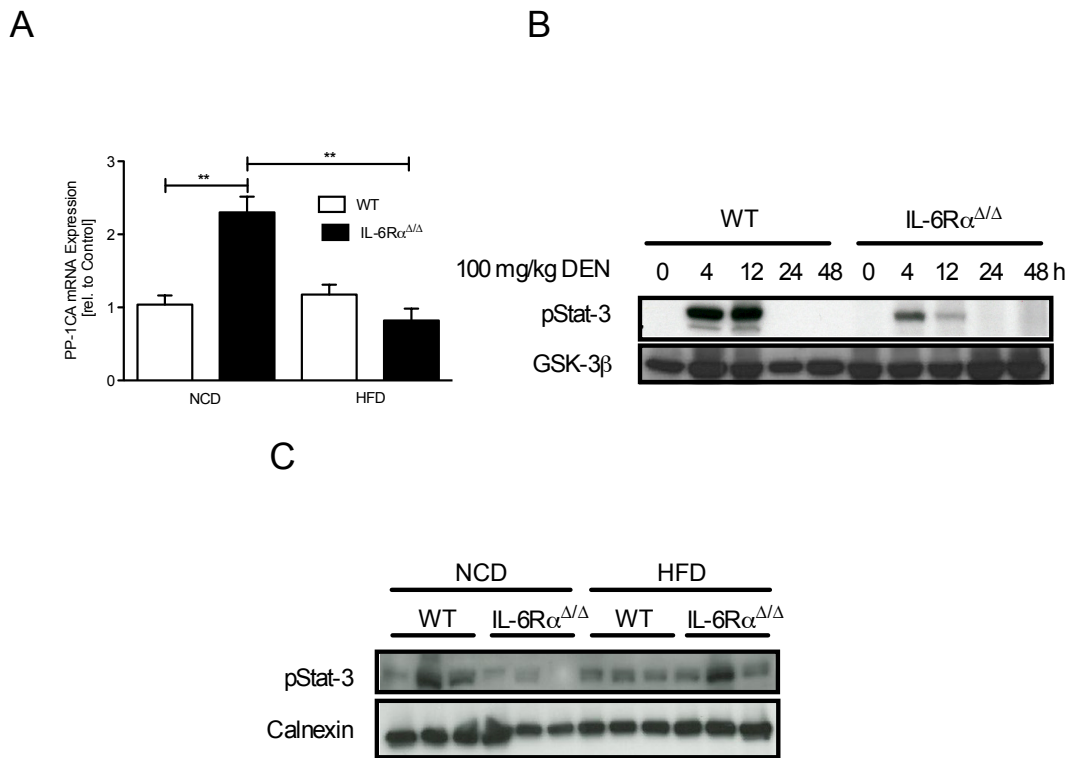


Figure 3.19: **PP-1 α expression and Stat-3 activation in control and IL-6R $\alpha^{\Delta/\Delta}$ mice**

(A) qPCR of PP-1CA in liver of DEN-injected 8 mo male control and IL-6R $\alpha^{\Delta/\Delta}$ mice (n=6). (B) Western blot analysis using pStat-3 and GSK-3 β antibodies on liver tissue from 8 wk control and IL-6R $\alpha^{\Delta/\Delta}$ mice after injection of 100 mg/kg DEN. (C) Western blot analysis using pStat-3 and Calnexin antibodies on liver tissue from DEN-injected 8 mo control and IL-6R $\alpha^{\Delta/\Delta}$ mice. Displayed values are means \pm S.E.M.; *, $p \leq 0.05$; **, $p \leq 0.01$; ***, $p \leq 0.001$ versus control.

Careful investigation of the PP-1 α promoter revealed a conserved Stat-3 binding site between mouse and human upstream of transcriptional initiation (Fig. 3.20A). To address whether this motif is bound by phosphorylated Stat-3 in response to IL-6, chromatin immunoprecipitation (ChIP) experiments of basal and IL-6-stimulated HepG2 cells were performed that demonstrated activated Stat-3 at this site under basal conditions but IL-6 stimulation increased the presence of Stat-3 at this motif (Fig. 3.20B). To determine whether PP-1 α is a direct IL-6 target in vivo and how expression is affected by IL-6-induced Stat-3 activation, a cohort of C57/BL6 mice were injected with IL-6 and relative hepatic expression of PP-1 α was examined in a time frame of 240 min after IL-6 injection. PP-1 α expression was significantly reduced upon IL-6 treatment 60 min post injection and progressively declined up to 240 min, indicating that PP-1 α is a transcriptional target for IL-6-induced repression (Fig. 3.20C). To examine whether PP-1 α inhibition is sufficient to stabilize Mcl-1 protein in acute DEN injection experiments in vivo, the specific PP-1 α inhibitor okadaic acid (OA) was applied 1 hour before DEN injection in lean control and in IL-6R α -deficient animals and the S9 phosphorylation of GSK-3 β was investigated as well as Mcl-1 protein abundance. Expectedly, PP-1 α inhibition resulted in the persistent phosphorylation of GSK-3 β in both IL-6R α -deficient and control mice (Fig. 3.20D). However, hepatic Mcl-1 protein levels in IL-6R α -deficient mice were still reduced when PP-1 α was inhibited (Fig. 3.20D), hinting to another synergistic pathway independent of PP-1 α and GSK-3 β that destabilizes Mcl-1 in lean IL-6R α -deficient mice.

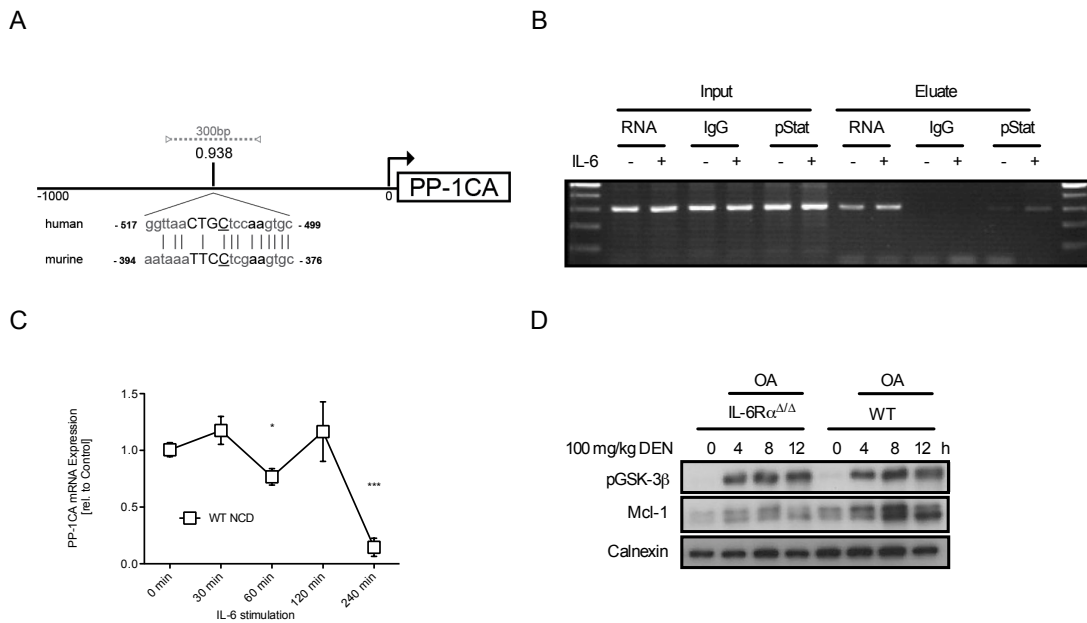


Figure 3.20: **PP-1 promoter analysis in control and IL-6R $\alpha^{\Delta/\Delta}$ mice**

(A) Illustration of PP-1CA promoter region for ChIP analysis. Putative Stat-3 binding sites are indicated by vertical black lines and include matrix similarity (above) and human and murine sequences with base pair precision (below). Capitals in the sequence indicate the core sequence, black letters a c_i -value > 60 . Oligos (5hPP1CAChip/3hPP1CAChip) used for PCR amplification are indicated by open triangles outside of the expected fragment. (B) ChIP using RNA PolIII, IgG and pStat-3 antibodies on sonicated DNA isolated from HepG2 cells stimulated with 200ng/ml IL-6 for 45 min using oligos 5hPP1CAChip and 3hPP1CAChip to examine PP-1CA promoter. (C) qPCR of PP-1CA in liver of 8 wk control mice fed on NCD after *i.v.* injection of 50 ng IL-6 ($n=5$). (D) Western blot analysis using pGSK-3 β , Mcl-1, and Calnexin antibodies on liver tissue from 8 wk old male control and IL-6R $\alpha^{\Delta/\Delta}$ mice fed on NCD pre-treated with 750 ng OA/g BW 1 hr before injection of a 100 mg/kg BW DEN dose. Displayed values are means \pm S.E.M.; *, $p \leq 0.05$; **, $p \leq 0.01$; ***, $p \leq 0.001$ versus control. Data in A/B produced in collaboration with Justus Ackermann

Recently, GSK-3 β -phosphorylated Mcl-1 has been shown to be recognized by either Mcl-1 ubiquitin ligase E3 (Mule) or the SKP1-cullin-F-box WD repeat-containing protein 7 (SCF-FBW7) E3 ligase both of which ligate polyubiquitin chains to Mcl-1 that lead to its proteasomal degradation [Wertz *et al.*, 2011; Zhong *et al.*, 2005]. In order to determine whether the expression of these E3 ligases correlate with Mcl-1 levels in lean and obese control and IL-6R $\alpha^{\Delta/\Delta}$ mice, qPCR analyses of tumor livers from these mice was performed.

Strikingly, while a 2-fold elevated expression of Mule could be observed in lean IL-6R $\alpha^{\Delta/\Delta}$ mice compared to lean controls, Mule expression was significantly reduced under obese conditions in mice of both genotypes (Fig. 3.21A). Interestingly, comparison of the expression levels of the subunits FBW7 and cullin 1 (Cul-1) of the SCF-FBW7 complex to Mule expression revealed a 20-fold lower FBW7 expression and 5-fold lower Cul-1 expression indicating that Mule rather than the SCF-FBW7 E3 ligase complex might play a role in liver carcinogenesis by interfering with Mcl-1 protein stability (Fig. 3.21A). Consistently, examination of Mule expression in acute DEN injection experiments revealed an impaired suppression of Mule IL-6R $\alpha^{\Delta/\Delta}$ mice in response to DEN when compared to controls (Fig. 3.21B).

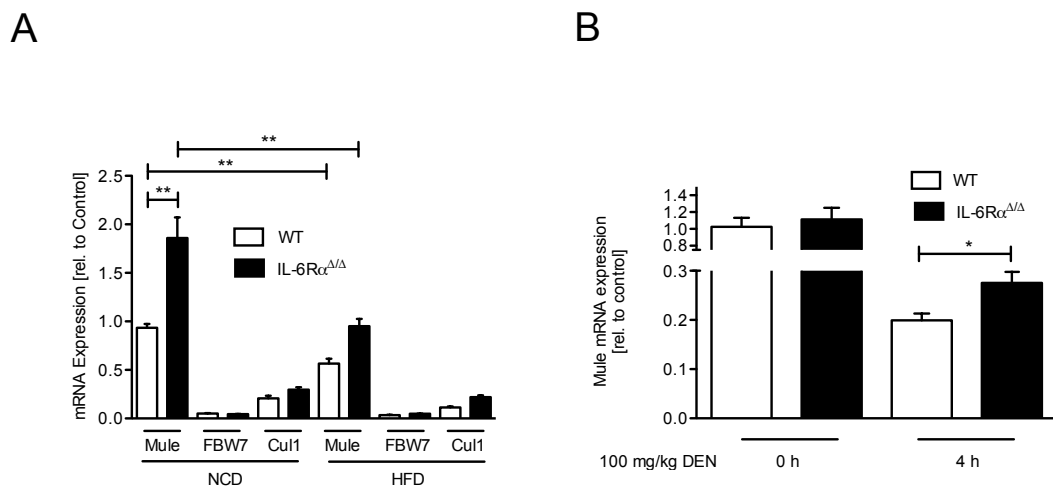


Figure 3.21: **Mule expression in control and IL-6R $\alpha^{\Delta/\Delta}$ mice**

(A) qPCR of Mule, FBW7 and Cul1 in liver of DEN-injected 8 mo male control and IL-6R $\alpha^{\Delta/\Delta}$ mice (n=6). (B) qPCR of Mule in liver of 8 wk control mice fed on NCD after injection of 100 mg/kg BW DEN (n=5). Displayed values are means \pm S.E.M.; *, $p \leq 0.05$; **, $p \leq 0.01$; ***, $p \leq 0.001$ versus control.

This result support the assumption that Mule expression is directly inhibited by IL-6 and that impaired suppression of Mule upon IL-6R α deficiency during HCC initiation might result in increased Mcl-1 protein turnover and apoptosis.

In line with these experiments that suggest an important role of IL-6-induced Stat-3 in the inhibition of Mule expression, the promoter region of Mule was analysed and two conserved Stat-3 binding motifs between mouse and human were identified within a region upstream of Mule transcriptional initiation (Fig. 3.22A). Chip experiments of basal and IL-6-stimulated HepG2 cells revealed active Stat-3 bound to the Mule promoter at the basal state, whereas IL-6 stimulation increased Stat-3 binding to these sites (Fig. 3.22B). Of note, binding of activated Stat-3 to the Stat-3 motifs in the Mule promoter was specific as using oligos more distal to these sites revealed still actively bound RNA pol II but not active Stat-3 (Fig. 3.22C).

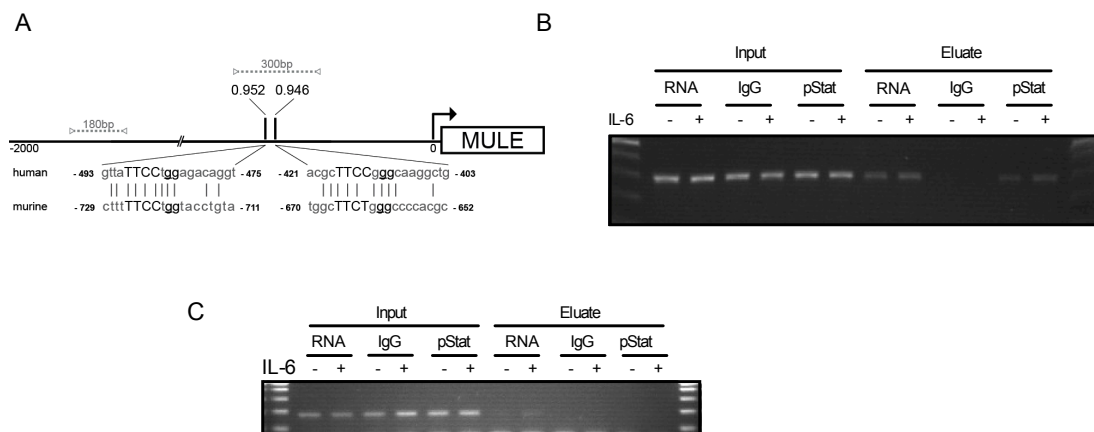


Figure 3.22: **ChIP experiments with Mule promoter**

(A) Illustration of Huwe1/Mule promoter region for ChIP analysis. Putative Stat-3 binding sites are indicated by vertical black lines and include matrix similarity (above) and human and murine sequences with basepair precision (below). Capitals in the sequence indicate the core sequence, black letters a ci -value > 60 . Oligos (5hMULEChip/3hMULEChip) used for PCR amplification are indicated by open triangles outside of the expected fragment. (B) ChIP using RNA PolII, IgG and p-Stat3 antibodies on sonicated DNA isolated from HepG2 cells stimulated with 200 ng/ml IL-6 for 45 min using oligos 5hMULEChip and 3hMULEChip to examine Mule promoter. (C) ChIP using RNA PolII, IgG and pStat-3 antibodies on sonicated DNA isolated from HepG2 cells stimulated with 200 ng/ml IL-6 for 45 min using oligos 5hMULEUSChIP and 3hMULEUSChIP to examine Mule promoter. Displayed values are means \pm S.E.M.; *, $p \leq 0.05$; **, $p \leq 0.01$; ***, $p \leq 0.001$ versus control. Data produced in collaboration with Justus Ackermann

To directly clarify whether Mule expression is subjected to IL-6-induced repression, 1000 bp upstream of Mule exon 1 that contains the promoter including regulatory elements was cloned in front of a firefly luciferase and this construct was transfected into HepG2 cells. Examination of luciferase activity revealed significantly 40% reduced Mule promoter activity upon IL-6 stimulation, whereas luciferase activity substantially increased when transfected cells were incubated in the presence of the Stat-3 inhibitor STATTIC (Fig. 3.23A). Accordingly, investigation of mice expressing a constitutive active Stat-3 variant in hepatocytes revealed a 40% reduced Mule expression similar to the *in vitro* findings (Fig. 3.23B).

Therefore, these analyses reveal that expression of the ubiquitin ligase Mule is regulated by IL-6- and obesity-controlled Stat-3 activation that impacts on Mcl-1 stability and thus alters apoptosis sensitivity.

In order to verify the mechanism of Mcl-1 stabilization *in vitro*, primary hepatocytes derived from control and IL-6R $\alpha^{\Delta/\Delta}$ animals were stimulated with 50 ng/ml IL-6 in a time frame and Western Blot analysis was performed. This analysis revealed that IL-6 treatment increased Mcl-1 protein, inhibited GSK-3 β activity and repressed Mule expression in control hepatocytes, whereas these processes were not present in IL-6R α -deficient cells (Fig. 3.23C). To prove the mechanism directly in tumor cells, Hep3B cells were stimulated with IL-6 for 1, 4 and 8 h. While IL-6 treatment increased Mcl-1 protein, this effect was blunted when IL-6R α action was inhibited through the supplementation of a neutralizing antibody (Fig. 3.23D). Similar to the *in vivo* data, IL-6 treatment inhibited GSK-3 β activity and repressed Mule expression, whereas these processes were not present when IL-6R α action was neutralized (Fig. 3.23D). Importantly, supplementation of IgG control antibody failed to affect IL-6-induced Mcl-1 stabilization.

In summary, these data clearly prove the key role of IL-6 mediated inhibition of Mule expression in the development of HCC.

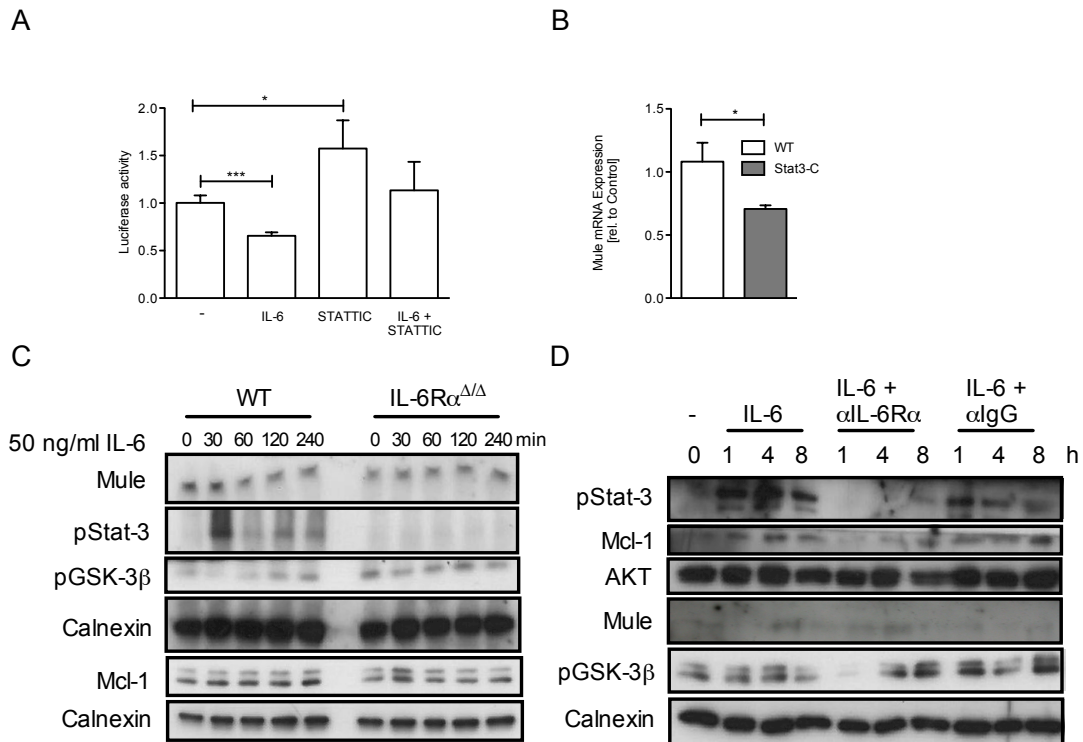


Figure 3.23: **Mule promoter analysis in control and IL-6R $\alpha^{\Delta/\Delta}$ mice**

(A) Luciferase activity of lysates obtained from HepG2 cells transfected with pTEMule-Luc and pRL-Null stimulated with IL-6 and/or preincubated with 20 μ M STATTC (n=9/stimulation). (B) qPCR of Mule in livers of 8 wk control and constitutive active Stat-3-C mice (n=4). (C) Western blot analysis using pStat-3, Mcl-1, AKT, Mule, pGSK-3 β and Calnexin antibodies of primary hepatocytes derived from control and IL-6R $\alpha^{\Delta/\Delta}$ mice stimulated with 50 ng/ml IL-6 for the indicated time points. (D) Western blot analysis using pStat-3, Mcl-1, AKT, Mule, pGSK-3 β and Calnexin antibodies of Hep3B cells stimulated with 50 ng/ml IL-6 and IL-6 plus 5 μ g/ml neutralizing IL-6R α antibody or control antibody. Displayed values are means \pm S.E.M.; *, $p \leq 0.05$; **, $p \leq 0.01$; ***, $p \leq 0.001$ versus control. Data in A/C produced in collaboration with Justus Ackermann

Increased Mcl-1 levels have previously been reported in a subset of human HCC [Fleischer *et al.*, 2006], however the correlation between Mcl-1 and Mule has never been addressed in HCC. Therefore, human HCC samples were examined in immunohistochemistry using anti-Mule and anti-Mcl-1 antibodies revealing that Mcl-1 expression in human HCC negatively correlated with Mule expression. Cases that showed no steatosis (#1, #2), steatosis (#3) and a steatohepatic pattern (#4, #5) were classified by visible lipid inclusions into the liver (Fig. 3.24). While, the non-steatotic cases #1, #2 revealed almost no Mcl-1 expression and high Mule expression, the steatohepatic HCC cases #4, #5 exhibited the most prominent Mcl-1 expression accompanied with a reduction in Mule expression (Fig. 3.24).

Collectively, the experiments demonstrate that obesity and IL-6 signaling synergize to affect the protein stability of the Bcl-2 family member Mcl-1 via GSK-3 β inhibition and repression of Mule expression to inhibit the mitochondrial apoptotic pathway during HCC development.

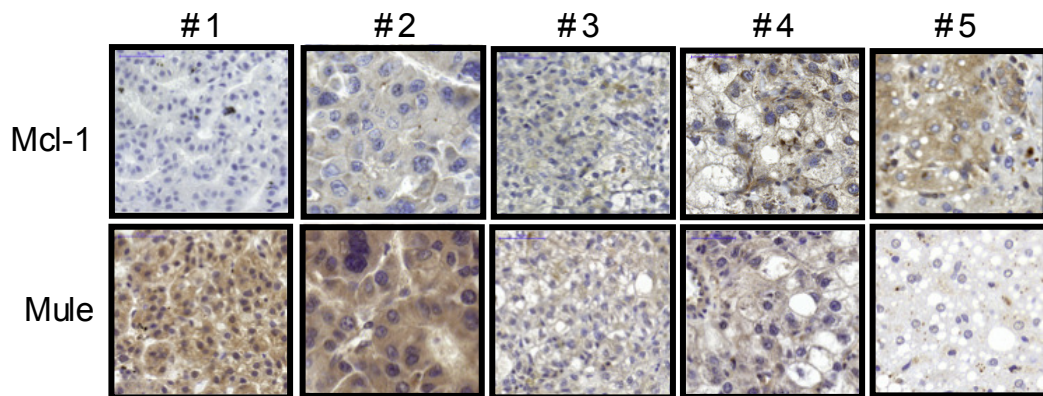


Figure 3.24: **Correlation between Mule and Mcl-1 level in human HCC**

(A) Mcl-1 and Mule stainings of 5 different human HCC sections. Data produced in collaboration with the group of Lukas Heukamp

3.8 Compensatory effects of IL-6 type cytokines and receptors

3.8.1 HFD causes obesity in control, IL-6R $\alpha^{\Delta/\Delta}$ and gp130 $^{L-KO}$ mice

While it is certainly not clear which factor in obesity compensates for IL-6R α deficiency in HCC development, another IL-6 type cytokine or receptor might account for this observation. The common feature of all IL-6 type cytokine receptors is the signaling transducing receptor unit glycoprotein 130 (gp130) [Zhang *et al.*, 1994]. To determine if another pathway of IL-6 type cytokines is involved in the development of HCC conditional gp130-deficient mice were generated allowing the cell type specific inactivation of gp130 in hepatocytes. Therefore, gp130 $^{f1/f1}$ mice were crossed to mice expressing the Cre recombinase under the control of both the mouse albumin regulatory elements and the α -fetoprotein enhancers (AlfpCre transgene) [Kellendonk *et al.*, 2000; Betz *et al.*, 1998]. These mice were further intercrossed with siblings leading to hepatocyte specific deletion of gp130 (gp130 $^{L-KO}$). To investigate whether gp130-deficiency in hepatocytes affects HCC development under normal and obese conditions, male gp130 $^{L-KO}$ mice were injected with 25 mg/kg BW DEN *i.p.* at 15 days of age and separated after weaning in cohorts fed either a NCD or HFD for 8 month.

As expected, HFD feeding significantly increased body weight in gp130 $^{L-KO}$ compared to mice upon NCD feeding, whereas no differences could be detected in comparison with IL-6R $\alpha^{\Delta/\Delta}$ and control mice neither upon NCD nor HFD feeding (Fig. 3.25). These data demonstrate that HFD exposure causes similar levels of obesity in both control, IL-6R $\alpha^{\Delta/\Delta}$ and gp130 $^{L-KO}$ mice.

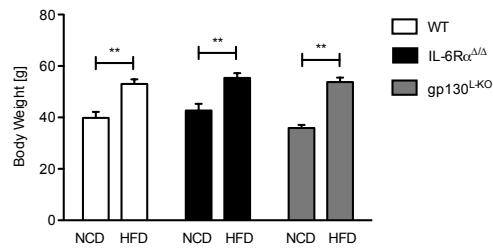


Figure 3.25: **Body weight of control, IL-6R $\alpha^{\Delta/\Delta}$ and gp130^{L-KO} mice**

(A) Weight determination of 8 mo control, IL-6R $\alpha^{\Delta/\Delta}$ and gp130^{L-KO} mice (n=15) injected with 25 mg/kg BW DEN at 15 days of age and exposed to NCD or HFD after weaning. Displayed values are means \pm S.E.M.; *, $p \leq 0.05$; **, $p \leq 0.01$; ***, $p \leq 0.001$ versus control.

3.8.2 Inactivation of gp130 in hepatocytes protected against DEN-induced HCC development even under obese conditions

To determine if another pathway of IL-6 type cytokines is involved in the development of HCC, tumor development in 8 month-old DEN-treated gp130^{L-KO} mice that had been exposed to either a NCD or HFD feeding was investigated by visual inspection and compared to control and IL-6R $\alpha^{\Delta/\Delta}$ mice. Similar to IL-6R $\alpha^{\Delta/\Delta}$ mice, gp130^{L-KO} mice upon NCD feeding developed significantly less macroscopically visible liver tumors compared to control mice (Fig. 3.26A/B). 90% of the tumors were smaller than 2 mm (Fig. 3.26C) whereas 10% reached a size of more than 2 mm (Fig. 3.26D). Surprisingly, in contrast to control and IL-6R $\alpha^{\Delta/\Delta}$ mice, obesity did not increase tumor burden in gp130^{L-KO} mice (Fig. 3.26A/B).

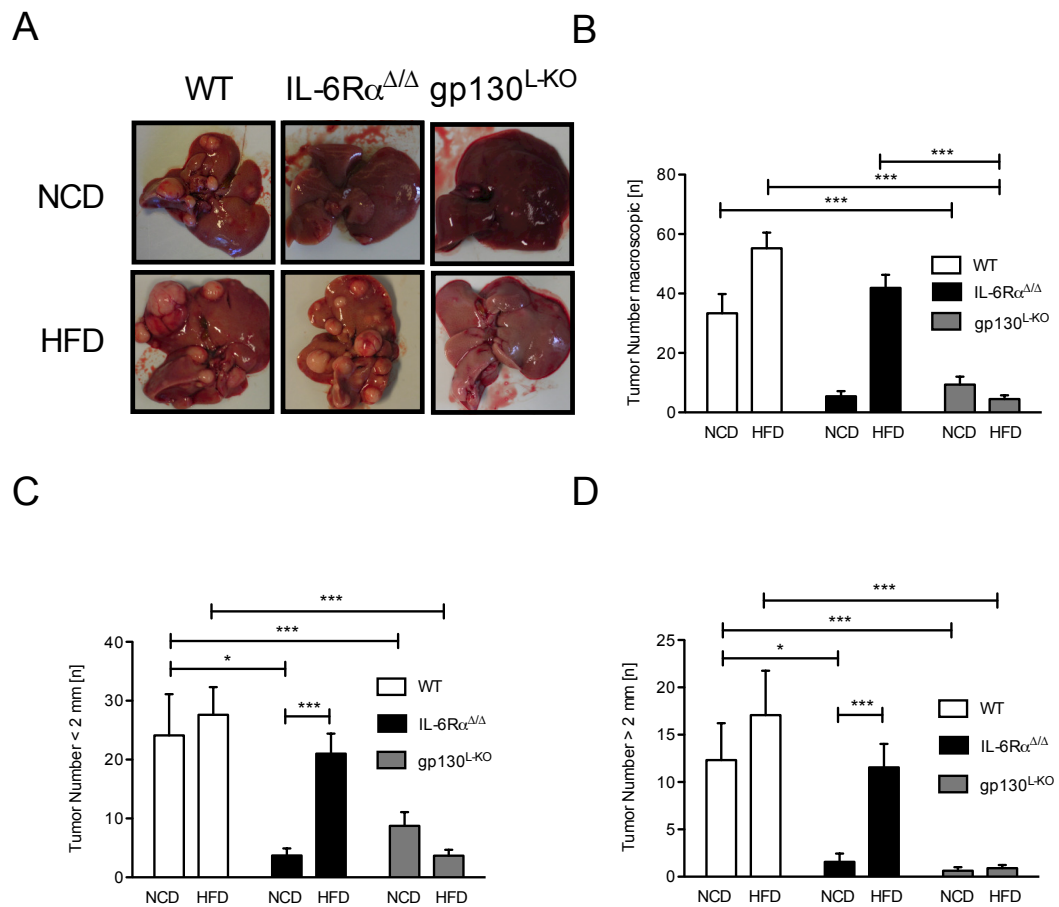


Figure 3.26: Tumor burden macroscopic in control, IL-6R $\alpha^{\Delta/\Delta}$ and gp130 $^{L-KO}$ mice
 (A) Livers of 8 mo control, IL-6R $\alpha^{\Delta/\Delta}$ and gp130 $^{L-KO}$ mice injected with 25 mg/kg BW DEN at 15 days of age. (B) Quantitation of macroscopic tumor multiplicity determined by visual inspection in DEN-injected 8 mo control, IL-6R $\alpha^{\Delta/\Delta}$ and gp130 $^{L-KO}$ mice (n=15). (C) Enumeration of tumor number for < 2 mm and (D) > 2 mm as determined by visual inspection of DEN-injected 8 mo control, IL-6R $\alpha^{\Delta/\Delta}$ and gp130 $^{L-KO}$ mice (n=15). Displayed values are means \pm S.E.M.; *, $p \leq 0.05$; **, $p \leq 0.01$; ***, $p \leq 0.001$ versus control.

Histological investigation of HE-stained liver sections confirmed that NCD-fed gp130 $^{L-KO}$ mice revealed significantly decreased number of HCC foci when compared to NCD-fed control mice, similar to IL-6R $\alpha^{\Delta/\Delta}$ mice (Fig. 3.27A). However, this difference was not as large as observed upon macroscopic inspection. Furthermore, tumor size was significantly decreased in gp130 $^{L-KO}$ mice upon NCD feeding compared to control mice, but comparable to IL-6R $\alpha^{\Delta/\Delta}$ mice (Fig. 3.27B).

HFD data were not available at this point.

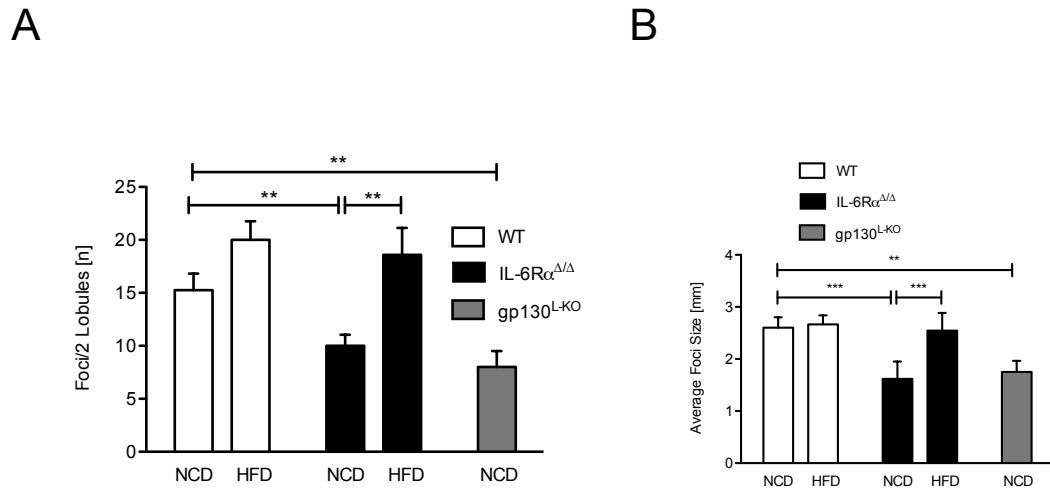


Figure 3.27: Tumor burden microscopic in control, IL-6R $\alpha^{\Delta/\Delta}$ and gp130 $^{L-KO}$ mice
 (A) Quantitation of tumor number per 2 lobules counted on liver sections from 8 mo control, IL-6R $\alpha^{\Delta/\Delta}$ and gp130 $^{L-KO}$ mice (n=15). (B) Quantitation of tumor size measured in the big liver lobe of DEN-injected 8 mo control, IL-6R $\alpha^{\Delta/\Delta}$ and gp130 $^{L-KO}$ mice (n=15). Displayed values are means \pm S.E.M.; *, $p \leq 0.05$; **, $p \leq 0.01$; ***, $p \leq 0.001$ versus control. Data produced in collaboration with Beate Straub.

The extent of inflammation, assessed by quantitation of infiltrating immune cells, was significantly reduced in livers of gp130 $^{L-KO}$ mice compared to control mice upon NCD feeding, but similar to IL-6R $\alpha^{\Delta/\Delta}$ mice (Fig. 3.28A). Liver steatosis was determined in control, IL-6R $\alpha^{\Delta/\Delta}$ and gp130 $^{L-KO}$ mice. Livers of gp130 $^{L-KO}$ mice fed a NCD revealed a significantly reduced extent of steatosis compared to control mice, similar to IL-6R $\alpha^{\Delta/\Delta}$ mice (Fig. 3.28B). Additionally, counting of necrotic hepatocytes per two lobules revealed a significant decrease in gp130 $^{L-KO}$ mice compared to control mice upon NCD feeding (Fig. 3.28C). As fibrosis is also connected to the development of liver cancer, the extent of fibrosis was determined by score. By comparison no significant alteration could be detected between the genotypes (Fig. 3.28D).

Taken together, these data demonstrate that gp130-deficiency in hepatocytes protected against DEN-induced HCC development even under obese conditions.

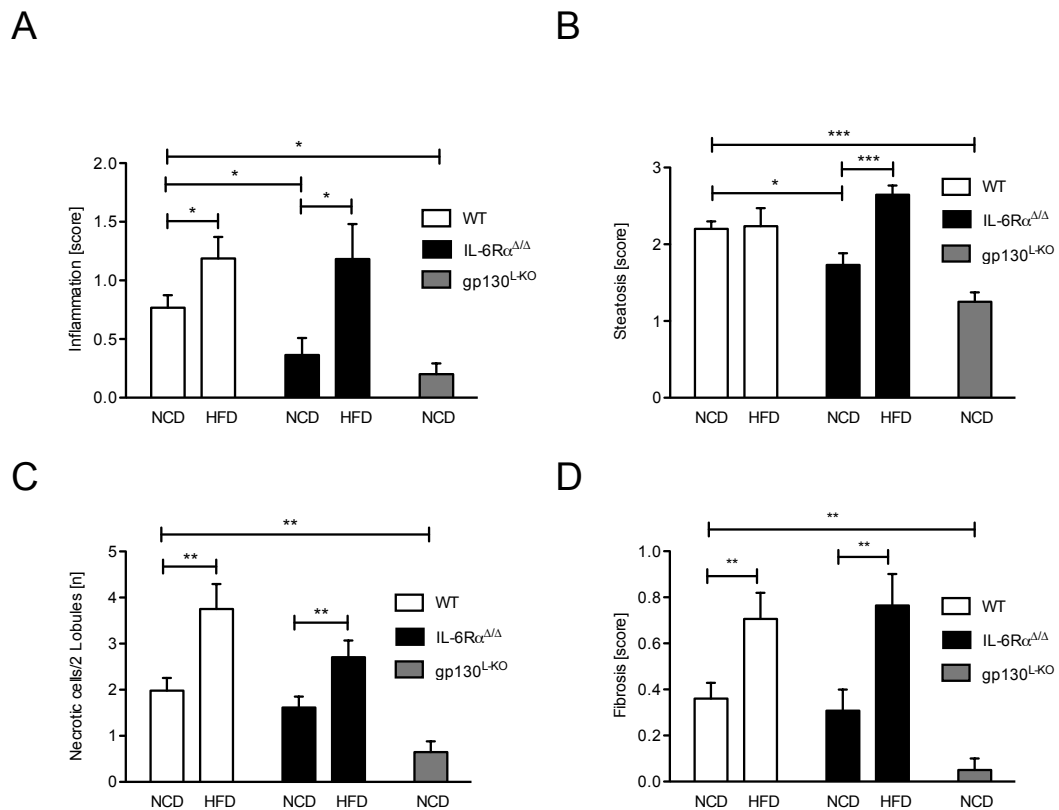


Figure 3.28: **Liver status of control, IL-6R $\alpha^{\Delta/\Delta}$ and gp130^{L-KO} mice**

(A) Quantitation of inflammation measured in the big liver lobe of DEN-injected 8 mo control, IL-6R $\alpha^{\Delta/\Delta}$ and gp130^{L-KO}. 1 = mild inflammation (mild portal inflammation, 3-5 single cell necrosis, no grouped necrosis); 2 = moderate inflammation (moderate portal inflammation, 6-9 single cell necrosis, 1 grouped necrosis); 3 = severe inflammation (severe portal inflammation, more than 10 single cell necrosis, more than 1 grouped necrosis) (n=15). (B) Quantitation of steatosis measured in the big liver lobe of DEN-injected 8 mo control, IL-6R $\alpha^{\Delta/\Delta}$ and gp130^{L-KO}. 1 = 0 - 10%; 2 = 11 - 50 %; 3 = above 50 % (C) Quantitation of necrotic cells measured in the big liver lobe of DEN-injected 8 mo control, IL-6R $\alpha^{\Delta/\Delta}$ and gp130^{L-KO}. (D) Quantitation of fibrosis measured in the big liver lobe of DEN-injected 8 mo control, IL-6R $\alpha^{\Delta/\Delta}$ and gp130^{L-KO}. 1 = increased portal connective tissue; 2 = early formation of septa (n = 15). Displayed values are means \pm S.E.M.; *, $p \leq 0.05$; **, $p \leq 0.01$; ***, $p \leq 0.001$ versus control. Data produced in collaboration with Beate Straub.

3.8.3 No compensation for IL-6R α deficiency by IL-6 type cytokines in HCC development upon HFD feeding

The gp130 subunit is part of every member of the IL-6 type cytokine receptor family [Zhang *et al.*, 1994]. To investigate which IL-6 type cytokine or receptor could compensate for IL-6R α deficiency in HCC development on HFD, expression of different IL-6 type cytokines and receptors were investigated (Fig. 3.29A-D), such as IL-6, IL-11, oncostatin M (OSM), ciliary neurotrophic factor (CNTF), IL-30, leukemia inhibitory factor (LIF), cardiothrophin 1 (CTF-1) and cardiotrophin-like cytokine factor 1 (CTCF-1) (Fig. 3.29A/B). As expected, IL-6 expression was increased in IL-6R $\alpha^{\Delta/\Delta}$ mice upon HFD feeding compared to control mice (Fig. 3.29A). Furthermore, OSM revealed a significant decrease in IL-6R $\alpha^{\Delta/\Delta}$ mice upon HFD feeding compared to control mice (Fig. 3.29A), whereas CTF-1 exhibited a significant decrease in control mice upon HFD feeding compared to control mice upon NCD feeding (Fig. 3.29B).

Investigation of the different IL-6 type cytokine receptors, IL-6R α , IL-11R, OSMR, CNTFR, IL-27R, Epstein-Barr virus induced gene 3 (EBI-3), LIFR and gp130, revealed a wide range of alterations between the diets and genotypes (Fig. 3.29C/D). As expected IL-6R α was significantly decreased in IL-6R $\alpha^{\Delta/\Delta}$ mice both upon NCD and HFD feeding (Fig. 3.29C). Furthermore, the IL-11R, whose structure is very similar to the IL-6R α , exhibited a significantly increase in IL-6R $\alpha^{\Delta/\Delta}$ mice upon NCD feeding compared to control mice upon NCD feeding as well as to IL-6R $\alpha^{\Delta/\Delta}$ mice upon HFD feeding (Fig. 3.29C). Similar to OSM, the OSMR was significantly increased in IL-6R $\alpha^{\Delta/\Delta}$ mice upon HFD feeding compared to control mice upon HFD feeding as well as to IL-6R $\alpha^{\Delta/\Delta}$ upon NCD feeding (Fig. 3.29C). The CNTFR revealed a significant decrease upon HFD feeding but no alterations between genotypes (Fig. 3.29C). EBI-3 was significantly increased in control mice upon HFD feeding whereas IL-6R $\alpha^{\Delta/\Delta}$ displayed only a tendency to increased EBI-3 upon HFD feeding compared to NCD feeding (Fig. 3.29D). Similar to CNTFR, LIFR was decreased upon HFD feeding both in control as well as in

IL-6R $\alpha^{\Delta/\Delta}$ mice (Fig. 3.29D). Surprisingly, gp130 revealed a significant decrease in IL-6R $\alpha^{\Delta/\Delta}$ mice upon HFD feeding compared to mice upon NCD feeding (Fig. 3.29D).

In summary, determination of IL-6 type cytokines and receptors expression in tumor livers of control and IL-6R α deficient animals under both dietary conditions failed to directly clarify which factor compensates for IL-6R α -deficiency in HCC development upon HFD feeding and needs further investigation.

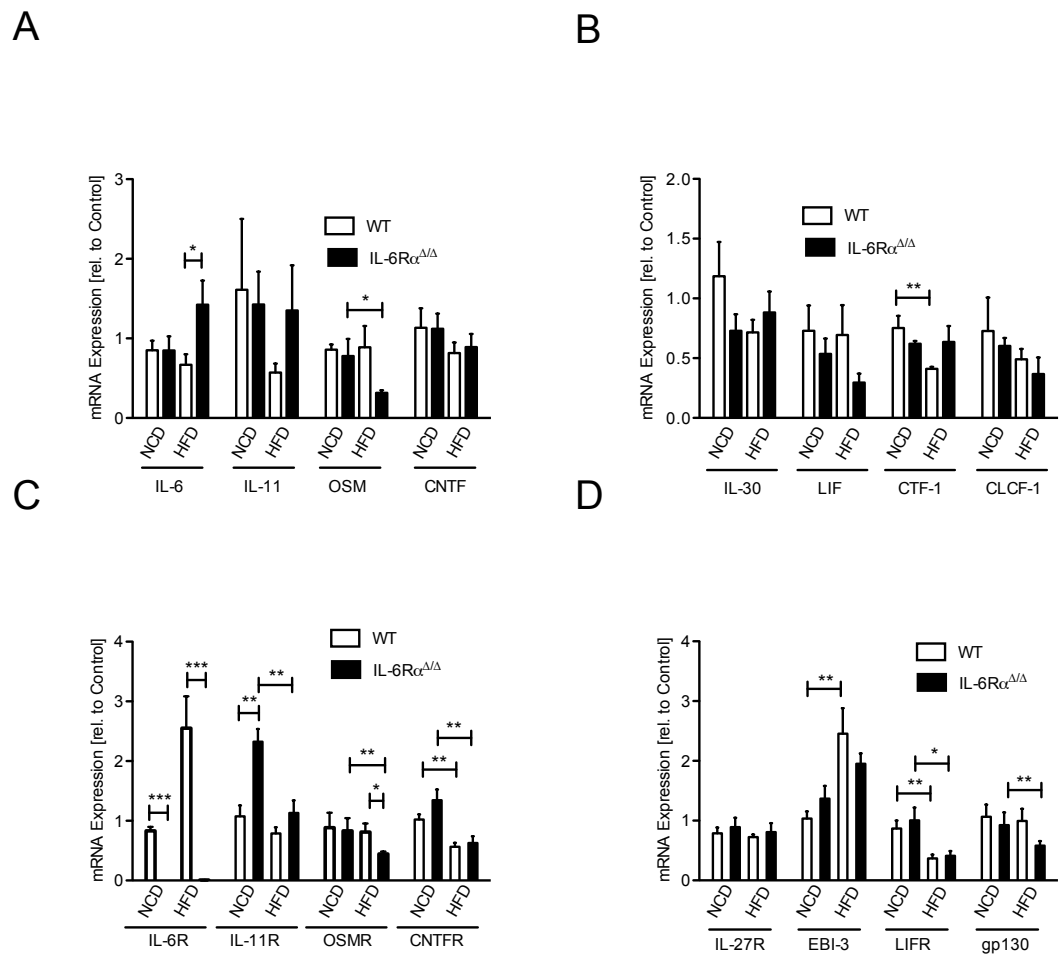


Figure 3.29: **IL-6 type cytokines and receptors in tumor livers of control and IL-6R $\alpha^{\Delta/\Delta}$ mice**

(A) qPCR of IL-6, IL-11, OSM and CNTF in livers from DEN-injected 8 month control and IL-6R $\alpha^{\Delta/\Delta}$ mice (n=6). (B) qPCR expression of IL-30, LIF, CTF-1 and CLCF-1 in livers from DEN-injected 8 month control and IL-6R $\alpha^{\Delta/\Delta}$ mice (n=6). (C) qPCR of IL-6R, IL-11R, OSMR and CNTFR in livers from DEN-injected 8 month control and IL-6R $\alpha^{\Delta/\Delta}$ mice (n=6). (D) qPCR of IL-27R, EBI-3, LIFR and gp130 in livers from DEN-injected 8 month control and IL-6R $\alpha^{\Delta/\Delta}$ mice (n=6). Displayed values are means \pm S.E.M.; *, $p \leq 0.05$; **, $p \leq 0.01$; ***, $p \leq 0.001$ versus control.

3.9 The cell-type specific role of the IL-6R α in the development of HCC

The expression of the IL-6R α is restricted to certain types of cells including hepatocytes, myeloid cells and T cells. To investigate the cell specific role of IL-6 signaling in the development of hepatocellular carcinoma, conditional IL-6R α -deficient mice were generated. Therefore IL-6R $\alpha^{fl/fl}$ mice were crossed to mice expressing the Cre recombinase under the control of both the mouse albumin regulatory elements and the α -fetoprotein enhancers (AlfpCre transgene), under the control of the murine lysozyme M gene (LysMcre) and under the control of the CD4 enhancer/ promoter/silencer, respectively [Wunderlich *et al.*, 2010; Lee *et al.*, 2001; Kellendonk *et al.*, 2000; Clausen *et al.*, 1999]. These mice were further intercrossed with siblings leading to hepatocyte specific (IL-6R α^{L-KO}), myeloid specific (IL-6R α^{M-KO}) and T cell specific (IL-6R α^{T-KO}) deletion of the IL-6R α . IL-6R $\alpha^{fl/fl}$ mice served as controls for all groups throughout experiments.

To investigate the cell-type specific role of IL-6 signaling in the development of hepatocellular carcinoma under normal and obese conditions, male IL-6R $\alpha^{fl/fl}$, IL-6R $\alpha^{\Delta/\Delta}$, IL-6R α^{L-KO} , IL-6R α^{M-KO} and IL-6R α^{T-KO} mice were treated with DEN as described before and separated after weaning in cohorts fed either a NCD or HFD for 8 month. To examine whether IL-6R α deficiency in different cell types has an impact on metabolic or inflammatory state, different parameters were measured.

3.9.1 Less effects on body weight through HFD feeding in IL-6R α^{L-KO} , IL-6R α^{M-KO} and IL-6R α^{T-KO} mice

Upon NCD feeding no differences in body weight could be detected between the genotypes (Fig. 3.30A). In contrast to control and IL-6R $\alpha^{\Delta/\Delta}$ mice upon HFD feeding, no differences could be detected in IL-6R α^{L-KO} , IL-6R α^{M-KO} and IL-6R α^{T-KO} mice between NCD and HFD feeding (Fig. 3.30A). To determine the extent of lipid burden in the blood, cholesterol and triglyceride level in the serum were measured (Fig. 3.30B/C). Cholesterol measurement revealed similar levels in all genotypes upon NCD feeding before DEN treatment (Fig. 3.30B). No alteration in Cholesterol levels could be detected in IL-6R α^{L-KO} , IL-6R α^{M-KO} and IL-6R α^{T-KO} mice after DEN treatment compared to non-treated animals whereas Cholesterol levels significantly increased in control and IL-6R $\alpha^{\Delta/\Delta}$ upon NCD feeding (Fig. 3.30B). HFD data were not available at this point. Triglyceride levels were completely unaltered between treated and non-treated mice and between genotypes (Fig. 3.30C).

Taken together, these data demonstrate that HFD exposure causes similar levels of obesity in control and IL-6R $\alpha^{\Delta/\Delta}$ mice upon DEN induction, but less effects of HFD feeding in IL-6R α^{L-KO} , IL-6R α^{M-KO} and IL-6R α^{T-KO} mice.

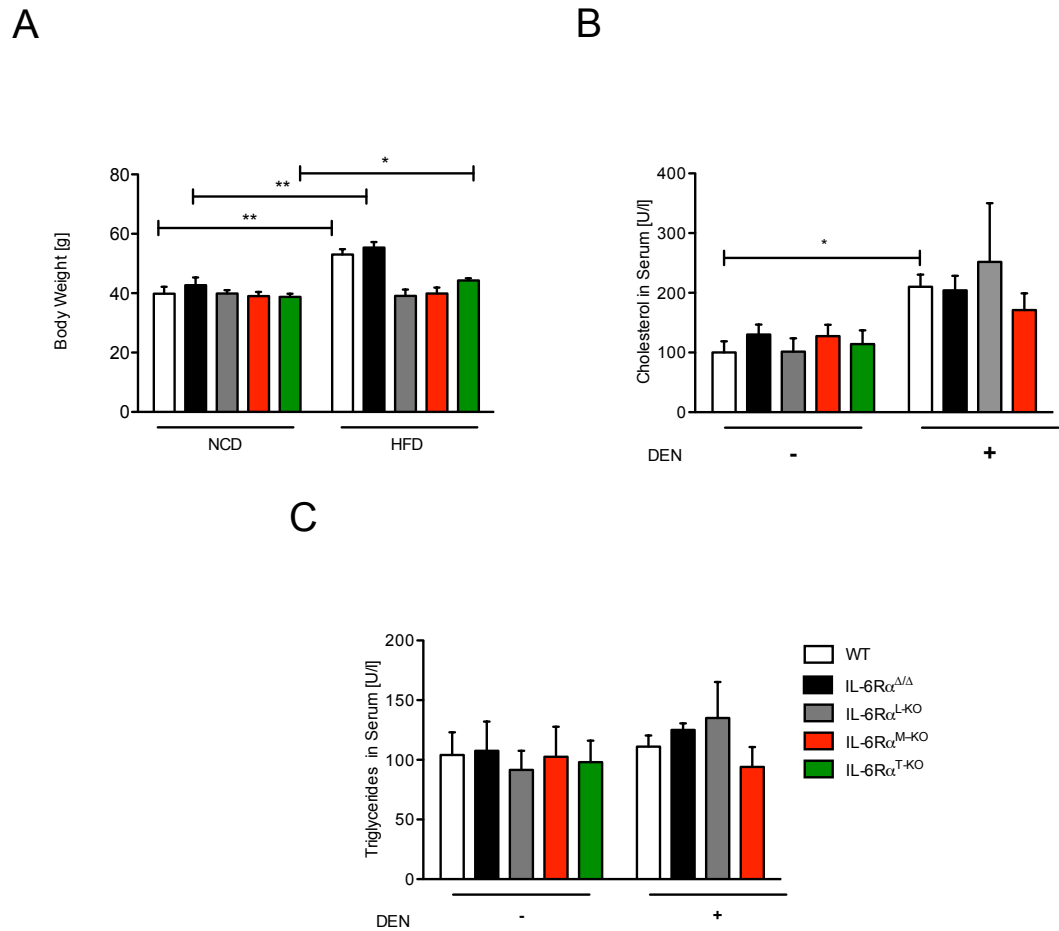


Figure 3.30: **Metabolic status of control, IL-6R $\alpha^{\Delta/\Delta}$, IL-6R α^{L-KO} , IL-6R α^{M-KO} and IL-6R α^{T-KO} mice**

(A) Weight determination of 8 mo DEN-injected control, IL-6R $\alpha^{\Delta/\Delta}$, IL-6R α^{L-KO} , IL-6R α^{M-KO} and IL-6R α^{T-KO} mice (n=15) (B) Examination of serum cholesterol level and (C) serum triglyceride level of untreated (-) or DEN-injected (+) 8 mo control, IL-6R $\alpha^{\Delta/\Delta}$, IL-6R α^{L-KO} , IL-6R α^{M-KO} and IL-6R α^{T-KO} mice (n=6). Displayed values are means \pm S.E.M.; *, $p \leq 0.05$; **, $p \leq 0.01$; ***, $p \leq 0.001$ versus control.

3.9.2 IL-6R α^{T-KO} mice are protected against DEN-induced HCC even on HFD

In the next step tumor development in 8 month old DEN-treated control, IL-6R $\alpha^{\Delta/\Delta}$, IL-6R α^{L-KO} , IL-6R α^{M-KO} and IL-6R α^{T-KO} mice that had been exposed to either a NCD or HFD were investigated by visual inspection. IL-6R α^{L-KO} mice on NCD revealed a tendency for decreased tumor numbers compared to control mice, whereas IL-6R α^{M-KO} mice had no differences in tumor burden upon NCD feeding (Fig. 3.31A/B). Surprisingly, IL-6R α^{T-KO} mice upon NCD feeding exhibited almost the same protection for tumor development as IL-6R $\alpha^{\Delta/\Delta}$ on NCD (Fig. 3.31A/B). In line with previous experiments, obesity increased tumor burden in control mice, IL-6R $\alpha^{\Delta/\Delta}$, IL-6R α^{L-KO} and IL-6R α^{M-KO} mice (Fig. 3.31A/B). Only IL-6R α^{T-KO} mice were almost protected against DEN-induced HCC even upon HFD feeding (Fig. 3.31A/B). In contrast to IL-6R $\alpha^{\Delta/\Delta}$ mice, IL-6R α^{T-KO} mice revealed no significant difference in tumor number <2mm upon NCD feeding whereas upon HFD feeding IL-6R α^{T-KO} mice had less tumors <2mm compared to control mice, similar to IL-6R $\alpha^{\Delta/\Delta}$ mice (Fig. 3.31C). Additionally, IL-6R α^{T-KO} mice exhibited significantly less tumors >2mm upon NCD feeding as well as upon HFD feeding compared to control mice (Fig. 3.31D).

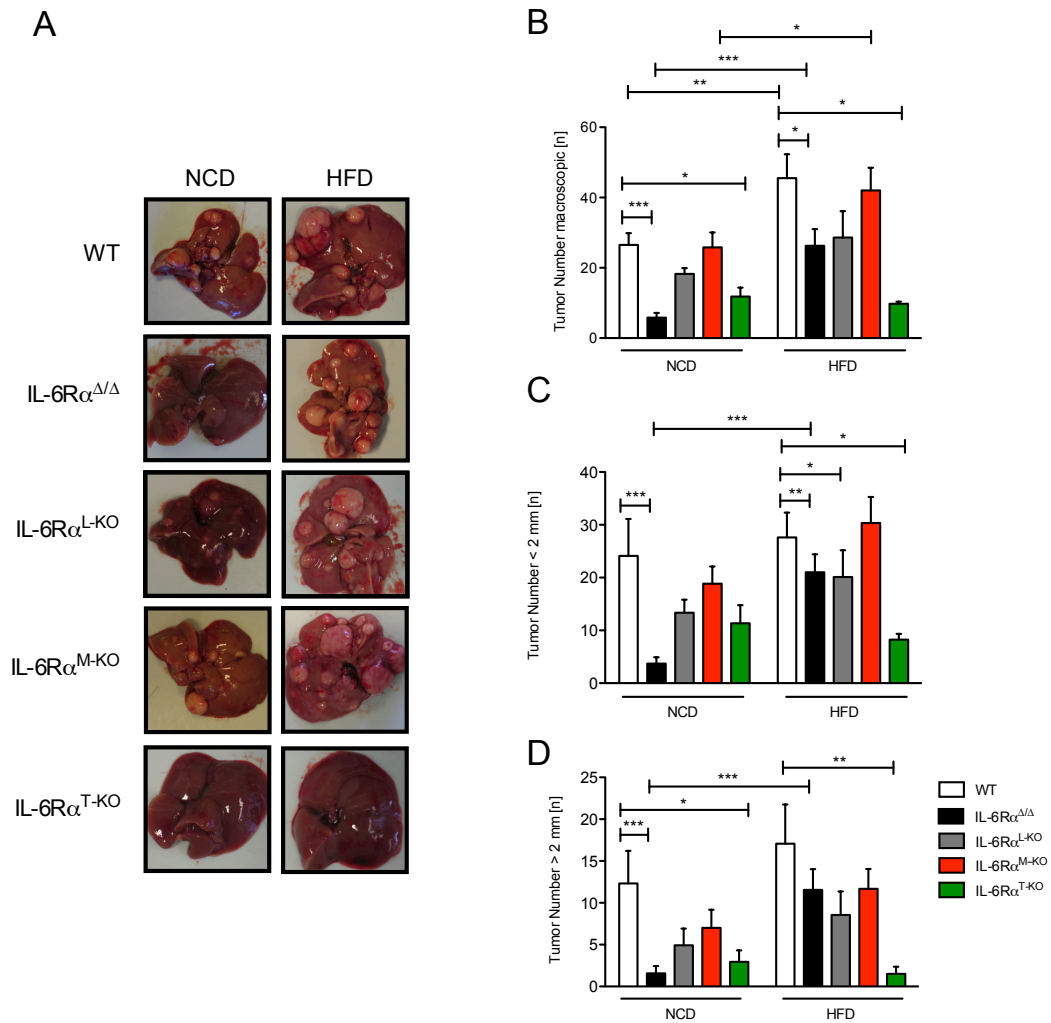


Figure 3.31: **Tumor burden macroscopic in control, IL-6R $\alpha^{\Delta/\Delta}$, IL-6R α^{L-KO} , IL-6R α^{M-KO} and IL-6R α^{T-KO} mice**

(A) Livers of 8 mo control, IL-6R $\alpha^{\Delta/\Delta}$, IL-6R α^{L-KO} , IL-6R α^{M-KO} and IL-6R α^{T-KO} mice injected with 25 mg/kg BW DEN at 15 days of age. (B) Quantitation of macroscopic tumor multiplicity determined by visual inspection in DEN-injected 8 mo control, IL-6R $\alpha^{\Delta/\Delta}$, IL-6R α^{L-KO} , IL-6R α^{M-KO} and IL-6R α^{T-KO} mice (n=15). (C) Enumeration of tumor number for < 2 mm (D) and > 2 mm as determined by visual inspection of DEN-injected 8 mo control, IL-6R $\alpha^{\Delta/\Delta}$, IL-6R α^{L-KO} , IL-6R α^{M-KO} and IL-6R α^{T-KO} mice (n=15). Displayed values are means \pm S.E.M.; *, $p \leq 0.05$; **, $p \leq 0.01$; ***, $p \leq 0.001$ versus control.

Hepatocyte steatosis can sequentially lead to the development of liver damage and steatohepatitis which are forerunners of HCC development. As an indirect indicator of liver damage, the activity of the liver AST and ALT were measured in control, IL-6R $\alpha^{\Delta/\Delta}$, IL-6R α^{L-KO} , IL-6R α^{M-KO} and IL-6R α^{T-KO} mice on NCD

before and after DEN treatment (Fig. 3.32A/B). AST and ALT level were not significantly different in the serum of control, IL-6R $\alpha^{\Delta/\Delta}$, IL-6R α^{L-KO} , IL-6R α^{M-KO} and IL-6R α^{T-KO} mice before DEN treatment (Fig. 3.32A/B). After DEN treatment serum AST level significantly increased to the same extent in control, IL-6R $\alpha^{\Delta/\Delta}$, IL-6R α^{M-KO} and IL-6R α^{T-KO} mice, whereas IL-6R α^{L-KO} revealed a significant increase after DEN treatment compared to other genotypes after DEN treatment (Fig. 3.32A). No alteration of serum ALT level could be observed between genotypes after DEN treatment (Fig. 3.32B).

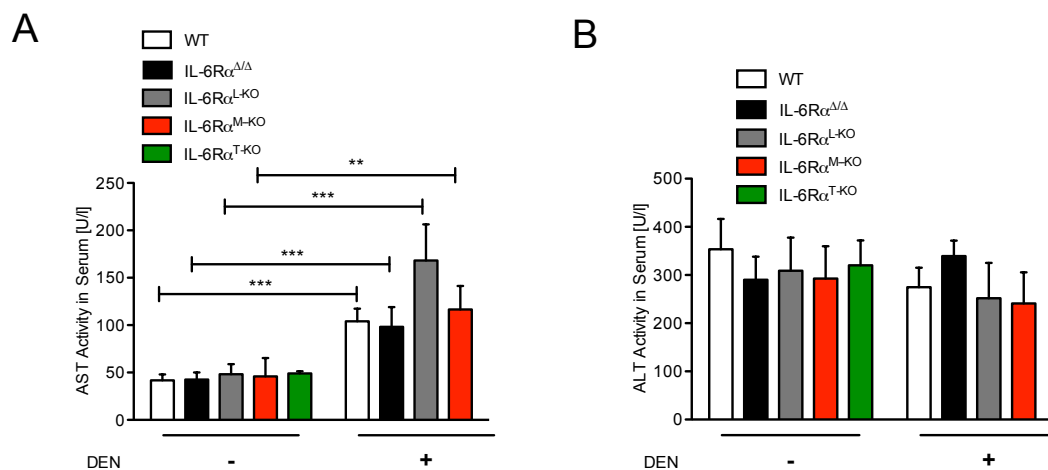


Figure 3.32: Liver damage of control, IL-6R $\alpha^{\Delta/\Delta}$, IL-6R α^{L-KO} , IL-6R α^{M-KO} and IL-6R α^{T-KO} mice

(A) Investigation of AST and (B) ALT activity in serum of untreated (-) or DEN-injected (+) 8 mo control, IL-6R $\alpha^{\Delta/\Delta}$, IL-6R α^{L-KO} , IL-6R α^{M-KO} and IL-6R α^{T-KO} mice (n=6). Displayed values are means \pm S.E.M.; *, $p \leq 0.05$; **, $p \leq 0.01$; ***, $p \leq 0.001$ versus control.

Histological investigation of HE-stained liver sections confirmed that NCD-fed IL-6R α^{L-KO} and IL-6R α^{M-KO} mice had no significant difference in number of HCC foci when compared to NCD-fed control mice (Fig. 3.33A). Strikingly, HFD feeding increased the carcinogenic capability of DEN in IL-6R α^{M-KO} animals but not in IL-6R α^{L-KO} mice (Fig. 3.33A). Furthermore decreased number of foci in IL-6R α^{T-KO} mice could not be confirmed by this analysis (Fig. 3.33A). HFD data for IL-6R α^{T-KO} mice were not available at this point. Determination of tumor size

exhibited significant increase of foci size in $IL-6R\alpha^{L-KO}$ and $IL-6R\alpha^{M-KO}$ mice upon NCD feeding compared to control mice, whereas $IL-6R\alpha^{T-KO}$ mice revealed no alterations in tumor size compared to control mice upon NCD feeding (Fig. 3.33B). Strikingly, tumor size in control, $IL-6R\alpha^{\Delta/\Delta}$, $IL-6R\alpha^{M-KO}$ and $IL-6R\alpha^{T-KO}$ mice did not change upon HFD feeding compared to NCD feeding, whereas foci size significantly decreased in $IL-6R\alpha^{L-KO}$ mice upon HFD feeding compared to NCD feeding (Fig. 3.33B).

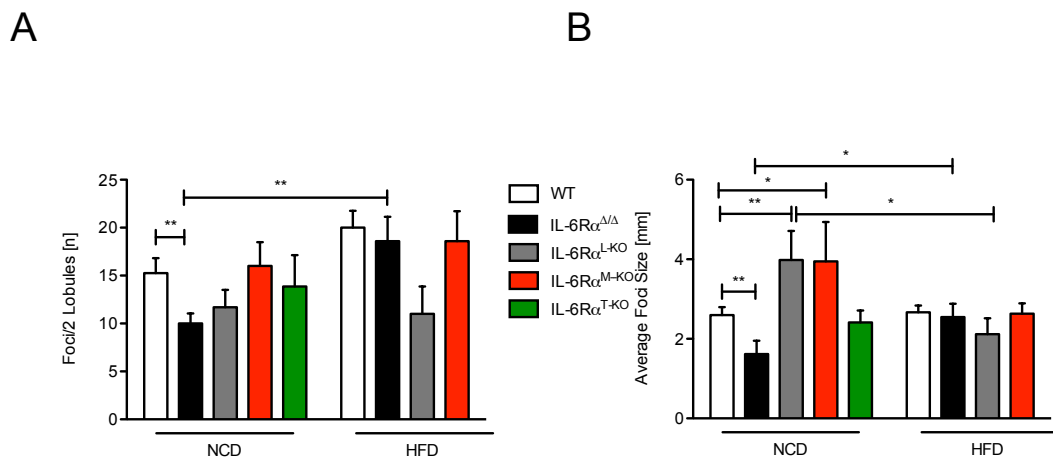


Figure 3.33: **Tumor burden microscopic in control, $IL-6R\alpha^{\Delta/\Delta}$, $IL-6R\alpha^{L-KO}$, $IL-6R\alpha^{M-KO}$ and $IL-6R\alpha^{T-KO}$ mice**

(A) Quantitation of tumor number per 2 lobules counted on liver sections from 8 mo control, $IL-6R\alpha^{\Delta/\Delta}$, $IL-6R\alpha^{L-KO}$, $IL-6R\alpha^{M-KO}$ and $IL-6R\alpha^{T-KO}$ mice (n=15). (B) Quantitation of tumor size measured in the big liver lobe of DEN-injected 8 mo control, $IL-6R\alpha^{\Delta/\Delta}$, $IL-6R\alpha^{L-KO}$, $IL-6R\alpha^{M-KO}$ and $IL-6R\alpha^{T-KO}$ mice (n=15). Displayed values are means \pm S.E.M.; *, $p \leq 0.05$; **, $p \leq 0.01$; ***, $p \leq 0.001$ versus control. Data produced in collaboration with Beate Straub.

To assess the extent of inflammation, infiltrating immune cells were quantitated. This analysis revealed a significant reduced inflammation in livers of $IL-6R\alpha^{T-KO}$ mice upon NCD feeding compared to control mice upon NCD feeding, similar to $IL-6R\alpha^{\Delta/\Delta}$ mice (Fig. 3.34A), whereas $IL-6R\alpha^{L-KO}$ and $IL-6R\alpha^{M-KO}$ mice exhibited no significant differences. Upon HFD feeding liver inflammation significantly increased in control, $IL-6R\alpha^{\Delta/\Delta}$ and $IL-6R\alpha^{L-KO}$ animals but not in

IL-6R α^{M-KO} mice (Fig. 3.34A). HFD data of IL-6R α^{T-KO} mice were not available at this point.

As mentioned before, HFD feeding was observed to induce hepatocyte steatosis that can result in HCC development. Similar to IL-6R $\alpha^{\Delta/\Delta}$ mice, livers of IL-6R α^{T-KO} mice fed a NCD revealed a significantly reduced extent of steatosis compared to control mice whereas IL-6R α^{L-KO} and IL-6R α^{M-KO} mice exhibited no alteration (Fig. 3.34B). In contrast to IL-6R $\alpha^{\Delta/\Delta}$ mice, the extent of steatosis did not increase both in IL-6R α^{L-KO} and IL-6R α^{M-KO} mice upon HFD feeding compared to NCD fed mice (Fig. 3.34B). HFD data of IL-6R α^{T-KO} mice were not available at this point.

Counting of necrotic hepatocytes per two lobules revealed significant reduction in IL-6R α^{T-KO} mice on NCD compared to control mice upon NCD feeding, contrary to IL-6R $\alpha^{\Delta/\Delta}$ mice (Fig. 3.34C). Similar to inflammation status upon HFD feeding, necrotic cells increased in IL-6R $\alpha^{\Delta/\Delta}$, IL-6R α^{L-KO} and IL-6R α^{M-KO} mice but not in IL-6R α^{M-KO} mice compared to HFD feeding (Fig. 3.34C). HFD data of IL-6R α^{T-KO} mice were not available at this point.

Assessment of fibrosis which is often connected with the development of liver cancer, revealed no significant alteration between the genotypes. Even upon HFD feeding no significant alteration could be detected in IL-6R α^{L-KO} and IL-6R α^{M-KO} mice compared to NCD feeding, contrary to IL-6R $\alpha^{\Delta/\Delta}$ mice after HFD feeding (Fig. 3.34D). HFD data of IL-6R α^{T-KO} mice were not available at this point.

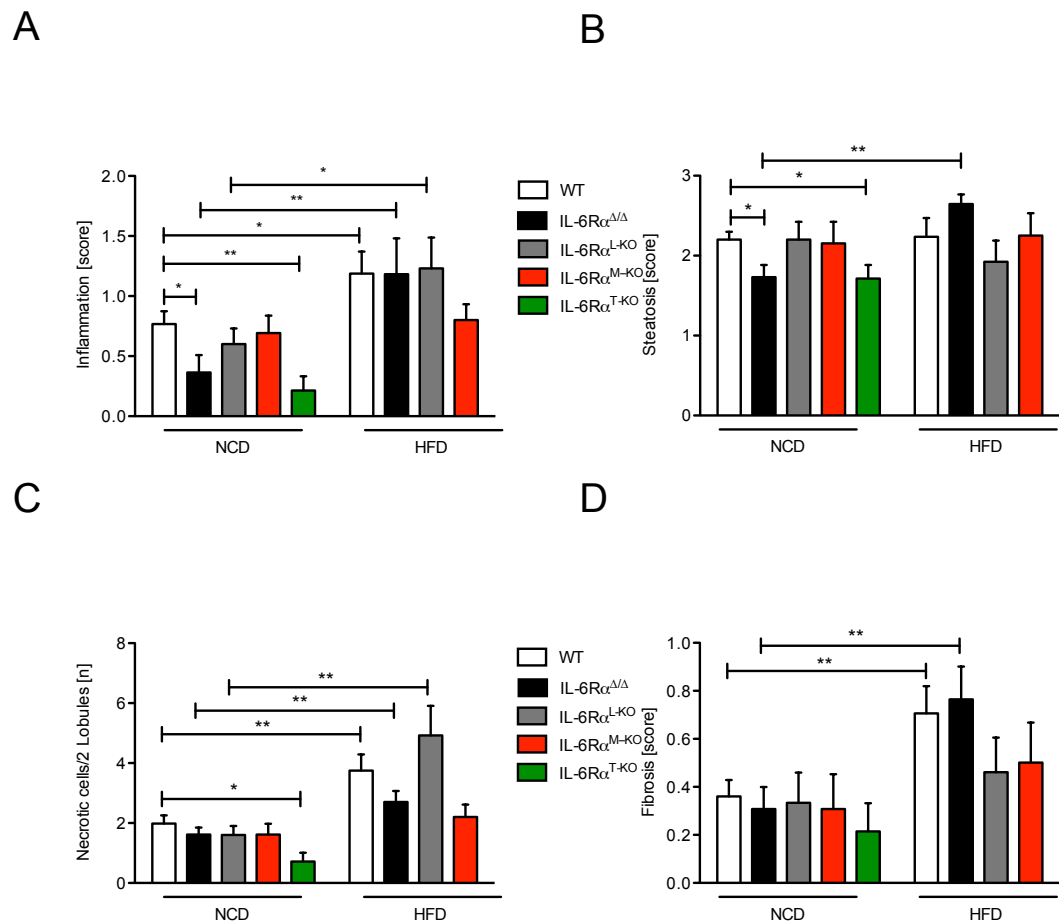


Figure 3.34: Liver status of control, IL-6R $\alpha^{\Delta/\Delta}$, IL-6R α^{L-KO} , IL-6R α^{M-KO} and IL-6R α^{T-KO} mice

(A) Quantitation of inflammation measured in the big liver lobe of DEN-injected 8 mo control, IL-6R $\alpha^{\Delta/\Delta}$, IL-6R α^{L-KO} , IL-6R α^{M-KO} and IL-6R α^{T-KO} . 1 = mild inflammation (mild portal inflammation, 3-5 single cell necrosis, no grouped necrosis); 2 = moderate inflammation (moderate portal inflammation, 6-9 single cell necrosis, 1 grouped necrosis); 3 = severe inflammation (severe portal inflammation, more than 10 single cell necrosis, more than 1 grouped necrosis) (n=15). (B) Quantitation of steatosis measured in the big liver lobe of DEN-injected 8 mo control, IL-6R $\alpha^{\Delta/\Delta}$, IL-6R α^{L-KO} , IL-6R α^{M-KO} and IL-6R α^{T-KO} . 1 = 0 - 10%; 2 = 11 - 50 %; 3 = above 50 % (n=15) (C) Quantitation of necrotic cells measured in the big liver lobe of DEN-injected 8 mo control, IL-6R $\alpha^{\Delta/\Delta}$, IL-6R α^{L-KO} , IL-6R α^{M-KO} and IL-6R α^{T-KO} . (n=15) (D) Quantitation of fibrosis measured in the big liver lobe of DEN-injected 8 mo control, IL-6R $\alpha^{\Delta/\Delta}$, IL-6R α^{L-KO} , IL-6R α^{M-KO} and IL-6R α^{T-KO} . 1 = increased portal connective tissue; 2 = early formation of septa (n = 15). Displayed values are means \pm S.E.M.; *, $p \leq 0.05$; **, $p \leq 0.01$; ***, $p \leq 0.001$ versus control. Data produced in collaboration with Beate Straub.

Regulatory T cells (T^{regs}) are the main regulators of the immune system. IL-6 plays a crucial role in differentiation and activation of regulatory T cells and it is known that different types of cancer are correlated with increased numbers of T^{regs} which suppress the immune response and promote cancer development [Haruta *et al.*, 2011; Mougiakakos, 2011; Mougiakakos *et al.*, 2010]. To investigate whether T^{regs} play a role in the IL-6 dependent development of HCC, control, IL-6R $\alpha^{\Delta/\Delta}$ and IL-6R α^{T-KO} mice were injected with 1 mg α -CD25 antibody *i.p.* at 13 days of age to deplete T^{regs} in the initial phase of tumor development. As before these mice were injected with 25 mg/kg BW DEN at 15 days of age *i.p.* and exposed to NCD. Tumor investigation after 8 month revealed a duplication of tumor number both in IL-6R $\alpha^{\Delta/\Delta}$ and IL-6R α^{T-KO} mice compared to control mice suggesting a crucial role of T^{regs} in the IL-6 mediated development of HCC (Fig. 3.35A). Collaboration with the lab of Ruslan Medzhitov indicated that IL-6 signaling on effector T cells is necessary to release them from suppression by T^{regs} . In this context natural killer like T cells (NKT cells) become the focus of attention. To investigate the role of NKT cells, eight weeks old control, IL-6R $\alpha^{\Delta/\Delta}$ and IL-6R α^{T-KO} mice were injected *i.p.* with 4 μ g α Galactosylceramide (α GalCer) to specifically activate NK T cells and sacrificed at different time points. This analysis revealed increased ALT and AST level in IL-6R $\alpha^{\Delta/\Delta}$ and IL-6R α^{T-KO} mice upon α GalCer induction (Fig. 3.35B/C). To determine expression of IL-6R α specifically on NKT cells, activated NKT cells were analysed by Fluorescence-activated cell sorting (Facs) analysis, revealing that maximum 2% of NKT cells express the IL-6R α (Fig. 3.35D).

Taken together, these data demonstrate that IL-6R α signaling in T cells play an essentielle role whereas IL-6R α signaling in hepatocytes and macrophages is only minor involved in HCC development. In contrast, IL-6R α signaling in macrophages seems to be more important upon HFD feeding indicated by missing alteration of liver damage and inflammation upon HFD feeding.

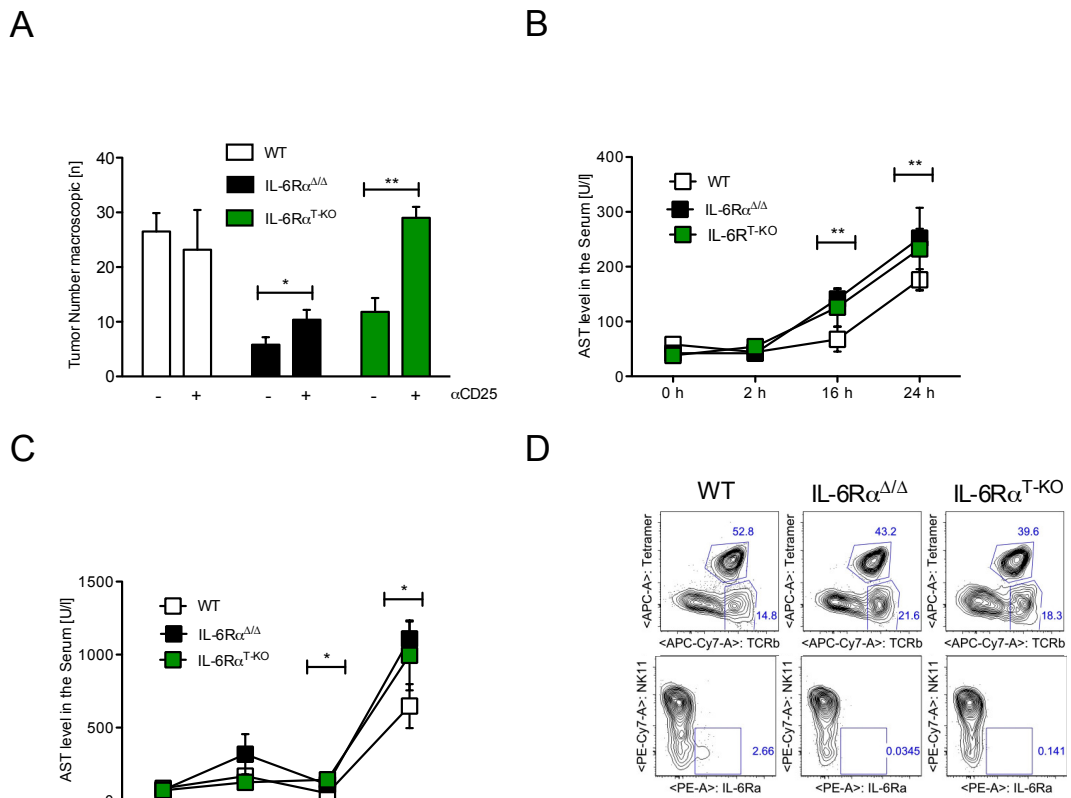


Figure 3.35: Tumor burden macroscopic in control, IL-6Rα^{Δ/Δ} and IL-6Rα^{T-KO} mice
(A) Quantitation of macroscopic tumor multiplicity determined by visual inspection in DEN-injected 8 mo control, IL-6Rα^{Δ/Δ} and IL-6Rα^{T-KO} mice (n=6) **(B)** Determination of serum AST (n=5) and **(C)** serum ALT activity to assess liver damage in 8 wk control, IL-6Rα^{Δ/Δ} and IL-6Rα^{T-KO} mice fed on a NCD sacrificed at the indicated time points after a 4 μg αGalCer injection (n=5). **(D)** FACS analysis of NKT cells, gated for tetramer and IL-6Rα (n=4). Data produced in collaboration with Christoph Vahl. Displayed values are means ± S.E.M.; *, p ≤ 0.05; **, p ≤ 0.01; ***, p ≤ 0.001 versus control.

4 Discussion

HCC is the most common primary liver cancer worldwide with about 700.000 new cases per year [El-Serag & Rudolph, 2007]. Only 3-5 % of the patients survive due to very limited treatment strategies. All main risk factors for HCC, such as Hepatitis B/C and alcoholic or non-alcoholic steatohepatitis, cause liver damage and chronic inflammation, characterizing HCC as a classic case of inflammation linked cancer [Mantovani *et al.*, 2008; Fattovich *et al.*, 2004]. This chronic hepatic inflammation leads to cell death and consequently to compensatory proliferation of hepatocytes and ultimately to tumor development [Bisgaard *et al.*, 1998].

Epidemiological studies identified HCC as the strongest obesity-associated cancer [Calle *et al.*, 2003]. The excessive weight gain during obesity is associated with a chronic low grade inflammatory state as a consequence of infiltrating immune cells into the white adipose tissue (WAT) and the liver [Xu *et al.*, 2003; Weisberg *et al.*, 2003; Olefsky & Glass, 2010]. During obesity, adipocytes rise in size and increasing mechanical stress results in ruption and leakage of adipocytes and in liberating of free fatty acids into circulation [Ferrante, 2007]. This in turn leads to the recruitment and activation of immune cells, such as macrophages and T cells, to the WAT. These immune cells release cytokines, such as $TNF\alpha$ and IL-6 [Nishimura *et al.*, 2009; Xu *et al.*, 2003; Hotamisligil *et al.*, 1993].

Human studies could demonstrate that the concentration of IL-6 in serum is increased in situations of chronic inflammation including alcoholic hepatitis, HBV and HCV infections and steatohepatitis, conditions that may lead to development of HCC [Abiru *et al.*, 2006]. IL-6 concentrations are also increased in patients with HCC compared to normal subjects, but whether IL-6 is causal or contributory to HCC is still unknown [Soresi *et al.*, 2006]. Recent studies in mouse models de-

scribed a pivotal role of IL-6 in the development of chemical induced HCC but the underlying mechanism is still poorly understood [Naugler *et al.*, 2007].

In contrast to other studies, the current study used the conditional gene targeting to disrupt the IL-6R α instead of IL-6 to examine the intracellular effect of IL-6 signaling in chemical induced HCC and the influence of obesity to this mechanism. To address this question, IL-6R $\alpha^{fl/fl}$ (controls) and IL-6R $\alpha^{\Delta/\Delta}$ mice were injected with DEN to induce HCC development and were exposed to either NCD or HFD feeding after weaning for 8 month.

Furthermore, conditional gene targeting has been applied to facilitate hepatocyte specific, myeloid specific and T cell specific disruption of the IL-6R to investigate the cell type specific role of IL-6 signaling in the development of HCC, which would be not possible if IL-6 knock out mice would be used. Therefore, IL-6R $\alpha^{fl/fl}$ (controls), IL-6R $\alpha^{\Delta/\Delta}$, IL-6R α^{L-KO} , IL-6R α^{M-KO} and IL-6R α^{T-KO} mice were injected with DEN to induce HCC development and were exposed to either NCD or HFD feeding for 8 month.

4.1 IL-6R α deficiency protects against DEN-induced liver carcinogenesis, but obesity abrogates this effect

The current study could demonstrate that IL-6R α signaling promotes DEN-induced liver carcinogenesis accompanied by increased inflammation. The macroscopic tumor investigation in the current study could confirm that IL-6R α -deficiency upon NCD feeding protects against DEN induced HCC - a finding that was also validated by pathological investigation [Naugler *et al.*, 2007]. Moreover, further pathological investigations of the tumor livers revealed decreased inflammation and steatosis upon IL-6R α -deficiency under NCD conditions, which is in line with Naugler *et al.* [2007] findings. However, abrogation of IL-6R α -signaling did not decrease liver AST level after DEN treatment in contrast to earlier observations in IL-6-deficient mice [Naugler *et al.*, 2007]. Also, the amount of necrotic

cells in livers lacking the IL-6R α upon NCD feeding were contradictory to previous results of Naugler *et al.* [2007]. While the authors postulate a decrease in necrosis in IL-6-deficient mice, the current study revealed similar amounts of necrotic cells in control and IL-6R $\alpha^{\Delta/\Delta}$ mice upon NCD feeding.

Additional studies of HCC development demonstrate that HFD-induced obesity increases DEN-induced HCC development in control mice which is in line with earlier observations [Park *et al.*, 2010]. Surprisingly, HFD feeding abrogates the protective effect of IL-6R α deficiency on HCC development which is in contrast to previous findings [Park *et al.*, 2010]. The results of the current study demonstrate that obesity abrogates the protective effect of IL-6R α deficiency and promotes HCC development by inducing inflammatory conditions mediated by elevated levels of TNF α and IL-6.

Earlier studies described that spontaneously developed liver damage in Nemo/IKK $\gamma^{\Delta hep}$ mice is promoted by HFD-feeding and results in tumor development [Wunderlich *et al.*, 2008]. Furthermore, Park *et al.* [2010] demonstrated recently that both dietary- and genetically-induced obesity in mice increased HCC development and progression in control mice compared to NCD-fed control mice. This study demonstrated that HFD-induced increase in HCC development and progression in control mice is a consequence of obesity-induced elevation of both TNF α and IL-6. In line with these findings, the current study can also confirm increased levels of TNF α and IL-6 in tumor livers upon obesity. Interestingly, also upon IL-6R α deficiency HFD feeding leads to an increase of TNF α and IL-6 in the tumor livers, underlining the differences in tumor development between IL-6- and IL-6R α -deficiency. Further investigation of inflammatory status of the liver revealed increased liver damage reflected by increased liver AST level after DEN treatment but no differences between genotypes or diets in contrast to earlier observations [Park *et al.*, 2010]. Moreover, pathological analysis of tumor livers of the different cohorts revealed increased inflammation upon HFD feeding, which was also demonstrated by Park *et al.* [2010]. Differences between IL-6-

and IL-6R α deficiency turn up again in inflammatory status, demonstrated by increased inflammation also in IL-6R α -deficient livers upon HFD feeding. However, the number of necrotic cells and the existing fibrosis were increased upon HFD feeding.

Taken together, there is a differential effect of previously described IL-6 deficiency versus the results on IL-6R α deficiency in obesity-induced HCC development. Both IL-6 and IL-6R α deficiency in lean mice protect against HCC development, whereas in the obese state IL-6R $\alpha^{\Delta/\Delta}$ mice exhibit similar tumor numbers as control mice but IL-6 knock out mice fail to develop HCC under these conditions [Park *et al.*, 2010]. In line with these reported differential effects, a recent publication demonstrated a similarly different experimental outcome in IL-6- and IL-6R α -deficient mice when addressing the function of IL-6 in wound healing [McFarland-Mancini *et al.*, 2010]. While IL-6-deficient mice demonstrated greatly reduced wound healing capacity, IL-6R α deficiency showed only slightly impaired wound healing. Further analysis of IL-6R α and IL-6 double knock out mice revealed that IL-6R α deficiency dominated wound healing capacity. Thus, these studies and the latest findings point towards a more complex role of IL-6R α signaling in inflammatory processes than assumed so far.

4.2 Similar extent of obesity in control and IL-6R $\alpha^{\Delta/\Delta}$ mice in the DEN-induced HCC model

One explanation for the different outcome of HCC incidence between IL-6 and IL-6R α deficient mice could be an altered influence of HFD feeding to these mice. However, the current study demonstrated that control and IL-6R $\alpha^{\Delta/\Delta}$ mice revealed no differences concerning glucose and fatty acid metabolism and that HFD exposure causes similar levels of obesity in both control and IL-6R $\alpha^{\Delta/\Delta}$ mice upon DEN induction. Moreover, HFD feeding results in IL-6 resistance in control mice resulting in impaired Stat-3 activation.

Investigation of glucose metabolism revealed no alterations in body weight and blood glucose clearance, which is surprising in reference to previous studies which revealed an impaired glucose metabolism in mice with impaired IL-6R α signaling in hepatocytes [Wunderlich *et al.*, 2010]. Hepatic insulin resistance as a consequence of HFD feeding leads to a diminished suppression of hepatic glucose production and thus exhibits a crucial impact on the impairment of whole body glucose metabolism [Li & Yang, 2004]. IL-6 signaling plays an important role in the development of hepatic insulin resistance during obesity and previous observations revealed that IL-6 treatment increases glucose tolerance in rats [Holmes *et al.*, 2008; Klover & Mooney, 2004; Senn *et al.*, 2002]. However, no effects of IL-6R α deficiency could be detected in the current study.

The Insulin levels in the current study revealed no difference between control and IL-6R $\alpha^{\Delta/\Delta}$ mice upon both NCD and HFD feeding. In contrast to that, Park *et al.* [2010] could demonstrate decreased Insulin levels upon IL-6-deficiency after HFD feeding. Furthermore, the decreased triglyceride levels in IL-6 deficient mice upon HFD feeding, could not be observed in IL-6R α deficient mice in the current study. No differences could be observed in fatty acid metabolism, measured by circulating cholesterol or triglycerides, as well as lipid accumulation in the liver.

IL-6 initiates downstream signaling by binding to the IL-6 receptor (IL-6R) whose activation results in multiple downstream signaling events in the liver such as activation of the JAK/Stat-3 pathways Heinrich *et al.* [2003]. Treatment of control mice with IL-6 revealed a robust Stat-3 phosphorylation in the liver. Interestingly, HFD feeding leads to an diminished Stat-3 activation in the liver suggesting an impaired responsiveness to acute IL-6 stimulation as a consequence of obesity. Recent studies could demonstrate that chronically raised IL-6 levels in obesity could cause Insulin resistance and IL-6 resistance [Wunderlich *et al.*, 2013]. This may involve basal increase of Socs protein levels in peripheral organs, such as the liver, similarly to the findings described for basal leptin-derived

signal transduction in the CNS [Wunderlich *et al.*, 2013].

4.3 Obesity and IL-6 increase HCC development through the inhibition of mitochondrial apoptosis

Increased IL-6 levels under inflammatory conditions and in obesity were predicted to inhibit hepatocyte apoptosis, a driving force in DEN-induced HCC development [Park *et al.*, 2010]. The current study could demonstrate that under NCD conditions, loss of IL-6 signaling sensitizes hepatocytes to damage-induced apoptosis by decreased protein levels of anti-apoptotic Bcl-2 protein family member Mcl-1 at the mitochondria without impairments in compensatory proliferation. However, under HFD conditions, hepatocyte apoptosis is inhibited – even in the absence of IL-6R α signaling.

Investigation of hepatocyte apoptosis in the DEN-induced HCC model revealed that IL-6R $\alpha^{\Delta/\Delta}$ mice, which have decreased tumor development, display increased Caspase 3 activity upon NCD feeding which is in line with induction of Caspase 3 as a potent cancer therapy [Tatsukawa *et al.*, 2011]. Furthermore, after acute induction with DEN, an increased Caspase 3 cleavage could be observed, translating into an increase of liver AST levels, which reflects liver damage. These effects were completely blunted upon HFD feeding, which was also reflected in abrogated tumor protection in IL-6R $\alpha^{\Delta/\Delta}$ mice.

Mitochondria represent a central sensory organelle that can respond to DNA damage by outer membrane permeabilization. The current study revealed that increased Caspase 3 activity in IL-6R $\alpha^{\Delta/\Delta}$ mice upon NCD feeding is a consequence of enhanced mitochondrial apoptotic response, demonstrated by elevated release of Cytochrome C from isolated mitochondria after Bax treatment. Consistently, IL-6R α -deficient hepatocytes demonstrated concentration dependent cytosolic Cytochrome C levels in response to DEN as well as increased Cytochrome C at the mitochondria itself. The increased hepatic apoptosis sensitivity of lean

IL-6R α -deficient mice is due to a decrease of anti-apoptotic protein Mcl-1. This effect is completely abolished under HFD conditions, which is reflected in the abrogated protection from tumor development in IL-6R α -deficient mice upon HFD feeding. Notably, protein levels of other Bcl-2 family members were only slightly altered between diets and genotypes.

The balance between anti- and pro-apoptotic members of the Bcl-2 protein family regulates mitochondrial outer membrane permeabilization and the efflux of Cytochrome C in response to cellular damage [Brunelle & Letai, 2009]. One of these anti-apoptotic proteins is Mcl-1 which keeps Bak and Bax separated at the outer membrane of the mitochondria [Tait & Green, 2010; Maurer *et al.*, 2006]. After phosphorylation Mcl-1 is ubiquitinated and degraded, Bax and Bak can assemble which leads to the release of Cytochrome C, activation of caspases and eventually to apoptosis [Tait & Green, 2010; Maurer *et al.*, 2006]. Immunohistochemistry of mouse liver sections and western blot analysis of dissected HCCs underlined the finding that Mcl-1 protein is decreased in HCCs of lean IL-6R α -deficient mice compared to controls, while HFD feeding significantly increased Mcl-1 protein abundance in HCCs of control as well as IL-6R $\alpha^{\Delta/\Delta}$ mice independent from IL-6R α signaling.

Strikingly, qPCR analyses of the Bcl-2 family members revealed largely unaltered transcriptional levels of the corresponding genes suggesting that the reduced Mcl-1 content at the mitochondria of IL-6R $\alpha^{\Delta/\Delta}$ mice might be caused by a posttranslational regulatory mechanism. This results are contrary to earlier findings that Mcl-1 expression is increased in HCC [?].

Along this line, previous studies have clearly demonstrated that Mcl-1 is an anti-apoptotic factor for a subset of human HCC, whose inhibition might have potential in human therapy, but may also result in liver damage and cancer development [Weber *et al.*, 2010; Vick *et al.*, 2009; Fleischer *et al.*, 2006; Schulze-Bergkamen *et al.*, 2006]. It has been previously demonstrated that hepatocyte-specific Mcl-1 inactivation causes spontaneous HCC in old mice as a consequence

of a microenvironment comprising apoptosis sensitive Mcl-1-deficient hepatocytes and compensating adjacent hepatocytes [Weber *et al.*, 2010]. Of note, HCC development in these mice occurs in the absence of chronic inflammation. The current DEN-induced HCC model depends on inflammation and high Mcl-1 protein levels. Moreover, the current study could demonstrate that DEN-induced compensatory proliferation of hepatocytes was comparable between control and IL-6R $\alpha^{\Delta/\Delta}$ mice. Interestingly, Bak protein level are slightly decreased in IL-6R $\alpha^{\Delta/\Delta}$ mice upon NCD feeding, which are protected against HCC. This result is underlined by the recent finding that the compound inactivation of Mcl-1 and BAK not only normalizes apoptosis sensitivity of hepatocytes but also prevents liver cancer development [Hikita *et al.*, 2012].

4.4 GSK-3 β inhibition stabilizes Mcl-1 via IL-6 signaling and under obese conditions in HCC development

The current study could demonstrate that IL-6R α -deficiency decreases Mcl-1 protein levels at the mitochondria without decreasing transcription, suggesting a posttranslational regulation of Mcl-1 within tumor lesions. The present work could provides evidence that GSK-3 β action increases the hepatic Mcl-1 turnover rate in IL-6R α deficiency, thereby decreasing Mcl-1 protein levels. Furthermore, it could be demonstrated that GSK-3 β inactivation by phosphorylation at S9 is required to stabilize Mcl1 during the initial phases of tumorigenesis

Unlike other Bcl-2 family members, Mcl-1 has a dynamic turnover rate [Maurer *et al.*, 2006; Kozopas *et al.*, 1993]. While Mcl-1 expression at the transcriptional level depends on PI3K-mediated signal transduction as well as IL-6-evoked signaling, the dynamic turnover rate of Mcl-1 is controlled by GSK-3 β [Maurer *et al.*, 2006; Jourdan *et al.*, 2003; Epling-Burnette *et al.*, 2001a,b]. Mcl-1 comprises a N-terminal proline, glutamic acid, serine, threonine peptide sequence (PEST domain), which is responsible for its short half-life. Phosphorylation of Mcl-1

in the PEST domain by GSK-3 β leads to its polyubiquitination and subsequent proteasome-mediated degradation, which initiates apoptosis [Maurer *et al.*, 2006].

Investigation of GSK-3 β in the current study revealed a remarkable decrease of phosphorylation in livers of IL-6R $\alpha^{\Delta/\Delta}$ mice upon NCD feeding, also reflected by decreased Mcl-1 protein levels which leads to increased mitochondrial apoptosis and subsequently to decreased tumor numbers. Moreover, in line with the stabilized Mcl-1 levels in IL-6R $\alpha^{\Delta/\Delta}$ mice upon HFD feeding, GSK-3 β phosphorylation is also restored. Consistent with these findings, direct assessment of GSK-3 β activity revealed a significant increase of activity in lean IL-6R $\alpha^{\Delta/\Delta}$ mice, an effect which is abrogated upon HFD feeding. Direct proof about the role of GSK-3 β regarding Mcl-1 stabilization *in vivo*, is provided by the injection of an adeno-associated virus containing a constitutive active GSK-3 β variant (GSK-3 β CA) in control mice. This GSK-3 β CA reduces Mcl-1 protein level in the liver to a similar extent as in IL-6R $\alpha^{\Delta/\Delta}$ mice.

Active GSK-3 β has been previously reported to regulate apoptosis through expression of the BH3 only member PUMA that antagonizes Mcl-1 to sensitize for apoptosis [Charvet *et al.*, 2011]. Investigation of PUMA expression in IL-6R $\alpha^{\Delta/\Delta}$ mice revealed 2-fold increase compared to control mice which is restored under obese conditions. However, in the initial phase of tumor development PUMA expression is unchanged between genotypes. Moreover, PUMA protein level peaked in both genotypes 24h after DEN injection, indicating a GSK-3 β independent mechanism controls PUMA expression under these conditions. This becomes even more clear by the fact that PUMA levels failed to correlate with GSK-3 β activity under acute DEN conditions.

The regulation of GSK-3 β is controlled at multiple levels and its misregulation is known to contribute to the development of numerous diseases such as diabetes, Alzheimer's disease, and cancer [Patel & Woodgett, 2008; Eldar-Finkelman *et al.*, 1999; Eldar-Finkelman & Krebs, 1997; Hanger *et al.*, 1992]. GSK-3 β is a serine/threonine protein kinase that is constantly active. Inactivation of GSK-3 β by

phosphorylation at serin residue 9 (S9) increases stabilization and accumulation of Mcl-1 and therefore prevents apoptosis [Ding *et al.*, 2007]. GSK-3 β S9 phosphorylation mainly occurs through the action of Phosphatidylinositol 3-kinases (PI3K) signaling as a substrate of AKT phosphorylation in response to insulin [Cross *et al.*, 1995]. The current work revealed that PI3K/AKT signaling is active but not altered in IL-6R $\alpha^{\Delta/\Delta}$ mice during HCC development independent from dietary conditions. Determination of the role of PI3K signaling in DEN-induced HCC development of HFD fed mice by treating HCC-bearing HFD fed control mice with a PI3K inhibitor resulted in reactivation of GSK-3 β leading to reduced levels of Mcl-1. This reduction of Mcl-1 transfers into increased number of apoptotic cells and a reduced proliferation in the liver of mice with inhibited PI3K. This results are in line with previous studies, demonstrating that the PI3K/AKT pathway transmits anti-apoptotic survival signals and is likely involved in mitigating apoptosis in a substantial fraction of human tumors [Jiang & Liu, 2008; Cully *et al.*, 2006]. Despite all that, the formation of PIP3 was similar between diets and genotypes. Even the activity of downstream kinases such as PDK and AKT were unaltered between diets and genotypes indicating the contribution of another factor which regulates GSK-3 β activity.

4.5 Obesity and IL-6 controlled expression of PP-1 α and Mule synergize to stabilize Mcl-1

The current study demonstrated that activation of PI3K/AKT signaling is not altered between diets and genotypes. Therefore, another regulatory element must be responsible for the differences in GSK-3 β activity between diets and genotypes. Protein phosphatase 1 α (PP-1 α) catalyzes the reverse reaction, namely GSK-3 β dephosphorylation at S9. Investigation of PP-1 α expression level revealed a 2-fold increase in IL-6R α -deficient mice upon NCD feeding, an effect which is completely blunted after HFD feeding. This increase in expression level

is due to decreased Stat-3 activation, which acts as a suppressor on the PP-1 α promoter, demonstrated by ChIP analysis of the PP-1 α promoter.

Transcriptional control of IL-6 regulated genes mainly occurs via the transcription factor Stat-3. Several studies demonstrated a key role of Stat-3 in cancer development. Grivennikov & Karin [2008] demonstrated a constitutive Stat-3 activation in different types of cancer. Furthermore, increased Stat-3 activity was found in chemical induced HCC in rats, indicating an essential role of Stat-3 in the formation of HCC [Sánchez *et al.*, 2003]. If activation of Stat-3 is inhibited, proliferation of HCC cells is suppressed, which is associated with increased apoptosis, cell arrest, reduced proliferation and inhibited expression of growth factors [Sun *et al.*, 2008; Li *et al.*, 2006]. In consequence, expression of Stat-3- regulated genes including B-cell lymphoma extra large (Bclxl), Cyclin D1 and c-Myc, which are involved in apoptosis and cell cycle progression, were downregulated [Sun *et al.*, 2008]. Interestingly, tumor cells use IL-6 to constitutively activate Stat-3 whereas other cytokines like IL-11 or IL-22 could also provoke Stat-3 phosphorylation and tumor development. One consideration is that inflammatory cells in close interaction to cancer cells can produce big amounts of “start-up” IL-6 which is required for early tumor production. IL-6 seems to have a dual role in the development of chemically induced HCC. At first, IL-6 advances cell injury and later the compensatory proliferation of hepatocytes. Secondly, IL-6 provides growth signals to transformed hepatocytes [Grivennikov & Karin, 2008].

However, PP-1 α inhibition by the inhibitor ocadaic acid is not sufficient to stabilize Mcl-1 protein level, suggesting another synergistic pathway independent from PP-1 α . These data confirm that IL6R α -deficiency increases PP1 α expression that regulates GSK-3 β activity, but it is not sufficient to reduce Mcl-1.

While the current study clearly demonstrate that PI3K/AKT action is not impaired in the absence of IL-6R α signaling, the experiments reveal a critical role of IL-6 signaling in the control of PP-1 α expression. However, while S9 phosphorylation dependent control of GSK-3 β activity was shown to regulate Mcl-1

protein stability, GSK-3 β action requires pre-phosphorylation of Mcl-1 in order to exert its regulatory function [Morel *et al.*, 2009; Maurer *et al.*, 2006]. Nevertheless, the experiments revealed a correlation between GSK-3 β phosphorylation and Mcl-1 protein stability in this mouse model. However, at this point it cannot be excluded that, depending on dietary conditions, IL-6R α signaling in addition to GSK-3 β regulation also controls the activity of additional Mcl-1 kinases, such as ERK or JNK. In line with this notion, previous studies have suggested that MAPK/ERK and JNK-dependent phosphorylation of Mcl-1 may also decrease Mcl-1 stability [Morel *et al.*, 2009; Kodama *et al.*, 2009; Domina *et al.*, 2004]. Furthermore, increased and sustained JNK-1 activity, as observed in obesity and during DEN-induced HCC development, can stabilize Mcl-1 [Kodama *et al.*, 2009; Hui *et al.*, 2008; Hirosumi *et al.*, 2002].

Recently, GSK-3 β -phosphorylated Mcl-1 has been shown to be recognized by either Mule or the SCFFBW7 E3 ligase both of which ligate polyubiquitin chains to Mcl-1 that lead to its proteasomal degradation [Wertz *et al.*, 2011; Zhong *et al.*, 2005]. Determination of the expression of these E3 ligases in the current study displayed a correlation of Mule expression with Mcl-1 levels in lean and obese control and IL-6R $\alpha^{\Delta/\Delta}$, whereas expression of the subunits FBW7 and cullin-1 of the SCF complex revealed only a minor expression in HCC. Promoter analysis of the Mule promoter could demonstrate that Mule expression is a direct target of IL-6-mediated Stat-3 repression which could be proven both *in vivo* by using mice with a constitutive active Stat-3 as well as *in vitro* by a Luciferase assay and ChIP analysis. These data clearly prove that expression of ubiquitin ligase Mule is directly regulated by IL-6 mediated Stat-3 activation in the development of HCC.

Interestingly, while the increased tumor burden in obese mice in the current study was accompanied with increased Mcl-1 levels in tumor lesions independent of IL-6R α signaling, the severity of tumor specific lipid accumulation in human HCC positively correlated with Mcl-1 abundance [Fleischer *et al.*, 2006]. Moreover, the current work could demonstrate a negative correlation between

Mcl-1 and Mule levels in human HCC, indicating this mechanism as translational to human disease.

4.6 Obesity promotes liver carcinogenesis via Mcl-1 stabilization independent of IL-6R α signaling

Considering the insights from the current work, the following model has the ability to clarify the role of IL-6 signaling in the development of HCC.

In lean control mice IL-6 decreases apoptosis sensitivity through Stat-3 activation and Mcl-1 stabilization. Stat-3 activation controls the synergistic actions of GSK-3 β via inhibition of PP-1 α expression and Mule via its inhibition which results in HCC development. Accordingly, IL-6R α -deficiency release PP-1 α and Mule expression from Stat-3-mediated inhibition, leading to an increased apoptosis sensitivity in hepatocytes. This sensitivity is caused by Mcl-1 degradation mediated by active GSK-3 β and Mule which protects against DEN-induced HCC.

In contrast in obesity, DEN-induced HCC development and progression occurred even in the absence of IL-6R α expression as a consequence of obesity-induced GSK-3 β inhibition and transcriptional repression of Mule leading to Mcl-1 stabilization. Along these lines, inhibitory S9 phosphorylation of GSK-3 β was increased upon HFD feeding both in control and IL-6R $\alpha^{\Delta/\Delta}$ mice, whereas Mule and PP-1 α expression was significantly inhibited under obese conditions not only in control but also in IL-6R α -deficient animals.

Therefore in lean mice, IL-6 appears to be the critical regulator of GSK-3 β as well as Mule-inhibition, while alternative signals may control these molecules in obese mice.

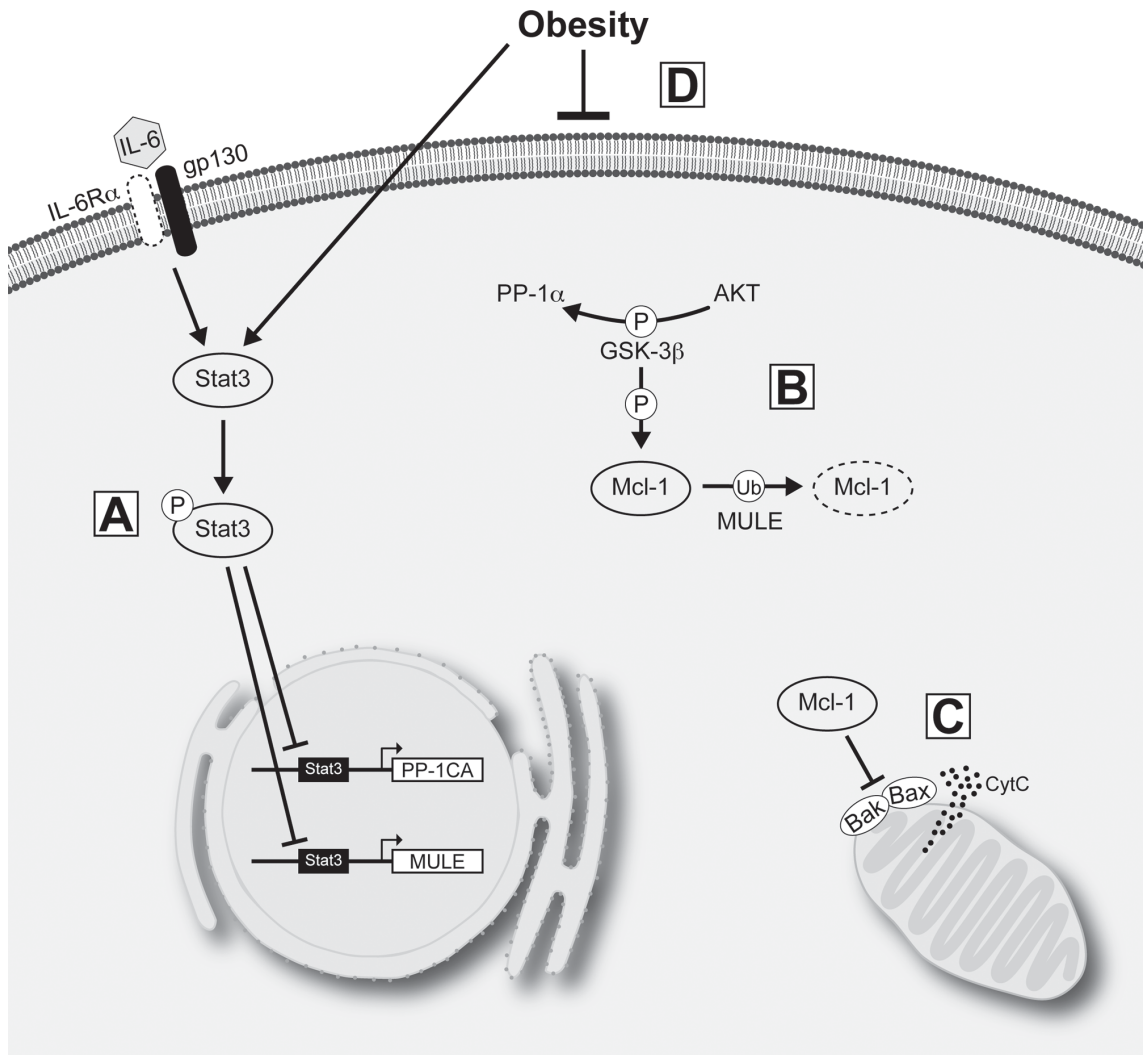


Figure 4.1: **Model of apoptosis-regulation in HCC via IL-6 signaling and obesity**

(A) IL-6 signaling activates Stat-3 which inhibits PP-1 α and Mule expression. (B) Since PP-1 α can not dephosphorylate GSK-3 β , phosphorylation at S9 by AKT inhibits GSK-3 β action which leads to stabilization of Mcl-1. (C) Mcl-1 keeps Bax and Bak separated at the mitochondria which prevents release of Cytochrome C and inhibits apoptosis. (D) Under obese conditions Stat-3-mediated inhibition of PP-1 α and Mule expression occurs independent from IL-6 signaling. Picture produced with the help of Justus Ackermann.

4.7 Inactivation of gp130 in hepatocytes protects against DEN-induced HCC development even under obese conditions

Apparently, the experiments refer to a not yet identified factor that compensates for IL-6R α deficiency in obesity-associated HCC development. In the pro-inflammatory state in obesity this factor could be increased, thereby elevating basal hepatic Stat-3 activation, but impairing acute responsiveness. Evidently, not only the restored hepatic Stat-3 activation in obese IL-6R $\alpha^{\Delta/\Delta}$ mice occurred independent of IL-6 but also the remaining DEN-induced Stat-3 activation in lean IL-6R $\alpha^{\Delta/\Delta}$ mice, thus indicating another obesity- and/or DEN-induced factor that activates Stat-3 in the absence of IL-6R α .

While it is certainly not clear which factor in obesity compensates for IL-6R α deficiency in HCC development, another IL-6 type cytokine or receptor might account for this observation. The common feature of all IL-6 type cytokine receptors is the signaling transducing receptor unit glycoprotein 130 (gp130) [Zhang *et al.*, 1994]. Although, determination of HCC development in hepatocyte specific gp130-deficient mice revealed a protection against DEN induced HCC even under obese conditions, investigation of IL-6 type cytokines and receptors expression in tumor livers of control and IL-6R α deficient mice under both dietary conditions failed to directly clarify which factor compensates for IL-6R α deficiency in HCC development upon HFD feeding. However, other signaling pathways, such as Leptin signaling, use Stat-3 to initiate gene expression [Yang & Barouch, 2007]. Indeed, Leptin levels in IL-6R α deficient mice upon HFD feeding are even more increased than levels in control mice. Moreover, pilot experiments revealed an increase in Leptin receptor expression in IL-6R α deficient mice after HFD feeding, indicating an unknown role of Leptin signaling in the development of HCC. Though, the role of Leptin in liver carcinogenesis has to be further elucidated.

4.8 IL-6R α ^{T-KO} mice are protected against DEN-induced HCC even on HFD

The tumormicroenvironment, especially the infiltrating immune cells play a major role in the development of cancer. In HCC development infiltrating immune cells create a tumor microenvironment releasing elevated levels of pro-inflammatory cytokines such as TNF α and IL-6, both of which are tumor-promoting cytokines [Newell *et al.*, 2008; Lin & Karin, 2007; Xu *et al.*, 2003]. In the liver these IL-6 levels can be recognized by hepatocytes, macrophages and T cells which all express the IL6R α .

The current work could demonstrate that IL-6R α signaling on T cells has a pivotal role in the development of HCC, whereas IL-6R α deficiency on hepatocytes has only minor effects on liver carcinogenesis.

Investigation of IL-6R α ^{L-KO}, IL-6R α ^{M-KO} and IL-6R α ^{T-KO} mice in a DEN-induced HCC approach revealed no differences in tumor development in IL-6R α ^{L-KO} and IL-6R α ^{M-KO} mice compared to control mice whereas IL-6R α ^{T-KO} mice are protected against DEN-induced HCC even upon HFD feeding indicating that IL-6 signaling on T cells promotes HCC development.

The CD4 cre construct which is used for the IL-6R α ^{T-KO} consists of the CD4 promoter, the Cre gene and a Poly A. The silencer from the CD4 is excised resulting in Cre expression in CD4⁺, CD8⁺ and NKT cells. IL-6 plays a pivotal role in differentiation and activation of different T cell subsets such as TH17 and regulatory T cells (T^{regs}) [Bettelli *et al.*, 2006]. Moreover it is known that IL-6 signaling deficient mice have an impaired TH17 differentiation and that IL-6 is required to overcome T^{regs} mediated suppression [Haruta *et al.*, 2011; Pasare, 2003]. Although, previous studys could observe an increase in T^{regs} in different types of cancer, such as pancreatic cancer or colorectal cancer [Mougiakakos, 2011; Mougiakakos *et al.*, 2010; Beyer, 2006; Wolf *et al.*, 2003], depletion of T^{regs} during the initial phase of HCC development doubled tumor number in IL-6R α ^{Δ/Δ}

and IL-6R α^{T-KO} mice compared to mice with T^{regs}.

Collaboration with Ruslan Medzhitov suggested that IL-6R α signaling on effector T cells is required to overcome repression by T^{regs} [personal communication]. Considering that HCC is an inflammation-linked cancer with increased levels of TNF α and IL-6 and that obesity increases HCC in this model, NKT cells could be a potential candidate for the crucial cell type concerning IL-6 signaling in HCC.

NKT cells are a subset of T cells often found in the liver [Swain, 2008]. It has been previously reported that NKT cells are associated with liver injury and inflammation [Gao *et al.*, 2009]. They express the inhibitory NK cell receptor NK1.1 and the semi-invariant T cell receptor Va14Ja18 [Harada *et al.*, 2004; Vivier & Anfossi, 2004]. This T cell receptor binds lipids and ceramides leading to crosslinking of the TCR receptor which results in an inflammatory response with release of TNF α and IL-6 [Gao *et al.*, 2009]. The endogenous ligand of the TCR receptor is still unknown but binding of α Galactosylceramide, a lipid of a marine sponge, leads to hepatic injury and release of TNF α and IL-6 [Van Der Vliet *et al.*, 1999]. Although, activation of NKT cells in control, IL-6R $\alpha^{\Delta/\Delta}$ and IL-6R α^{T-KO} mice by α GalCer mediates an increase liver damage in IL-6R $\alpha^{\Delta/\Delta}$ and IL-6R α^{T-KO} mice, only a very small fraction of NKT cells could be detected which express the IL-6R α .

IL-6-stimulation of primary hepatocytes and human liver tumor cells to verify the mechanism of Mcl-1 stabilization in HCC *in vitro*, revealed a less potent effect than observed *in vivo* indicating another factor which could contribute to inhibition of apoptosis by stabilizing Mcl-1. Therefore, the question raises whether there is another factor which contributes to the inhibition of hepatocyte apoptosis in HCC, which could be released by activated T cells.

Since the repression of Mule and PP-1 α expression by activated Stat-3 could be shown *in vivo* and *in vitro*, another synergistic pathway, which uses Stat-3 as signal transducer, could be involved in the observed effects. Considering that Dominik Schenten from the group of Ruslan Medzhitov could demonstrate that

L-6R α signaling on effector T cells is required to overcome T^{regs}-mediated suppression, a signal from activated effector T cells could be in part responsible for the Stat-3-mediated inhibition of apoptosis in hepatocytes [personal communication]. One potential candidate for this signal could be Interleukin 22. IL-22 is a cytokines released by activated effector T cells, whose receptor is expressed on hepatocytes [Rutz *et al.*, 2013]. Radaeva *et al.* [2004] could demonstrate that IL-22 has a protective effect in T cell-mediated hepatitis in mice. This effect is mediated by Stat-3 activation which serves as a survival factor for hepatocytes. Therefore, IL-22 could be a potential candidate to inhibit Stat-3-mediated inhibition of apoptosis in hepatocytes, together with IL-6.

4.9 Conclusion

Collectively, this study has clearly identified IL-6- and obesity-induced Mcl-1 stabilization as a critical factor for HCC development and progression. Moreover, this study provides evidence that under obese conditions IL-6R α -dependent regulation of GSK-3 β and Mule is compensated for by an alternative mechanism, which has to be further elucidated.

Moreover, it could be demonstrated that IL-6R α signaling on T cells has a pivotal role in the development of HCC, which might be mediated by another cytokine released from activated T cells.

Thus, the current work has strong implications for current translational research on HCC and the development of novel therapeutic strategies aiming at reactivating the mitochondrial apoptotic pathway under inflammatory and obese conditions.

Therefore, the current study implicate the provided mechanism as translational to human disease in the light of increasing obesity in western countries.

5 Bibliography

- ABIRU, S, MIGITA, K, MAEDA, Y, DAIKOKU, M, ITO, M, OHATA, K, NAGAOKA, S, MATSUMOTO, T, TAKII, Y, KUSUMOTO, K, NAKAMURA, M, KOMORI, A, YANO, K, YATSUHASHI, H, EGUCHI, K, & ISHIBASHI, H. 2006. Serum cytokine and soluble cytokine receptor levels in patients with non-alcoholic steatohepatitis. *Liver international : official journal of the international association for the study of the liver*, **26**(1), 39–45. [3, 102]
- AKIRA, S. 1997. IL-6-regulated transcription factors. *The international journal of biochemistry & cell biology*. [10]
- ALWAN, A. 2011. Global status report on noncommunicable diseases 2010. *Who journal*. [1]
- ANGEL, P, & KARIN, M. 1991. The role of Jun, Fos and the AP-1 complex in cell-proliferation and transformation. *Biochimica et biophysica acta*, **1072**(2-3), 129–157. [12]
- ARKAN, M. C, HEVENER, A. L, GRETEN, F. R, MAEDA, S, LI, Z.-W, LONG, J. M, WYNSHAW-BORIS, A, POLI, G, OLEFSKY, J, & KARIN, M. 2005. IKK- β links inflammation to obesity-induced insulin resistance. *Nature medicine*, **11**(2), 191–198. [7]
- BALKWILL, F, & MANTOVANI, A. 2001. Inflammation and cancer: back to Virchow? *The lancet*. [2]
- BARTHOLOMEUSZ, C, GONZALEZ-ANGULO, A. M, LIU, P, HAYASHI, N, LLUCH, A, FERRER-LOZANO, J, & HORTOBAGYI, G. N. 2012. High ERK Protein Expression Levels Correlate with Shorter Survival in Triple-Negative Breast Cancer Patients. *The oncologist*, **17**(6), 766–774. [12]
- BARTON, B. E. 1996. The biological effects of interleukin 6. *Medicinal research reviews*, **16**(1), 87–109. [8]
- BASTARD, J. P, JARDEL, C, BRUCKERT, E, BLONDY, P, CAPEAU, J, LAVILLE, M, VIDAL, H, & HAINQUE, B. 2000. Elevated levels of interleukin 6 are reduced in serum and subcutaneous adipose tissue of obese women after weight loss. *The journal of clinical endocrinology and metabolism*, **85**(9), 3338–3342. [6]

- BAUD, V, LIU, Z.-G, BENNETT, B, SUZUKI, N, XIA, Y, & KARIN, M. 1999. Signaling by proinflammatory cytokines: oligomerization of TRAF2 and TRAF6 is sufficient for JNK and IKK activation and target gene induction via an amino-terminal effector domain. *Genes & . . .* [12]
- BENOIT, S. C, CLEGG, D. J, SEELEY, R. J, & WOODS, S. C. 2004. Insulin and leptin as adiposity signals. *Recent progress in hormone research*, **59**, 267–285. [48]
- BETTELLI, E, CARRIER, Y, GAO, W, KORN, T, STROM, T. B, OUKKA, M, WEINER, H. L, & KUCHROO, V. K. 2006. Reciprocal developmental pathways for the generation of pathogenic effector TH17 and regulatory T cells. *Nature*, **441**(7090), 235–238. [117]
- BETZ, U. A, BLOCH, W, VAN DEN BROEK, M, YOSHIDA, K, TAGA, T, KISHIMOTO, T, ADDICKS, K, RAJEWSKY, K, & MÜLLER, W. 1998. Postnatally induced inactivation of gp130 in mice results in neurological, cardiac, hematopoietic, immunological, hepatic, and pulmonary defects. *The journal of experimental medicine*, **188**(10), 1955–1965. [83]
- BEYER, M. 2006. Regulatory T cells in cancer. *Blood*, **108**(3), 804–811. [117]
- BHARDWAJ, A, & AGGARWAL, B. B. 2003. Receptor-mediated choreography of life and death. *Journal of clinical immunology*, **23**(5), 317–332. [14]
- BIANCHINI, F, KAAKS, R, & VAINIO, H. 2002. Overweight, obesity, and cancer risk. *The lancet oncology*, **3**(9), 565–574. [4]
- BISGAARD, H. C, NAGY, P, SANTONI-RUGIU, E, & THORGEIRSSON, S. S. 1998. Proliferation, apoptosis, and induction of hepatic transcription factors are characteristics of the early response of biliary epithelial (oval) cells to chemical carcinogens. *Hepatology*, **23**(1), 62–70. [63, 102]
- BJØRBAEK, C, ELMQUIST, J. K, FRANTZ, J. D, SHOELSON, S. E, & FLIER, J. S. 1998. Identification of SOCS-3 as a potential mediator of central leptin resistance. *Molecular cell*, **1**(4), 619–625. [10]
- BRINKMANN, K, ZIGRINO, P, WITT, A, SCHELL, M, ACKERMANN, L, BROXTERMANN, P, SCHÜLL, S, ANDREE, M, COUTELLE, O, YAZDANPANA, B, SEEGER, J. M, KLUBERTZ, D, DREBBER, U, HACKER, U. T, KRÖNKE, M, MAUCH, C, HOPPE, T, & KASHKAR, H. 2013. Ubiquitin C-Terminal Hydrolase-L1 Potentiates Cancer Chemosensitivity by Stabilizing NOXA. *Cell-reports*, **3**(3), 881–891. [16]

- BROOKS, K, FERNANDEZ, R, & VITETTA, E. S. 1985. B cell growth and differentiation factors. *Methods in enzymology*, **116**, 372–379. [8]
- BRUNELLE, J. K, & LETAI, A. 2009. Control of mitochondrial apoptosis by the Bcl-2 family. *Journal of cell science*, **122**(Pt 4), 437–441. [16, 60, 62, 108]
- CAJA, L, SANCHO, P, BERTRAN, E, IGLESIAS-SERRET, D, GIL, J, & FABREGAT, I. 2009. Overactivation of the MEK/ERK pathway in liver tumor cells confers resistance to TGF-beta-induced cell death through impairing up-regulation of the NADPH oxidase NOX4. *Cancer research*, **69**(19), 7595–7602. [12]
- CALDWELL, S. H, CRESPO, D. M, KANG, H. S, & AL-OSAIMI, A. M. S. 2004. Obesity and hepatocellular carcinoma. *Ygast*, **127**(5 Suppl 1), S97–103. [5]
- CALLE, E. E, & KAAKS, R. 2004. Overweight, obesity and cancer: epidemiological evidence and proposed mechanisms. *Nature reviews cancer*, **4**(8), 579–591. [4]
- CALLE, E. E, RODRIGUEZ, C, WALKER-THURMOND, K, & THUN, M. J. 2003. Overweight, obesity, and mortality from cancer in a prospectively studied cohort of U.S. adults. *New england journal of medicine*, **348**(17), 1625–1638. [4, 5, 102]
- CHALARIS, A, RABE, B, PALIGA, K, LANGE, H, LASKAY, T, FIELDING, C. A, JONES, S. A, ROSE-JOHN, S, & SCHELLER, J. 2007. Apoptosis is a natural stimulus of IL6R shedding and contributes to the proinflammatory trans-signaling function of neutrophils. *Blood*, **110**(6), 1748–1755. [9]
- CHARVET, C, WISSLER, M, BRAUNS-SCHUBERT, P, WANG, S.-J, TANG, Y, SIGLOCH, F. C, MELLERT, H, BRANDENBURG, M, LINDNER, S. E, BREIT, B, GREEN, D. R, MCMAHON, S. B, BORNER, C, GU, W, & MAURER, U. 2011. Phosphorylation of Tip60 by GSK-3 determines the induction of PUMA and apoptosis by p53. *Molecular cell*, **42**(5), 584–596. [67, 110]
- CHIPUK, J. E, BOUCHIER-HAYES, L, & GREEN, D. R. 2006. Mitochondrial outer membrane permeabilization during apoptosis: the innocent bystander scenario. *Cell death and differentiation*, **13**(8), 1396–1402. [14]
- CLAUSEN, B. E, BURKHARDT, C, REITH, W, RENKAWITZ, R, & FÖRSTER, I. 1999. Conditional gene targeting in macrophages and granulocytes using LysMcre mice. *Transgenic research*, **8**(4), 265–277. [91]

- CRESSMAN, D. E, GREENBAUM, L. E, DEANGELIS, R. A, CILIBERTO, G, FURTH, E. E, POLI, V, & TAUB, R. 1996. Liver failure and defective hepatocyte regeneration in interleukin-6-deficient mice. *Science*, **274**(5291), 1379–1383. [63]
- CROCE, C. M. 2008. Oncogenes and Cancer. *New england journal of medicine*, **358**(5), 502–511. [1]
- CROSS, D. A, ALESSI, D. R, COHEN, P, ANDJELKOVICH, M, & HEMMINGS, B. A. 1995. Inhibition of glycogen synthase kinase-3 by insulin mediated by protein kinase B. *Nature*, **378**(6559), 785–789. [66, 71, 111]
- CULLY, M, YOU, H, LEVINE, A. J, & MAK, T. W. 2006. Beyond PTEN mutations: the PI3K pathway as an integrator of multiple inputs during tumorigenesis. *Nature reviews cancer*, **6**(3), 184–192. [71, 111]
- DANDONA, P, WEINSTOCK, R, THUSU, K, ABDEL-RAHMAN, E, ALJADA, A, & WADDEN, T. 1998. Tumor necrosis factor-alpha in sera of obese patients: fall with weight loss. *The journal of clinical endocrinology and metabolism*, **83**(8), 2907–2910. [6]
- DAVIS, P. J, TILLMANN, H. C, DAVIS, F. B, & WEHLING, M. 2002. Comparison of the mechanisms of nongenomic actions of thyroid hormone and steroid hormones. *Journal of endocrinological investigation*, **25**(4), 377–388. [11]
- DAVIS, R. J. 2000. Signal transduction by the JNK group of MAP kinases. *Cell*, **103**(2), 239–252. [11, 12]
- DING, Q, HE, X, HSU, J. M, XIA, W, CHEN, C. T, LI, L. Y, LEE, D. F, LIU, J. C, ZHONG, Q, WANG, X, & HUNG, M. C. 2007. Degradation of Mcl-1 by -TrCP Mediates Glycogen Synthase Kinase 3-Induced Tumor Suppression and Chemosensitization. *Molecular and cellular biology*, **27**(11), 4006–4017. [66, 111]
- DOMINA, A. M, VRANA, J. A, GREGORY, M. A, HANN, S. R, & CRAIG, R. W. 2004. MCL1 is phosphorylated in the PEST region and stabilized upon ERK activation in viable cells, and at additional sites with cytotoxic okadaic acid or taxol. *Oncogene*, **23**(31), 5301–5315. [113]
- DONATO, F, TAGGER, A, GELATTI, U, PARRINELLO, G, BOFFETTA, P, ALBERTINI, A, DECARLI, A, TREVISI, P, RIBERO, M. L, MARTELLI, C, PORRU, S, & NARDI, G. 2002. Alcohol and Hepatocellular Carcinoma: The Effect of Lifetime Intake and Hepatitis Virus Infections in Men and Women. *American journal of . . .* [2]
- EL-SERAG, H. B, & RUDOLPH, K. L. 2007. Hepatocellular carcinoma: epidemiology and molecular carcinogenesis. *Ygast*, **132**(7), 2557–2576. [1, 5, 102]

- EL-SERAG, H. B, DAVILA, J. A, PETERSEN, N. J, & MCGLYNN, K. A. 2003. The continuing increase in the incidence of hepatocellular carcinoma in the United States: an update. *Annals of internal medicine*, **139**(10), 817–823. [1]
- ELDAR-FINKELMAN, H, & KREBS, E. G. 1997. Phosphorylation of insulin receptor substrate 1 by glycogen synthase kinase 3 impairs insulin action. *Proceedings of the national academy of sciences of the united states of america*, **94**(18), 9660–9664. [110]
- ELDAR-FINKELMAN, H, SCHREYER, S. A, SHINOHARA, M. M, LEBOEUF, R. C, & KREBS, E. G. 1999. Increased glycogen synthase kinase-3 activity in diabetes- and obesity-prone C57BL/6J mice. *Diabetes*, **48**(8), 1662–1666. [110]
- ENDO, T. A, MASUHARA, M, YOKOUCHI, M, SUZUKI, R, SAKAMOTO, H, MITSUI, K, MATSUMOTO, A, TANIMURA, S, OHTSUBO, M, MISAWA, H, MIYAZAKI, T, LEONOR, N, TANIGUCHI, T, FUJITA, T, KANAKURA, Y, KOMIYA, S, & YOSHIMURA, A. 1997. A new protein containing an SH2 domain that inhibits JAK kinases. *Nature*, **387**(6636), 921–924. [10]
- EPLING-BURNETTE, P. K, ZHONG, B, BAI, F, JIANG, K, BAILEY, R. D, GARCIA, R, JOVE, R, DJEU, J. Y, LOUGHRAN, T. P, & WEI, S. 2001a. Cooperative regulation of Mcl-1 by Janus kinase/stat and phosphatidylinositol 3-kinase contribute to granulocyte-macrophage colony-stimulating factor-delayed apoptosis in human neutrophils. *Journal of immunology (baltimore, md. : 1950)*, **166**(12), 7486–7495. [109]
- EPLING-BURNETTE, P. K, LIU, J. H, CATLETT-FALCONE, R, TURKSON, J, OSHIRO, M, KOTHAPALLI, R, LI, Y, WANG, J. M, YANG-YEN, H. F, KARRAS, J, JOVE, R, & LOUGHRAN, T. P. 2001b. Inhibition of STAT3 signaling leads to apoptosis of leukemic large granular lymphocytes and decreased Mcl-1 expression. *Journal of clinical investigation*, **107**(3), 351–362. [109]
- ESKES, R, DESAGHER, S, ANTONSSON, B, & MARTINOU, J. C. 2000. Bid induces the oligomerization and insertion of Bax into the outer mitochondrial membrane. *Molecular and cellular biology*, **20**(3), 929–935. [16]
- FATTOVICH, G, STROFFOLINI, T, ZAGNI, I, & DONATO, F. 2004. Hepatocellular carcinoma in cirrhosis: Incidence and risk factors. *Gastroenterology*, **127**(5), S35–S50. [2, 102]
- FAUSTO, N. 1999. Mouse liver tumorigenesis: models, mechanisms, and relevance to human disease. *Seminars in liver disease*, **19**(3), 243–252. [3]

- FERRANTE, A. W. 2007. Obesity-induced inflammation: a metabolic dialogue in the language of inflammation. *Journal of internal medicine*, **262**(4), 408–414. [102]
- FLEISCHER, B, SCHULZE-BERGMANN, H, SCHUCHMANN, M, WEBER, A, BIESTERFELD, S, MÜLLER, M, KRAMMER, P. H, & GALLE, P. R. 2006. Mcl-1 is an anti-apoptotic factor for human hepatocellular carcinoma. *International journal of oncology*, **28**(1), 25–32. [82, 108, 113]
- FORD, E. S, & MOKDAD, A. H. 2008. Epidemiology of obesity in the Western Hemisphere. *The journal of clinical endocrinology and metabolism*, **93**(11 Suppl 1), S1–8. [4]
- FUJII, M, SHIBAZAKI, Y, WAKAMATSU, K, HONDA, Y, KAWAUCHI, Y, SUZUKI, K, ARUMUGAM, S, WATANABE, K, ICHIDA, T, ASAKURA, H, & YONEYAMA, H. 2013. A murine model for non-alcoholic steatohepatitis showing evidence of association between diabetes and hepatocellular carcinoma. *Medical molecular morphology*, **46**(3), 141–152. [54, 56]
- GAO, B, RADAIEVA, S, & PARK, O. 2009. Liver natural killer and natural killer T cells: immunobiology and emerging roles in liver diseases. *Journal of leukocyte biology*, **86**(3), 513–528. [118]
- GONZALEZ, F, THUSU, K, ABDEL-RAHMAN, E, PRABHALA, A, TOMANI, M, & DANDONA, P. 1999. Elevated serum levels of tumor necrosis factor alpha in normal-weight women with polycystic ovary syndrome. *Metabolism: clinical and experimental*, **48**(4), 437–441. [6]
- GRAEVE, L, KOROLENKO, T. A, HEMMANN, U, WEIERGRÄBER, O, DITTRICH, E, & HEINRICH, P. C. 1996. A complex of the soluble interleukin-6 receptor and interleukin-6 is internalized via the signal transducer gp130. *Febs letters*, **399**(1-2), 131–134. [8]
- GREEN, D. R. 2005. Apoptotic pathways: ten minutes to dead. *Cell*, **121**(5), 671–674. [13, 14]
- GRIVENNIKOV, S, & KARIN, M. 2008. Autocrine IL-6 Signaling: A Key Event in Tumorigenesis? *Cancer cell*, **13**(1), 7–9. [112]
- GRUBER, S. 2009. The Role of Interleukin 6 in the Development of Hepatocellular carcinoma. *Diploma thesis*, Mar., 1–96. [46]
- HANAHAN, D, & WEINBERG, R. A. 2000. The hallmarks of cancer. *Cell*, **100**(1), 57–70. [13]

- HANAHAHAN, D, & WEINBERG, R. A. 2011. Hallmarks of cancer: the next generation. *Cell*, **144**(5), 646–674. [13]
- HANGER, D. P, HUGHES, K, WOODGETT, J. R, BRION, J. P, & ANDERTON, B. H. 1992. Glycogen synthase kinase-3 induces Alzheimer's disease-like phosphorylation of tau: generation of paired helical filament epitopes and neuronal localisation of the kinase. *Neuroscience letters*, **147**(1), 58–62. [110]
- HARADA, M, SEINO, K.-I, WAKAO, H, SAKATA, S, ISHIZUKA, Y, ITO, T, KOJO, S, NAKAYAMA, T, & TANIGUCHI, M. 2004. Down-regulation of the invariant Valpha14 antigen receptor in NKT cells upon activation. *International immunology*, **16**(2), 241–247. [118]
- HARUTA, H, OHGURO, N, FUJIMOTO, M, HOHKI, S, TERABE, F, SERADA, S, NOMURA, S, NISHIDA, K, KISHIMOTO, T, & NAKA, T. 2011. Blockade of Interleukin-6 Signaling Suppresses Not Only Th17 but Also Interphotoreceptor Retinoid Binding Protein-Specific Th1 by Promoting Regulatory T Cells in Experimental Autoimmune Uveoretinitis. *Investigative ophthalmology & visual science*, **52**(6), 3264–3271. [13, 100, 117]
- HEINRICH, P. C, BEHRMANN, I, MULLER-NEWEN, G, SCHAPER, F, & GRAEVE, L. 1998. Interleukin-6-type cytokine signalling through the gp130/Jak/STAT pathway1. *Biochem. j*, **334**, 297–314. [44]
- HEINRICH, P. C, BEHRMANN, I, HAAN, S, HERMANNNS, H. M, MULLER-NEWEN, G, & SCHAPER, F. 2003. Principles of interleukin (IL)-6-type cytokine signalling and its regulation. *Biochem. j*, **374**(Pt 1), 1–20. [106]
- HENGARTNER, M. O. 2000. The biochemistry of apoptosis. *Nature*, **407**(6805), 770–776. [14]
- HIBI, M, NAKAJIMA, K, & HIRANO, T. 1996. IL-6 cytokine family and signal transduction: a model of the cytokine system. *Journal of molecular medicine (berlin, germany)*, **74**(1), 1–12. [8]
- HIKITA, H, KODAMA, T, SHIMIZU, S, LI, W, SHIGEKAWA, M, TANAKA, S, HOSUI, A, MIYAGI, T, TATSUMI, T, KANTO, T, HIRAMATSU, N, MORII, E, HAYASHI, N, & TAKEHARA, T. 2012. Bak deficiency inhibits liver carcinogenesis: A causal link between apoptosis and carcinogenesis. *Journal of hepatology*, **57**(1), 92–100. [109]
- HIROSUMI, J, TUNCMAN, G, CHANG, L, GÖRGÜN, C. Z, UYSAL, K. T, MAEDA, K, KARIN, M, & HOTAMISLIGIL, G. S. 2002. A central role for JNK in obesity and insulin resistance. *Nature*, **420**(6913), 333–336. [113]

- HOLMES, A. G, MESA, J. L, NEILL, B. A, CHUNG, J, CAREY, A. L, STEINBERG, G. R, KEMP, B. E, SOUTHGATE, R. J, LANCASTER, G. I, BRUCE, C. R, WATT, M. J, & FEBBRAIO, M. A. 2008. Prolonged interleukin-6 administration enhances glucose tolerance and increases skeletal muscle PPARalpha and UCP2 expression in rats. *The journal of endocrinology*, **198**(2), 367–374. [106]
- HOTAMISLIGIL, G. S, SHARGILL, N. S, & SPIEGELMAN, B. M. 1993. Adipose expression of tumor necrosis factor-alpha: direct role in obesity-linked insulin resistance. *Science*, **259**(5091), 87–91. [6, 102]
- HOTAMISLIGIL, G. S, ARNER, P, CARO, J. F, ATKINSON, R. L, & SPIEGELMAN, B. M. 1995. Increased adipose tissue expression of tumor necrosis factor-alpha in human obesity and insulin resistance. *Journal of clinical investigation*, **95**(5), 2409–2415. [6]
- HOTAMISLIGIL, G. S. 2006. Inflammation and metabolic disorders. *Nature*, **444**(7121), 860–867. [7]
- HUEBER, A. O, ZÖRNIG, M, LYON, D, SUDA, T, NAGATA, S, & EVAN, G. I. 1997. Requirement for the CD95 receptor-ligand pathway in c-Myc-induced apoptosis. *Science*, **278**(5341), 1305–1309. [17]
- HUI, L, ZATLOUKAL, K, SCHEUCH, H, STEPNIAK, E, & WAGNER, E. F. 2008. Proliferation of human HCC cells and chemically induced mouse liver cancers requires JNK1-dependent p21 downregulation. *Journal of clinical investigation*, **118**(12), 3943–3953. [3, 113]
- JIANG, B.-H, & LIU, L.-Z. 2008. PI3K/PTEN signaling in tumorigenesis and angiogenesis. *Biochimica et biophysica acta (bba) - proteins and proteomics*, **1784**(1), 150–158. [71, 111]
- JIN, F, IRSHAD, S, YU, W, BELAKAVADI, M, CHEKMAREVA, M, ITTMANN, M. M, ABATE-SHEN, C, & FONDELL, J. D. 2013. ERK and AKT Signaling Drive MED1 Overexpression in Prostate Cancer in Association with Elevated Proliferation and Tumorigenicity. *Molecular cancer research*, **11**(7), 736–747. [12]
- JONES, S. A, NOVICK, D, HORIUCHI, S, YAMAMOTO, N, SZALAI, A. J, & FULLER, G. M. 1999. C-reactive protein: a physiological activator of interleukin 6 receptor shedding. *The journal of experimental medicine*, **189**(3), 599–604. [8]
- JOURDAN, M, VEYRUNE, J.-L, DE VOS, J, REDAL, N, COUDERC, G, & KLEIN, B. 2003. A major role for Mcl-1 antiapoptotic protein in the IL-6-induced survival of human myeloma cells. *Oncogene*, **22**(19), 2950–2959. [109]

- KARIN, M, & CHANG, L. 2001. AP-1–glucocorticoid receptor crosstalk taken to a higher level. *Journal of endocrinology*, **169**(3), 447–451. [12]
- KARIN, M. 2008. The I κ B kinase - a bridge between inflammation and cancer. *Cell research*, **18**(3), 334–342. [3, 9]
- KARIN, M, & GALLAGHER, E. 2005. From JNK to pay dirt: jun kinases, their biochemistry, physiology and clinical importance. *Iubmb life*, **57**(4-5), 283–295. [9]
- KARIN, M, & GRETEN, F. R. 2005. NF- κ B: linking inflammation and immunity to cancer development and progression. *Nature reviews immunology*, **5**(10), 749–759. [2]
- KARIN, M, LAWRENCE, T, & NIZET, V. 2006. Innate Immunity Gone Awry: Linking Microbial Infections to Chronic Inflammation and Cancer. *Cell*, **124**(4), 823–835. [2]
- KAWAZOE, Y, NAKA, T, FUJIMOTO, M, KOHZAKI, H, MORITA, Y, NARAZAKI, M, OKUMURA, K, SAITOH, H, NAKAGAWA, R, UCHIYAMA, Y, AKIRA, S, & KISHIMOTO, T. 2001. Signal Transducer and Activator of Transcription (Stat)-Induced Stat Inhibitor 1 (Ssi-1)/Suppressor of Cytokine Signaling 1 (Socs1) Inhibits Insulin Signal Transduction Pathway through Modulating Insulin Receptor Substrate 1 (Irs-1) Phosphorylation. *The journal of . . .* [10]
- KELLENDONK, C, OPPERK, C, ANLAG, K, SCHÜTZ, G, & TRONCHE, F. 2000. Hepatocyte-specific expression of Cre recombinase. *Genesis (new york, n.y. : 2000)*, **26**(2), 151–153. [83, 91]
- KERN, P. A, SAGHIZADEH, M, ONG, J. M, BOSCH, R. J, DEEM, R, & SIMSOLO, R. B. 1995. The expression of tumor necrosis factor in human adipose tissue. Regulation by obesity, weight loss, and relationship to lipoprotein lipase. *Journal of clinical investigation*, **95**(5), 2111–2119. [6]
- KERR, J. F, WYLLIE, A. H, & CURRIE, A. R. 1972. Apoptosis: a basic biological phenomenon with wide-ranging implications in tissue kinetics. *British journal of cancer*, **26**(4), 239–257. [13]
- KLOVER, P. J, & MOONEY, R. A. 2004. Hepatocytes: critical for glucose homeostasis. *The international journal of biochemistry & cell biology*, **36**(5), 753–758. [106]

- KODAMA, Y, TAURA, K, MIURA, K, SCHNABL, B, OSAWA, Y, & BRENNER, D. A. 2009. Antiapoptotic Effect of c-Jun N-terminal Kinase-1 through Mcl-1 Stabilization in TNF-Induced Hepatocyte Apoptosis. *Ygast*, **136**(4), 1423–1434. [113]
- KOZOPAS, K. M, YANG, T, BUCHAN, H. L, ZHOU, P, & CRAIG, R. W. 1993. MCL1, a gene expressed in programmed myeloid cell differentiation, has sequence similarity to BCL2. *Proceedings of the national academy of sciences of the united states of america*, **90**(8), 3516–3520. [109]
- LEE, P. P, FITZPATRICK, D. R, BEARD, C, JESSUP, H. K, LEHAR, S, MAKAR, K. W, PÉREZ-MELGOSA, M, SWEETSER, M. T, SCHLISSEL, M. S, NGUYEN, S, CHERRY, S. R, TSAI, J. H, TUCKER, S. M, WEAVER, W. M, KELSO, A, JAENISCH, R, & WILSON, C. B. 2001. A critical role for Dnmt1 and DNA methylation in T cell development, function, and survival. *Immunity*, **15**(5), 763–774. [91]
- LI, L, & YANG, G.-Y. 2004. Effect of hepatic glucose production on acute insulin resistance induced by lipid-infusion in awake rats. *World journal of gastroenterology*, **10**(21), 3208–3211. [106]
- LI, W.-C, YE, S.-L, SUN, R.-X, LIU, Y.-K, TANG, Z.-Y, KIM, Y, KARRAS, J. G, & ZHANG, H. 2006. Inhibition of growth and metastasis of human hepatocellular carcinoma by antisense oligonucleotide targeting signal transducer and activator of transcription 3. *Clinical cancer research : an official journal of the american association for cancer research*, **12**(23), 7140–7148. [112]
- LIN, W.-W, & KARIN, M. 2007. A cytokine-mediated link between innate immunity, inflammation, and cancer. *Journal of clinical investigation*, **117**(5), 1175–1183. [7, 117]
- LUEDDE, T, & SCHWABE, R. F. 2011. NF- κ B in the liver[mdash]linking injury, fibrosis and hepatocellular carcinoma : Abstract : Nature Reviews Gastroenterology and Hepatology. *Nature reviews gastroenterology and . . .* [57]
- LUEDDE, T, BERAZA, N, KOTSIKORIS, V, VAN LOO, G, NENCI, A, DE VOS, R, ROSKAMS, T, TRAUTWEIN, C, & PASPARAKIS, M. 2007. Deletion of NEMO/IKK γ in liver parenchymal cells causes steatohepatitis and hepatocellular carcinoma. *Cancer cell*, **11**(2), 119–132. [3, 6]
- MAEDA, S, KAMATA, H, LUO, J.-L, LEFFERT, H, & KARIN, M. 2005. IKK β Couples Hepatocyte Death to Cytokine-Driven Compensatory Proliferation that Promotes Chemical Hepatocarcinogenesis. *Cell*, **121**(7), 977–990. [3, 63]

- MALHI, H, GUICCIARDI, M. E, & GORES, G. J. 2010. Hepatocyte death: a clear and present danger. *Physiological reviews*, **90**(3), 1165–1194. [14, 16]
- MANTOVANI, A, ALLAVENA, P, SICA, A, & BALKWILL, F. 2008. Cancer-related inflammation. *Nature*, **454**(7203), 436–444. [2, 102]
- MARIA, N. D, MANNO, M, & VILLA, E. 2002. Sex hormones and liver cancer. *Molecular and cellular endocrinology*, **193**(1-2), 59–63. [1]
- MAURER, U, CHARVET, C, WAGMAN, A. S, DEJARDIN, E, & GREEN, D. R. 2006. Glycogen Synthase Kinase-3 Regulates Mitochondrial Outer Membrane Permeabilization and Apoptosis by Destabilization of MCL-1. *Molecular cell*, **21**(6), 749–760. [66, 108, 109, 110, 113]
- McFARLAND-MANCINI, M. M, FUNK, H. M, PALUCH, A. M, ZHOU, M, GIRIDHAR, P. V, MERCER, C. A, KOZMA, S. C, & DREW, A. F. 2010. Differences in wound healing in mice with deficiency of IL-6 versus IL-6 receptor. *The journal of immunology*, **184**(12), 7219–7228. [105]
- MOHAMED-ALI, V, GOODRICK, S, RAWESH, A, KATZ, D. R, MILES, J. M, YUDKIN, J. S, KLEIN, S, & COPPACK, S. W. 1997. Subcutaneous Adipose Tissue Releases Interleukin-6, But Not Tumor Necrosis Factor- α , in Vivo. *Journal of clinical . . .* [6]
- MOREL, C, CARLSON, S. M, WHITE, F. M, & DAVIS, R. J. 2009. Mcl-1 Integrates the Opposing Actions of Signaling Pathways That Mediate Survival and Apoptosis. *Molecular and cellular biology*, **29**(14), 3845–3852. [113]
- MOUGIAKAKOS, D. 2011. Regulatory T Cells in Colorectal Cancer: From Biology to Prognostic Relevance. *Cancers*, **3**(4), 1708–1731. [100, 117]
- MOUGIAKAKOS, D, CHOUDHURY, A, LLADSER, A, KIESSLING, R, & JOHANSSON, C. C. 2010. *Chapter 3 - Regulatory T Cells in Cancer*. 1 edn. Vol. 107. Elsevier Inc. [100, 117]
- NAKA, T, NARAZAKI, M, HIRATA, M, & MATSUMOTO, T. 1997. STAT-induced STAT inhibitor. *Nature*. [10]
- NAKA, T, FUJIMOTO, M, & KISHIMOTO, T. 1999. Negative regulation of cytokine signaling: STAT-induced STAT inhibitor. *Trends in biochemical sciences*. [10]
- NAUGLER, W. E, SAKURAI, T, KIM, S, MAEDA, S, KIM, K, ELSHARKAWY, A. M, & KARIN, M. 2007. Gender Disparity in Liver Cancer Due to Sex Differences in MyD88-Dependent IL-6 Production. *Science*, **317**(5834), 121–124. [1, 3, 7, 18, 53, 63, 103, 104]

- NAULT, J.-C, & ZUCMAN-ROSSI, J. 2010. Building a bridge between obesity, inflammation and liver carcinogenesis. *Journal of hepatology*, **53**(4), 777–779. [54, 56]
- NEWELL, P, VILLANUEVA, A, FRIEDMAN, S. L, KOIKE, K, & LLOVET, J. M. 2008. Experimental models of hepatocellular carcinoma. *Journal of hepatology*, **48**(5), 858–879. [3, 117]
- NISHIMURA, S, MANABE, I, NAGASAKI, M, ETO, K, YAMASHITA, H, OHSUGI, M, OTSU, M, HARA, K, UEKI, K, SUGIURA, S, YOSHIMURA, K, KADOWAKI, T, & NAGAI, R. 2009. CD8+ effector T cells contribute to macrophage recruitment and adipose tissue inflammation in obesity. *Nature medicine*, **15**(8), 914–920. [6, 102]
- OLEFSKY, J. M, & GLASS, C. K. 2010. Macrophages, Inflammation, and Insulin Resistance. *Annual review of physiology*, **72**(1), 219–246. [102]
- O'SHEA, J. J, GADINA, M, & SCHREIBER, R. D. 2002. Cytokine signaling in 2002: new surprises in the Jak/Stat pathway. *Cell*, **109 Suppl**(Apr.), S121–31. [10]
- PAREKH, R. B, DWEK, R. A, RADEMACHER, T. W, OPDENAKKER, G, & VAN DAMME, J. 1992. Glycosylation of interleukin-6 purified from normal human blood mononuclear cells. *European journal of biochemistry / febs*, **203**(1-2), 135–141. [8]
- PARK, E. J, LEE, J. H, YU, G.-Y, HE, G, ALI, S. R, HOLZER, R. G, OSTERREICHER, C. H, TAKAHASHI, H, & KARIN, M. 2010. Dietary and Genetic Obesity Promote Liver Inflammation and Tumorigenesis by Enhancing IL-6 and TNF Expression. *Cell*, **140**(2), 197–208. [5, 7, 18, 53, 104, 105, 106, 107]
- PASARE, C. 2003. Toll Pathway-Dependent Blockade of CD4+CD25+ T Cell-Mediated Suppression by Dendritic Cells. *Science*, **299**(5609), 1033–1036. [117]
- PATEL, S, & WOODGETT, J. 2008. Glycogen Synthase Kinase-3 and Cancer: Good Cop, Bad Cop? *Cancer cell*, **14**(5), 351–353. [110]
- PIKARSKY, E, PORAT, R. M, STEIN, I, ABRAMOVITCH, R, AMIT, S, KASEM, S, GUTKOVICH-PYEST, E, URIELI-SHOVAL, S, GALUN, E, & BEN-NERIAH, Y. 2004. NF- κ B functions as a tumour promoter in inflammation-associated cancer. *Nature*, **431**(7007), 461–466. [3]
- RADAEVA, S, SUN, R, PAN, H.-N, HONG, F, & GAO, B. 2004. Interleukin 22 (IL-22) plays a protective role in T cell-mediated murine hepatitis: IL-22 is a

- survival factor for hepatocytes via STAT3 activation. *Hepatology*, **39**(5), 1332–1342. [119]
- RAMADORI, G, & CHRIST, B. 1999. Cytokines and the hepatic acute-phase response. *Seminars in liver disease*, **19**(2), 141–155. [10, 11]
- REN, D, TU, H. C, KIM, H, WANG, G. X, BEAN, G. R, TAKEUCHI, O, JEFFERS, J. R, ZAMBETTI, G. P, HSIEH, J. J. D, & CHENG, E. H. Y. 2010. BID, BIM, and PUMA Are Essential for Activation of the BAX- and BAK-Dependent Cell Death Program. *Science*, **330**(6009), 1390–1393. [16]
- ROHN, T. T. 2010. The role of caspases in Alzheimer's disease; potential novel therapeutic opportunities. *Apoptosis : an international journal on programmed cell death*, **15**(11), 1403–1409. [13]
- RUTZ, S, EIDENSCHENK, C, & OUYANG, W. 2013. IL-22, not simply a Th17 cytokine. *Immunological reviews*, **252**(1), 116–132. [119]
- SAKURAI, T, MAEDA, S, CHANG, L, & KARIN, M. 2006. Loss of hepatic NF- κ B activity enhances chemical hepatocarcinogenesis through sustained c-Jun N-terminal kinase 1 activation. *Proceedings of the national academy of sciences of the united states of america*, **103**(28), 10544–10551. [3]
- SÁNCHEZ, A, NAGY, P, & THORGEIRSSON, S. S. 2003. STAT-3 activity in chemically-induced hepatocellular carcinoma. *European journal of cancer (oxford, england : 1990)*, **39**(14), 2093–2098. [112]
- SANZ-CAMENO, P, TRAPERO-MARUGÁN, M, CHAPARRO, M, JONES, E. A, & MORENO-OTERO, R. 2010. Angiogenesis: From Chronic Liver Inflammation to Hepatocellular Carcinoma. *Journal of oncology*, **2010**(2), 1–7. [2]
- SCHULZE-BERGMANN, H, FLEISCHER, B, SCHUCHMANN, M, WEBER, A, WEINMANN, A, KRAMMER, P. H, & GALLE, P. R. 2006. Suppression of Mcl-1 via RNA interference sensitizes human hepatocellular carcinoma cells towards apoptosis induction. *Bmc cancer*, **6**, 232. [108]
- SCHWENK, F, BARON, U, & RAJEWSKY, K. 1995. A cre-transgenic mouse strain for the ubiquitous deletion of loxP-flanked gene segments including deletion in germ cells. *Nucleic acids research*, **23**(24), 5080–5081. [46]
- SENN, J. J, KLOVER, P. J, NOWAK, I. A, & MOONEY, R. A. 2002. Interleukin-6 induces cellular insulin resistance in hepatocytes. *Diabetes*, **51**(12), 3391–3399. [106]

- SHERMAN, M. 2005. Hepatocellular carcinoma: epidemiology, risk factors, and screening. *Seminars in liver disease*, **25**(2), 143–154. [1, 3]
- SHI, Y, & GAESTEL, M. 2002. In the cellular garden of forking paths: how p38 MAPKs signal for downstream assistance. *Biological chemistry*, **383**(10), 1519–1536. [12]
- SHOELSON, S. E, HERRERO, L, & NAAZ, A. 2007. Obesity, Inflammation, and Insulin Resistance. *Gastroenterology*, **132**(6), 2169–2180. [7]
- SOLINAS, G, VILCU, C, NEELS, J. G, BANDYOPADHYAY, G. K, LUO, J.-L, NAUGLER, W, GRIVENNIKOV, S, WYNshaw-BORIS, A, SCADENG, M, OLEFSKY, J. M, & KARIN, M. 2007. JNK1 in hematopoietically derived cells contributes to diet-induced inflammation and insulin resistance without affecting obesity. *Cell metabolism*, **6**(5), 386–397. [7]
- SORESI, M, GIANNITRAPANI, L, D'ANTONA, F, FLORENA, A.-M, LA SPADA, E, TERRANOVA, A, CERVELLO, M, D'ALESSANDRO, N, & MONTALTO, G. 2006. Interleukin-6 and its soluble receptor in patients with liver cirrhosis and hepatocellular carcinoma. *World journal of gastroenterology*, **12**(16), 2563–2568. [102]
- SUN, X, ZHANG, J, WANG, L, & TIAN, Z. 2008. Growth inhibition of human hepatocellular carcinoma cells by blocking STAT3 activation with decoy-ODN. *Cancer letters*, **262**(2), 201–213. [112]
- SWAIN, M. G. 2008. Hepatic NKT cells: friend or foe? *Clinical science*, **114**(7), 457. [118]
- TAIT, S. W. G, & GREEN, D. R. 2010. Mitochondria and cell death: outer membrane permeabilization and beyond. *Nature publishing group*, **11**(9), 621–632. [108]
- TATSUKAWA, H, SANO, T, FUKAYA, Y, ISHIBASHI, N, WATANABE, M, OKUNO, M, MORIWAKI, H, & KOJIMA, S. 2011. Dual induction of caspase 3- and transglutaminase-dependent apoptosis by acyclic retinoid in hepatocellular carcinoma cells. *Molecular cancer*, **10**(1), 4. [107]
- THOMAS, L. W, LAM, C, & EDWARDS, S. W. 2010. Mcl-1; the molecular regulation of protein function. *Febs letters*, **584**(14), 2981–2989. [16]
- THORGEIRSSON, S. S, & GRISHAM, J. W. 2002. Molecular pathogenesis of human hepatocellular carcinoma. *Nature genetics*, **31**(4), 339–346. [2]
- TIBBLES, L. A, & WOODGETT, J. R. 1999. The stress-activated protein kinase pathways. *Cellular and molecular life sciences : Cmls*, **55**(10), 1230–1254. [12]

- VAN DER VLIET, H. J, NISHI, N, KOEZUKA, Y, PEYRAT, M. A, VON BLOMBERG, B. M, VAN DEN EERTWEGH, A. J, PINEDO, H. M, GIACCONE, G, & SCHEPER, R. J. 1999. Effects of alpha-galactosylceramide (KRN7000), interleukin-12 and interleukin-7 on phenotype and cytokine profile of human Valpha24+ Vbeta11+ T cells. *Immunology*, **98**(4), 557–563. [118]
- VAUX, D. L, CORY, S, & ADAMS, J. M. 1988. Bcl-2 gene promotes haemopoietic cell survival and cooperates with c-myc to immortalize pre-B cells. *Nature*, **335**(6189), 440–442. [17]
- VENTURA, J.-J, KENNEDY, N. J, LAMB, J. A, FLAVELL, R. A, & DAVIS, R. J. 2003. c-Jun NH(2)-terminal kinase is essential for the regulation of AP-1 by tumor necrosis factor. *Molecular and cellular biology*, **23**(8), 2871–2882. [9]
- VICK, B, WEBER, A, URBANIK, T, MAASS, T, TEUFEL, A, KRAMMER, P. H, OPFERMAN, J. T, SCHUCHMANN, M, GALLE, P. R, & SCHULZE-BERGMANN, H. 2009. Knockout of myeloid cell leukemia-1 induces liver damage and increases apoptosis susceptibility of murine hepatocytes. *Hepatology*, **49**(2), 627–636. [108]
- VILLANUEVA, A, NEWELL, P, CHIANG, D. Y, FRIEDMAN, S. L, & LLOVET, J. M. 2007. Genomics and signaling pathways in hepatocellular carcinoma. *Seminars in liver disease*, **27**(1), 55–76. [2]
- VILLANUEVA, A, HOSHIDA, Y, TOFFANIN, S, LACHENMAYER, A, ALSINET, C, SAVIC, R, CORNELLA, H, & LLOVET, J. M. 2010. New strategies in hepatocellular carcinoma: genomic prognostic markers. *Clinical cancer research : an official journal of the american association for cancer research*, **16**(19), 4688–4694. [1]
- VIVIER, E, & ANFOSSI, N. 2004. Inhibitory NK-cell receptors on T cells: witness of the past, actors of the future. *Nature reviews immunology*, **4**(3), 190–198. [118]
- WANG, J. M, CHAO, J. R, CHEN, W, KUO, M. L, YEN, J. J, & YANG-YEN, H. F. 1999. The antiapoptotic gene mcl-1 is up-regulated by the phosphatidylinositol 3-kinase/Akt signaling pathway through a transcription factor complex containing CREB. *Molecular and cellular biology*, **19**(9), 6195–6206. [-]
- WANG, Y, AUSMAN, L. M, GREENBERG, A. S, RUSSELL, R. M, & WANG, X.-D. 2009. Nonalcoholic steatohepatitis induced by a high-fat diet promotes diethylnitrosamine-initiated early hepatocarcinogenesis in rats. *International journal of cancer*, **124**(3), 540–546. [5]

- WEBER, A, BOGER, R, VICK, B, URBANIK, T, HAYBAECK, J, ZOLLER, S, TEUFEL, A, KRAMMER, P. H, OPFERMAN, J. T, GALLE, P. R, SCHUCHMANN, M, HEIKENWALDER, M, & SCHULZE-BERGMANN, H. 2010. Hepatocyte-specific deletion of the antiapoptotic protein myeloid cell leukemia-1 triggers proliferation and hepatocarcinogenesis in mice. *Hepatology*, **51**(4), 1226–1236. [108, 109]
- WEISBERG, S. P, MCCANN, D, DESAI, M, ROSENBAUM, M, LEIBEL, R. L, & FERRANTE, A. W. 2003. Obesity is associated with macrophage accumulation in adipose tissue. *Journal of clinical investigation*, **112**(12), 1796–1808. [102]
- WERTZ, I. E, KUSAM, S, LAM, C, OKAMOTO, T, SANDOVAL, W, ANDERSON, D. J, HELGASON, E, ERNST, J. A, EBY, M, LIU, J, BELMONT, L. D, KAMINKER, J. S, O’ROURKE, K. M, PUJARA, K, KOHLI, P. B, JOHNSON, A. R, CHIU, M. L, LILL, J. R, JACKSON, P. K, FAIRBROTHER, W. J, SESHAGIRI, S, LUDLAM, M. J. C, LEONG, K. G, DUEBER, E. C, MAECKER, H, HUANG, D. C. S, & DIXIT, V. M. 2011. Sensitivity to antitubulin chemotherapeutics is regulated by MCL1 and FBW7. *Nature*, **471**(7336), 110–114. [77, 113]
- WESTON, C. R, & DAVIS, R. J. 2002. The JNK signal transduction pathway. *Current opinion in genetics & development*. [11, 12]
- WOLF, A. M, WOLF, D, STEURER, M, GASTL, G, GUNSILIUS, E, & GRUBECK-LOEBENSTEIN, B. 2003. Increase of regulatory T cells in the peripheral blood of cancer patients. *Clinical cancer research : an official journal of the american association for cancer research*, **9**(2), 606–612. [117]
- WUNDERLICH, C. M, HÖVELMEYER, N, & WUNDERLICH, F. T. 2013. Mechanisms of chronic JAK-STAT3-SOCS3 signaling in obesity. *Jak-stat*, **2**(2), e23878. [106, 107]
- WUNDERLICH, F. T, LUEDDE, T, SINGER, S, SCHMIDT-SUPPRIAN, M, BAUMGARTL, J, SCHIRMACHER, P, PASPARAKIS, M, & BRÜNING, J. C. 2008. Hepatic NF- κ B essential modulator deficiency prevents obesity-induced insulin resistance but synergizes with high-fat feeding in tumorigenesis. *Proceedings of the national academy of sciences of the united states of america*, **105**(4), 1297–1302. [6, 18, 104]
- WUNDERLICH, F. T, STRÖHLE, P, KÖNNER, A. C, GRUBER, S, TOVAR, S, BRÖNNEKE, H. S, JUNTTI-BERGGREN, L, LI, L.-S, VAN ROOIJEN, N, LIBERT, C, BERGGREN, P.-O, & BRÜNING, J. C. 2010. Interleukin-6 Signaling in Liver-Parenchymal Cells Suppresses Hepatic Inflammation and Improves Systemic Insulin Action. *Cell metabolism*, **12**(3), 237–249. [46, 91, 106]

- XU, H, BARNES, G. T, YANG, Q, TAN, G, YANG, D, CHOU, C. J, SOLE, J, NICHOLS, A, ROSS, J. S, TARTAGLIA, L. A, & CHEN, H. 2003. Chronic inflammation in fat plays a crucial role in the development of obesity-related insulin resistance. *Journal of clinical investigation*, **112**(12), 1821–1830. [3, 6, 48, 102, 117]
- YANG, R, & BAROUCH, L. A. 2007. Leptin signaling and obesity: cardiovascular consequences. *Circulation research*, **101**(6), 545–559. [116]
- YOSHIOKA, Y, HASHIMOTO, E, YATSUJI, S, KANEDA, H, TANIAI, M, TOKUSHIGE, K, & SHIRATORI, K. 2004. Nonalcoholic steatohepatitis: cirrhosis, hepatocellular carcinoma, and burnt-out NASH. *Journal of gastroenterology*, **39**(12), 1215–1218. [2, 5]
- YU, M.-W, YANG, Y.-C, YANG, S.-Y, CHENG, S.-W, LIAW, Y.-F, LIN, S.-M, & CHEN, C.-J. 2001. Hormonal Markers and Hepatitis B Virus-Related Hepatocellular Carcinoma Risk: a Nested Case–Control Study Among Men. *Journal of the* [2]
- ZHANG, S. Q, YANG, W, KONTARIDIS, M. I, BIVONA, T. G, WEN, G, ARAKI, T, LUO, J, THOMPSON, J. A, SCHRAVEN, B. L, PHILIPS, M. R, & NEEL, B. G. 2004. Shp2 regulates SRC family kinase activity and Ras/Erk activation by controlling Csk recruitment. *Molecular cell*, **13**(3), 341–355. [12]
- ZHANG, X. G, GU, J. J, LU, Z. Y, YASUKAWA, K, YANCOPOULOS, G. D, TURNER, K, SHOYAB, M, TAGA, T, KISHIMOTO, T, & BATAILLE, R. 1994. Ciliary neurotropic factor, interleukin 11, leukemia inhibitory factor, and oncostatin M are growth factors for human myeloma cell lines using the interleukin 6 signal transducer gp130. *The journal of experimental medicine*, **179**(4), 1337–1342. [8, 83, 88, 116]
- ZHONG, Q, GAO, W, DU, F, & WANG, X. 2005. Mule/ARF-BP1, a BH3-Only E3 Ubiquitin Ligase, Catalyzes the Polyubiquitination of Mcl-1 and Regulates Apoptosis. *Cell*. [16, 77, 113]

6 Acknowledgments

Als letztes möchte ich mich bei allen bedanken, die mich in den letzten Jahren unterstützt haben und mir auf so vielfältige Weise geholfen haben es bis hierhin zu schaffen. Mein besonderer Dank gilt dabei:

- **PD. Dr. F. Thomas Wunderlich** für mein spannendes Projekt und dafür einfach ein großartiger Chef zu sein. Ich danke Dir für deine unglaubliche Geduld und dein Verständnis in jeder Lebenslage. Es sollte mehr Chefs wie dich geben!
- **Prof. Dr. Jens C Brüning** für die Begutachtung meiner Doktorarbeit und die Möglichkeit in einem interessanten und produktiven Umfeld zu arbeiten.
- **Prof. Dr. Peter Kloppenburg** für den Vorsitz meines Prüfungskomitees.
- **Dr. Tim C. Klöckener** für Problemlösungen in jeder Lebenslage, für Motivation und Aufmunterung, wenn ich schon aufgeben wollte, für Rückhalt und Unterstützung, wenn ich unsicher war und für einfach alles. Danke, dass Du für mich da warst!
- **Dr. Claudia M. Wunderlich** für unermüdliches Korrekturlesen, für deine Geduld, für jede Menge Hilfe in praktischen und theoretischen Dingen und für ganz viel Spaß im Labor. Ohne dich wäre es nicht gegangen!
- **P. Justus Ackermann** für die tolle Hilfe bei unserem Paper, für großartige gemeinsame Meetings und für ganz viele Lacher im Laboralltag.
- **Cathy Baitzel und Anke Lietzau** für Western, ELISAs, Mausearbeit, Realties und und und! Danke für eure großartige Hilfe!
- **Mona Al-Maari, Peter Ströhle und der AG Wunderlich im allgemeinen** für eine unglaublich großartige Zeit im Labor. Jeder sollte eine Gruppe wie euch haben!
- **Martin E. Hess, M.Sc.** für jede Menge Hilfe bei Präsentationen und vor allem für deine Hilfe bei Latex. Ohne dich wäre ich verzweifelt!
- **AG Brüning** für Hilfe aller Art, ein tolle Arbeitumfeld und eine gute Zeit.
- **meiner Familie** für einfach unbeschreiblich viel Unterstützung und Hilfe. Ihr seid einzigartig!

7 Erklärung

Die vorliegende Arbeit wurde in der Zeit von November 2009 bis Oktober 2013 am Institut für Genetik, Arbeitsgruppe Mouse Genetics and Obesity-associated Cancer, Universität zu Köln unter Anleitung von Herrn PD Dr. F. Thomas Wunderlich angefertigt.

Ich versichere, dass ich die von mir vorgelegte Dissertation selbständig angefertigt, die benutzten Quellen und Hilfsmittel vollständig angegeben und die Stellen der Arbeit einschließlich Tabellen, Karten und Abbildungen, die anderen Werken im Wortlaut oder dem Sinn nach entnommen sind, in jedem Einzelfall als Entlehnung kenntlich gemacht habe; dass diese Dissertation noch keiner anderen Fakultät oder Universität zur Prüfung vorgelegen hat; dass sie abgesehen von unten angegebenen Teilpublikationen noch nicht veröffentlicht worden ist sowie, dass ich eine solche Veröffentlichung vor Abschluss des Promotionsverfahrens nicht vornehmen werde. Die Bestimmungen der Promotionsordnung sind mir bekannt. Die von mir vorgelegte Dissertation ist von Prof. Dr. Jens C. Brüning betreut worden.

Teilpublikationen:

Obesity Promotes Liver Carcinogenesis via Mcl-1 Stabilization Independent of IL-6R α Signaling.

Sabine Gruber, Beate K. Straub, P. Justus Ackermann, Claudia M. Wunderlich, Jan Mauer, Jens M. Seeger, Hildegard Büning, Lukas Heukamp, Hamid Kashkar, Peter Schirmacher, Jens C. Brüning, and F. Thomas Wunderlich

Cell reports, August 2013

<http://dx.doi.org/10.1016/j.celrep.2013.07.023>

Köln, den 07. Oktober 2013

(Sabine Gruber)

8 Curriculum vitae

Dipl. Biol. Sabine Gruber

Name: Sabine Gruber

Geburt: 18.04.1984 in Köln

Adresse: Vorgebirgsplatz 10, 50969 Köln

E-Mail: sabine_gruber_bio@yahoo.de

Staatsangehörigkeit: Deutsch

AUSBILDUNG

- | | |
|-------------|---|
| 2009 – 2013 | Universität zu Köln, Institut für Genetik
Promotion in der Abteilung Mausgenetiks and Metabolism des Instituts für Genetik, Labor von Prof. Dr. Jens C. Brüning.
Thema: „ <i>The Role of Interleukin 6 and Obesity in the Development of Hepatocellular Carcinoma</i> ”. |
| 2008 – 2009 | Universität zu Köln, Institut für Genetik
Diplomarbeit in der Abteilung Mausgenetiks and Metabolism des Instituts für Genetik, im Labor von Prof. Dr. Jens C. Brüning. Thema: „ <i>The role of Interleukin-6 in the development of hepatocellular carcinoma</i> ”. |
| 2008 | Universität zu Köln, Institut für Genetik
Diplomprüfungen im Hauptfach Genetik und in den Nebenfächern Biochemie und Zoologie. |
| 2000 – 2003 | Gymnasium der Stadt Kerpen
Allgemeine Hochschulreife |
| 1994 – 2000 | Realschule Mater Salvatoris, Kerpen
Fachoberschulreife |
| 1990 – 1994 | kath. Grundschule Theodor Heuss, Kerpen |

PUBLIKATIONEN

- 2013 **Obesity Promotes Liver Carcinogenesis via Mcl-1 Stabilization Independent of IL-6R α Signaling**
Sabine Gruber, Beate K. Straub, P. Justus Ackermann, Claudia M. Wunderlich, Jan Mauer, Jens M. Seeger, Hildegard Büning, Lukas Heukamp, Hamid Kashkar, Peter Schirmacher, Jens C. Brüning, and F. Thomas Wunderlich
 Cell Reports, August 2013
- 2010 **Interleukin-6 Signaling in Liver-Parenchymal Cells Suppresses Hepatic Inflammation and Improves Systemic Insulin Action**
F. Thomas Wunderlich, Peter Ströhle, A. Christine Könner, Sabine Gruber, Sulay Tovar, Hella S. Brönneke, Lisa Juntti-Berggren, Luo-Sheng Li, Nico van Rooijen, Claude Libert, Per-Olof Berggren, and Jens C. Brüning
 Cell Metabolism, September 2010

POSTER & PRÄSENTATIONEN

- 2013, *Mai* **Immunity and Tolerance**
 Poster
- 2013, *Januar* **Breakthroughs in Cancer Research and Therapy**
 Poster
- 2012, *November* **Metabolism 2012: From Signaling to Disease**
 Poster
- 2012, *September* **Diabetes and Obesity**
 Poster
- 2012, *Mai* **The Role of Inflammation during Carcinogenesis**
 Poster and Presentation

AWARDS

- 2013, *Januar* **Young Investigator Award**
 Charles Rodolphe Brupbacher Foundation